H_∞ and LQG Optimal Control for the Rejection of Persistent Disturbances: Analysis, Design and Experiment

by

Graham K. Ellis

Dissertation submitted to the Faculty of the

Virginia Polytechnic Institute and State University

in partial fulfillment of the requirements for the degree of

Doctor of Philosophy

in

Mechanical Engineering

APPROVED:

Harry H. Robertshaw, Committee Chairman
Mechanical Engineering Department

Robert G. Leonard
Mechanical Engineering Department

David L. Russell
Mathematics Department

Alfred L. Wicks
Mechanical Engineering Department

William T. Baumann
Electrical Engineering Department

February, 1992
Blacksburg, Virginia

H_∞ and LQG Optimal Control for the Rejection of Persistent Disturbances: Analysis, Design and Experiment

by

Graham K. Ellis

Committee Chairman: Harry H. Robertshaw
Mechanical Engineering

Abstract

This dissertation presents a discussion of the asymptotic behavior and estimation structure of the H_∞ central controllers in terms of the well-known behavior of the LQG controller and gives some insight into the physics of the H_∞ controller that is often presented in an unclear manner in the current literature. The connections to LQ game theory that underlie this confusion are discussed. Augmented systems that are typically used in disturbance rejection problems are also analyzed. Additionally, a controlled output equation for disturbance rejection is developed based on the physics of the problem rather than the typical ad hoc approaches of the past. These controlled output equations are also appropriate for LQG compensators. In order to verify the proposed approach, an experiment in harmonic and narrowband disturbance rejection using a simply supported steel plate is presented. Discrete-time LQG, and continuous-time H_∞ and LQG controllers that have been transformed to discrete-time are used to determine the attainable performance of each approach. The results indicate that the H_∞ controller provides more damping than either LQG approach and that discrete-time design procedures are necessary for maximum disturbance rejection.

Acknowledgements

Whew! Where to begin? I think that getting a Ph.D. is interesting – interesting in the same sense of the Chinese curse: *May your life be interesting.* All seriousness aside though, there are many people who have contributed to this endeavor called a Ph.D. and any omissions and missed thanks should not be taken personally; they should be attributed to the current state of my mental faculties.

First, I must thank my friend and committee chairman Harry Robertshaw for his tolerance of my antics and his guidance and advice that I was sometimes smart enough to heed. Besides, Harry is one of the few people that actually thinks my jokes are funny – at least initially. A special thanks to David Russell from whom I learned a modicum of mathematical rigor (only a modicum due to my limitations, not his) and fortunately only an insignificant amount of mortis. Rarely at a loss for words, you seem to have an astounding collection of stories – something for any occasion. You know David, I'd even bet that some of them are true! Thanks also to the rest of my committee members: Bill Baumann, Bob Leonard and Al Wicks, all of whom can see through the fluff and get right to the crux of a problem. Although, in retrospect, I'm not sure whether that's good or bad. I must also thank Joe Ball who provided valuable preprints of papers that saved me more than just a few hours of reinventing the wheel.

A special thanks goes to all my cohorts in the lab (and elsewhere) without whom this work would not have been and certainly would have been less enjoyable: Will (what do you mean *almost* always right?), Robert and Carol (thanks for everything), Buddy, Steve, Tom E., Tom W. and Dan. What a group! Can motley be an un-

derstatement? All the gripe sessions where we solved the worlds problems were a welcome diversion to the daily grind. And you all know how easily I was diversed.

To my family, thanks for the love and support that helped me persevere throughout the last three-plus years. You helped more than you can imagine. Also, a special acknowledgement to my sister, N, who summed it up best when she said, "Ken, you're weird." It's nice to have someone who at least pretends to understand my version of craziness.

And to Xiaohong, thank you for your love and support. I could not have done this without you. You kicked me when I needed kicking and hugged my when I needed hugging. Thanks for being there.

And finally, a thought on how things should be done, expressed much more eloquently than I am capable of doing. This quote is by the late Nobel laureate Richard Feynman excerpted from Appendix F of the Rogers Commission report on the space shuttle Challenger accident:

> For a successful technology, reality must take precedence over public relations, for Nature cannot be fooled.

Contents

List of Figures

List of Tables

Nomenclature

Symbol	Definition
R	field of real numbers
C	field of complex numbers
L_2	Lebesgue space (domain based on context)
L_∞	Lebesgue space (domain based on context)
H_2	Hardy space
H_∞	Hardy space
prefix R	real rational
$\|\cdot\|_2$	norm on L_2
$\|\cdot\|_\infty$	norm on L_∞
$\|\cdot\|_F$	Frobenius norm
$\langle\cdot,\cdot\rangle$	inner product
$\sigma_j(A)$	j^{th} singular value of A
$\bar{\sigma}(A)$	maximum singular value of A
$\mu(A)$	structured singluar value of A
$\rho(A)$	spectral radius of A
$F_l(\cdot,\cdot)$	lower linear fractional transformation
$F_u(\cdot,\cdot)$	upper linear fractional transformation
$\equiv$	equivalent to
$\triangleq$	defined as
$\hat{x}_{k\|k-1}$	estimate of the k^{th} value of x given measurments up to the $(k-1)^{st}$ step
$\hat{x}_{k\|k}$	estimate of the k^{th} value of x given measurments up to the k^{th} step

Chapter 1

Introduction

One of the difficulties with H_∞ control is that it is so new that there are few practitioners of the "art" and consequently no clear presentation of the H_∞ related material. To make matters worse, some of the material in the literature uses incorrect or perhaps more correctly "inexact" descriptions to describe the behavior of H_∞ controllers.

In an effort to "extract" the H_∞ controller theory from the world of analysis presented in journal articles to the world of controller design, we thoroughly analyze the asymptotic and error behavior of the H_∞ controller and attempt to frame the behavior in terms the well known LQG controller and in terms of systems physics rather than mathematical esoterica. We will show that the H_∞ controller does not generate a state estimate like the LQG controller. Additionally, we develop an approach to choosing controlled outputs (quadratic cost weights in LQG) based on the physics of the problem rather than the ad hoc approaches of the past. In this case, we choose to use a "minimum acceleration" cost as a basis for the controller design. The importance of this new design procedure is that is shows how weighting the augmented disturbance states can be important for disturbance rejection problems.

This approach is not immediately obvious if only time-domain cost functions are used. The cost weights obtained using this approach are appropriate for both LQG and H_∞ disturbance rejection compensators.

Once the theory has been presented, we will show the results of an experiment in disturbance rejection on a simply-supported steel plate using the minimum acceleration cost controller design procedure. In order to narrow the scope of this work, we will concentrate on the following disturbance rejection problems: *design a controller to reject the effects of a persistent sinusoidal or narrow-band disturbance on a dynamic system.*

The main emphasis of the experiment will involve selecting the controlled output equation appropriately to achieve the best possible disturbance rejection while maintaining closed-loop stability on an actual system. We will show that more disturbance rejection can be achieved using the H_∞ controller when compared to the LQG controller in certain cases. This is especially apparent when driving systems near resonances. This additional rejection does not come without cost however. Since the H_∞ controller minimizes the worst case system "gain", the side bands (away from the disturbance spectrum) can grow to possibly unacceptable levels using the H_∞ approach. The advantages to the proposed controlled output equations in terms of overall performance compared to the traditional ad hoc approach will be discussed.

The rest of this dissertation is organized as follows: Chapter 2 presents an introduction to H_∞ control theory in a tutorial fashion and attempts to consolidate much of the material that is "dispersed" throughout technical journals. Both forms of the

H_∞ central controllers are covered as well as loop scaling and μ-analysis techniques. Chapter 3 provides an analysis of the asymptotic and error behavior of the H_∞ central controllers and shows that the H_∞ controllers do not provide state estimates. It also presents the connections to LQ game theory and a discussion of why certain terminology associated with the H_∞ controllers is misleading. Chapter 4 develops controlled output (weighting matrices) based on a "minimum acceleration" cost for both LQG and H_∞ controllers for use in disturbance rejection problems. An example problem is used to show the characteristics of the various controlled output equations obtained using the proposed method. Chapter 5 presents the simulations and the experiments for the harmonic and narrowband disturbance rejection problem on a simply-supported steel plate using both LQG and H_∞ controllers and the new design methods presented in Chapter 4. Chapter 6 concludes the report with a brief summary and some recommendations for future research.

Chapter 2

Recent Developments in State-Space Optimal Control Theory

This chapter focuses on some of the recent developments in control theory with specific emphasis on state-space H_∞ control. The review of the control literature is presented mostly in chronological order and the H_∞ discussion is designed to be a limited tutorial since many control engineers are not familiar with H_∞ techniques. The primary purpose of the tutorial part of the discussion is to familiarize the reader with the notation used in the current literature. Those familiar with H_∞ controllers can skip this material and proceed directly to the next chapter.

2.1 Historical Background

In broad brush, the evolution of control theory can be grouped into three major periods: classical, modern, and robust. Table 2.1 divides these three time frames into analysis and synthesis methods appropriate for each period. There is some difference of opinion as to when the robust control period actually started; however,

Table 2.1: Chronology of Control Theory Development [7]

	Classical Control 1930-1960	Modern Control 1960-1980	Robust Control 1980-present
Analysis	Bode plots Nyquist stability test Routh stability test Evans root locus Gain and phase margins	State-space models Controllability Observability Random processes	Singular value plots μ-analysis Balanced Realizations Spectral factorization
Synthesis	PID controllers Lead-lag compensation	Kalman-Bucy filters LQR state feedback LQG	H_∞ synthesis μ-synthesis LQG/LTR Youla Q-parameterization
Chief Paradigm	Frequency domain	Time domain	Frequency domain with state-space models

1975-1980 is typically mentioned as the beginning of the period.

A brief summary of the development of robust control, although one that is more thorough than the one printed here, can be found in the IEEE collection of papers on robust control [1]. This volume contains reprints of the important papers on robust control from around 1975 to 1985. Many of the papers discussed below appear in this work. Additionally, the collection contains 385 references on general robust control analysis and design techniques.

For the sake of brevity, we start our discussion with the modern control era. The work of this period was couched in terms of state variables and analysis was performed in the time domain. Kalman [2] introduced a number of key state-variable concepts such as controllability, observability, optimal linear-quadratic state feed-

back, and optimal state estimation (Kalman-Bucy filtering). The results from this work can be found in any textbook on modern control theory [3, 4] and the reader is assumed to be familiar with this material.

What is interesting to note is that the issue of plant uncertainty was, for the most part, ignored during this period. Attempts at dealing with plant uncertainty was largely dealt with in terms of differential sensitivity. That is, the types of plant uncertainties (perturbations) were restricted to those described by (typically) first order variations in the plant's mathematical description [5]. Additionally, modal control methods dealing with eigenvalue/eigenvector sensitivities were also developed in order to deal with differential plant uncertainties [6]. One problem with the sensitivity approach is that it does not allow for arbitrary norm-bounded (i.e. finite not differential) perturbations. It was this inability to deal with general norm-bounded perturbations that lead to the renewed interest in robustness issues in control system design.

Although the state-space methods theoretical development was well established, there was no rush to apply these methods on real systems [7]. These so called "optimal" controllers were found to give either poor performance or even destabilize real systems because of high sensitivity to modelling errors. It was these types of difficulties that drove researchers to investigate the stability margins available when using the various modern control techniques for control system design.

Kalman in 1964 [8] showed that for Single-Input-Single-Output (SISO) systems, the LQR controller (state-feedback with no observer) gave infinite gain margins and

60 degree phase margins. Safanov and Athans [9] extended these results to Multi-Input-Multi-Output (MIMO) systems in 1977. However, in 1978 Doyle [10] showed if an estimator is used to construct the plant states (LQG control), the stability margins disappear entirely. In 1979, Doyle and Stein [11] showed that the desirable LQR characteristics were obtainable with LQG by suitable design of the Kalman filter. This work was further expanded in their now classic Linear Quadratic Gaussian/Loop Transfer Recovery (LQG/LTR) paper in 1981 [12].

At around the same time, in the late 1970's and early 1980's, other researchers were pursuing the problem of plant uncertainty with analyses in the frequency domain. Youla et al. in 1976 [13], and Desoer et al. in 1980 [14] presented the idea of the coprime matrix fraction description of MIMO systems as a design tool. The parameterization of all stabilizing controllers discussed in Youla's paper was important to the early H_∞ synthesis research and is often referred to as the *Youla* or *Q-parameterization.* In another extension from SISO to MIMO systems, McFarlane et al. generalized the Nyquist stability criteria and root locus method to the multivariable case in 1977 [15].

In 1981, Safanov et al. [16], wrote on the feedback properties of multivariable systems. They showed how the feedback properties of plant disturbance attenuation, sensor noise response, and sensitivity to plant and sensor variations are quantitatively related to the Bode magnitude-versus-frequency plots of the singular values of the return difference matrix $I + GK$ and the corresponding inverse return difference matrix, $I + (GK)^{-1}$, where $G(s)$ is the plant transfer matrix, and $K(s)$ is the controller transfer matrix. One result from this analysis shows the necessary tradeoff

between attenuating disturbances and filtering out measurement errors. Basically, the performance and robustness tradeoffs present in SISO systems also apply for MIMO systems.

Many of the results for robust multivariable control methods involving both LQG, LQG/LTR, and the loop shaping ideas of Safanov can be found in the 1986 book by Ridgely and Banda [17] and in the 1989 book by Maciejowski [18]. The book by Maciejowski also contains some information on the Youla Q-parameterization and H_∞ theory through 1988.

2.2 H_∞ Synthesis

The seminal paper on the use of the H_∞ norm as a metric for robust stability was written by Zames in 1981 [19] although the emphasis in this paper was on SISO systems. He formulated the idea of treating the idea of sensitivity reduction by feedback as an optimization problem with an operator norm, in this case, the H_∞ norm.

Typically, H_∞ problems are cast in an input-output (operator) framework and for simplicity, the numerical computations are performed in a state-space framework. Much of the H_∞ research has involved the development of state-space methods for solving the H_∞ optimization problem.

The "standard" H_∞ problem as presented by Doyle [20] is shown in figure 2.1. All signals are assumed to be vector-valued and are defined as follows: u_1 is the exoge-

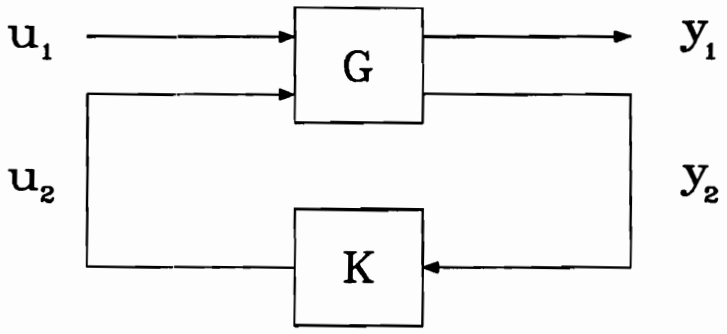

Figure 2.1: The Standard H_∞ Problem Block Diagram

nous input which consists of command signals, disturbances, and sensor noise; u_2 is the control signal; y_1 is the controlled output, i.e. the error signals; and y_2 is the measured output. The transfer matrices G and K are assumed to be real-rational and proper: G represents the plant, and K represents the controller.

The purpose of the H_∞ synthesis (optimization) problem is to find a stabilizing feedback, K, that minimizes the H_∞ norm of the transfer function matrix from u_1 to y_1.

An excellent exposition of the mathematical underpinnings of the H_∞ theory is presented in Francis and Doyle [21]. This paper provides a thorough overview of the various H_∞ problem formulations; however, it does not deal with any computational methods for obtaining solutions to the problems posed. The paper also includes a substantial review of the robust control literature of the time (prior to 1987).

In order to adequately describe the H_∞ theory, a few preliminary mathematical concepts are given below. These definitions are not as complete as the ones provided

by Francis and Doyle; however, they are adequate for the scope of the discussion below.

The Hardy space H_∞ is the class of matrix-valued functions which are analytic and bounded in the open right half-plane.

Definition 2.1 *The transfer function* ∞**-norm** *is defined as:*

$$\| G \|_\infty \triangleq \operatorname{ess\,sup}_{w \in \mathbf{R}} \overline{\sigma}(G(jw)) \tag{2.1}$$

This simply says that the maximum singular value of $G(jw)$ has bounded gain on the jw-axis (except possibly on a set of measure zero).

Also, the infinity norm can be thought of as the maximum transfer function matrix "gain" on the jw-axis and as the maximum induced gain for signals in $L_2(\mathbf{R})$:

$$\| G \|_\infty = \sup_{u \neq 0} \frac{\| Gu \|_2}{\| u \|_2} = \sup_{\|u\|_2 = 1} \| Gu \|_2 \tag{2.2}$$

We will also make use of the transfer function **2-norm** which is the norm minimized in LQG control.

Definition 2.2 *The transfer function* **2-norm** *is defined as:*

$$\begin{aligned} \|G\|_2^2 &\triangleq \langle G, G \rangle \\ &= \frac{1}{2\pi} \int_{-\infty}^{\infty} \operatorname{trace}[G(jw)^* G(jw)]\, dw \end{aligned} \tag{2.3}$$

$$
\begin{aligned}
&= \int_{-\infty}^{\infty} \sum_{i=1}^{n} \sigma_i(jw)^2 \, dw \\
&= \frac{1}{2\pi} \int_{-\infty}^{\infty} \|G(jw)\|_F^2 \, dw \\
&= \langle g, g \rangle \\
&= \int_{-\infty}^{\infty} \mathrm{trace}[g(t)^T g(t)] \, dt \\
&= \int_{-\infty}^{\infty} \|g(t)\|_F^2 \, dt
\end{aligned}
$$

The notation used in the literature to describe the standard H_∞ problem takes several forms. This notation is summarized in the sections below.

2.2.1 Linear Fractional Transformations (LFT)

Let a 2×2 block transfer function relating the input vectors u_1 and u_2 to the output vectors y_1 and y_2 be defined as

$$
G(s) = \begin{bmatrix} G_{11} & G_{12} \\ G_{21} & G_{22} \end{bmatrix} \tag{2.4}
$$

When we connect the feedback matrix K as in figure 2.1, the closed-loop transfer function from u_1 to y_1 we get the following:

$$
y_1 = G_{11}u_1 + G_{12}u_2 \tag{2.5}
$$

$$
y_2 = G_{21}u_1 + G_{22}u_2 \tag{2.6}
$$

$$
u_2 = Ky_2 \tag{2.7}
$$

And if we eliminate u_2 and y_2 we find:

$$y_1 = (G_{11} + G_{12}K(I - G_{22}K)^{-1}G_{21})u_1 \quad (2.8)$$

$$\triangleq F_l(G, K)u_1 \quad (2.9)$$

where $F_l(G, K)$ is called the *lower linear fractional transformation* of G and K. The same operations can be performed when the upper loop is closed. When the upper loop is closed, say with a transfer function Δ, and the transfer function is from u_2 to y_2, the notation $F_u(G, \Delta)$ is used. We call this the *upper linear fractional transformation.* Upper linear fractional transformations will be discussed later in the μ-analysis section.

2.2.2 State-Space Realizations of LFTs

When we get to the more recent developments in H_∞ control theory, much of the design is performed in the frequency domain using state-space models. The general state space formulation of the standard problem is given below:

$$\dot{x} = Ax + B_1u_1 + B_2u_2 \quad (2.10)$$

$$y_1 = C_1x + D_{11}u_1 + D_{12}u_2 \quad (2.11)$$

$$y_2 = C_2x + D_{21}u_1 + D_{22}u_2 \quad (2.12)$$

with $x \in \mathbf{R}^n, u_1 \in \mathbf{R}^{m_1}, u_2 \in \mathbf{R}^{m_2}, y_1 \in \mathbf{R}^{p_1}$, and $y_2 \in \mathbf{R}^{p_2}$.

These equations are often denoted in the literature in the following forms:

$$G = \left[\begin{array}{c|cc} A & B_1 & B_2 \\ \hline C_1 & D_{11} & D_{12} \\ C_2 & D_{21} & D_{22} \end{array}\right] = \begin{bmatrix} G_{11} & G_{12} \\ G_{21} & G_{22} \end{bmatrix} \tag{2.13}$$

Note that the state-space depiction of the transfer function G is *not* a transfer function matrix, it is only a notational convenience.

2.2.3 Solving the Standard H_∞ Problem

Francis [22], in the first book on H_∞ control theory expands on the material presented in Francis and Doyle [21]. He shows that the standard problem can be recast in three different forms that are easier to solve than the originally posed standard problem. The first form is called the model-matching problem. There is also the tracking problem and the robust stabilization problem.

By using the previously mentioned Youla Q-parameterization, the standard problem can be recast into the model-matching problem. A block diagram of the model matching problem is shown in figure 2.2. The transfer matrix T_1 represents a model which is to be matched by the transfer matrix T_2QT_3. The transfer matrix Q is the "controller" which needs to be specified to minimize the following model matching criteria:

$$\sup\{\| z \|_2 : w \in H_2, \| w \|_2 \leq 1\} = \text{minimum.}$$

Which, in view of equation 2.2 is equivalent to:

$$\| T_1 - T_2QT_3 \|_\infty = \text{minimum.}$$

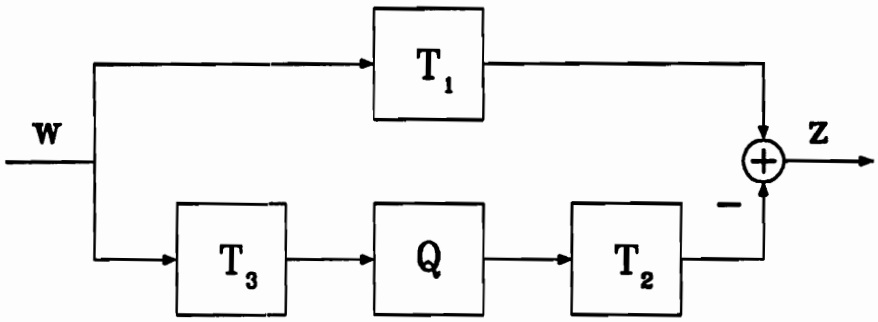

Figure 2.2: The Model-Matching Problem Block Diagram

The model-matching problem can be recast as a standard problem by defining:

$$\begin{aligned} G &\triangleq \begin{bmatrix} T_1 & T_2 \\ T_3 & 0 \end{bmatrix} \\ K &\triangleq -Q \end{aligned}$$

which gives us the standard form shown in figure 2.1. We should note that the model-matching problem is not important per se; its only significance is that the standard problem can be transformed to the model-matching form which is easier to solve.

Another important transformation of the standard problem is the robust stabilization problem. In this case, we wish to find a stabilizing controller for not only a single plant $G(s)$, but a set of transfer functions, say $\mathbf{G} \triangleq G(s) + \Delta G(s)$. Suppose

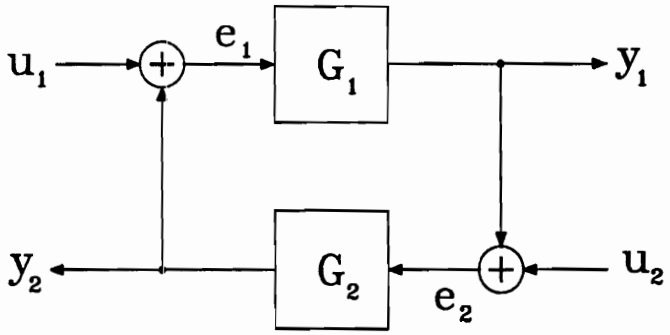

Figure 2.3: Block Diagram for Small Gain Theorem

the perturbation ΔG is defined by:

$$|\Delta G(jw)| < |R(jw)| \qquad \forall\, w \in [0, \infty)$$

or equivalently,

$$\|R^{-1}\Delta G\|_\infty < 1$$

For robust stability, we require a K that stabilizes all plants in the set $\mathbf{G}$. To deal with this problem, we need the following theorem. A block diagram for the proof is given in figure 2.3.

Theorem 2.1 (Small Gain Theorem [7]) *Assume that G_1 and $G_2 \in H_\infty$ are both stable, bounded-gain transfer functions. Then if $\|G_1G_2\|_\infty < 1$ the closed-loop system is stable. Furthermore, since $\|G_1G_2\|_\infty \leq \|G_1\|_\infty\|G_2\|_\infty < 1$ then,*

$$\|G_1\|_\infty \|G_2\|_\infty < 1 \Rightarrow \text{closed-loop stability.}$$

Proof:

Let $u_1 = 0$. *Then* $e_2 = (I - G_1 G_2)^{-1} u_2$.

$$\begin{aligned}
&\Leftrightarrow && e_2 = u_2 + G_1 G_2 e_2 \\
&\Rightarrow && \|e_2\|_2 \leq \|u_2\|_2 + \|G_1 G_2\|_\infty \|e_2\|_2 \qquad \forall\, u_2 \in L_2[0,\infty) \\
&\Leftrightarrow && (1 - \|G_1 G_2\|_\infty)\, \|e_2\|_2 \leq \|u_2\|_2
\end{aligned}$$

therefore,

$$\begin{aligned}
\|G_1 G_2\|_\infty < 1 \;&\Rightarrow\; \|e_2\|_2 \leq \frac{1}{1 - \|G_1 G_2\|_\infty} \|u_2\|_2 \\
&\Rightarrow \text{ closed-loop gain is bounded} \\
&\Rightarrow \text{ closed-loop system is stable.} \quad \square
\end{aligned}$$

Note that this is only a sufficient condition for stability.

The importance of $\|\cdot\|_\infty$ in this case is that we can bound the norm of the products by the product of the norms. This is not possible when using $\|\cdot\|_2$.

The small gain theorem is the basis for stability robustness tests using singular values as well as the Structured Singular Value (SSV) that we will discuss below when

we talk about structured perturbations.

One problem with treating plant perturbations in terms of just a norm bound is that any structure inherent in the perturbations is lost. This typically leads to an overly conservative controller and many times yields a closed-loop system that has poor performance. In an effort to circumvent this problem, Doyle [23] introduced the Structured Singular Value (SSV), denoted μ, as a new metric for robustness measure. At around the same time, Safanov [24] introduced the related robustness metric called the Multivariable Stability Margin, k_m. It turns out that $k_m = 1/\mu$ so we will restrict our discussion to the SSV.

Definition 2.3 *The SSV of the matrix* $M \in \mathbf{C}^{m \times m}$, *denoted* $\mu(M)$ *is defined as:*

$$\frac{1}{\mu(M)} = k_m \triangleq \inf_{\Delta \in \underline{\Delta}} \{\overline{\sigma}(\Delta) \mid \det(I - \Delta M) = 0\}$$

where $\underline{\Delta}$ *is the set of all* Δ *matrices with fixed, block-diagonal structure. If no* $\Delta \in \underline{\Delta}$ *satisfies the above definition, we let* $\mu(M) = 0$. *Here,* $1/\mu$ *is the size of the smallest* destabilizing Δ *satisfying the above equation.*

Instead of a general norm bound perturbation, the SSV approach allows any arbitrary set of perturbations to be written as a block-diagonal perturbation problem that can then be dealt with using μ. The SSV, μ is designed to be proportional to the "size" of a matrix as measured by singular values or eigenvalues. One of the important relations derived by Doyle is the following:

$$\rho(M) \leq \mu(M) \leq \overline{\sigma}(M)$$

where $\rho(\cdot)$ is the spectral radius and $\overline{\sigma}(\cdot)$ is the maximum singular value.

These Δ matrices are used to describe the plant uncertainties. This μ-analysis gives a "yes" or "no" answer to the question of closed-loop stability with assumed perturbations Δ with a previously designed feedback transfer matrix K. If the system fails the μ test, a new K needs to be computed using H_∞ synthesis and then the μ-analysis needs to be repeated. It is this iterative procedure that is called μ-synthesis. We will discuss μ-synthesis in more detail after the presentation of the state-space formulation of H_∞ control.

2.3 Recent Developments in H_∞ Theory

A major problem when trying to use the early H_∞ synthesis techniques for controller design was the complexity in terms of the types of operations required to construct a controller. Techniques such as the Youla Q-parameterization, inner-outer and spectral factorizations, and Hankel optimal model matching added states to the overall closed-loop system. In some cases, these methods required from 10 to 30 times more states than the original plant. The only practical approach with so many states was a model reduction technique such as balancing truncation or optimal projection. Even after the order reduction process, the controller typically had many more states than the plant being controlled and there was no consistent

structure to the controller analogous to an LQG type controller [7]. Only recently has the factorization theory been developed to the point where low order H_∞ compensators the same order as the plant can be computed [25].

In an early attempt at a state-space solution to the H_∞ synthesis problem, Doyle [20] presented a suboptimal controller that added $2n$-states to the plant. In a major breakthrough, Glover and Doyle [26] presented a general, state-space H_∞ controller that was posed as a two matrix Ricatti equation problem with the controller the same order as the plant. They also showed the relation of the H_∞ controller to risk sensitive LQG control and maximum entropy controllers. Unfortunately, the results of this paper were stated without proof. Proofs were first given for several special cases in Doyle, Glover, Khargonekar, and Francis [27], hereafter denoted DGKF.

The special cases presented in DGKF require some not so routine, and overly restrictive assumptions on the structure of the plant to be controlled. These assumptions are listed below.

i) (A, B_1) is stabilizable and (C_1, A) is detectable.

ii) (A, B_2) is stabilizable and (C_2, A) is detectable.

iii) $D_{12}^T \begin{bmatrix} C_1 & D_{12} \end{bmatrix} = \begin{bmatrix} 0 & I \end{bmatrix}$.

iv) $\begin{bmatrix} B_1 \\ D_{21} \end{bmatrix} D_{21}^T = \begin{bmatrix} 0 \\ I \end{bmatrix}$.

v) $D_{11} = 0$.

vi) $D_{22} = 0$.

The detectability and stabilizability conditions above are required for solutions to exist and are standard assumptions. Assumption *iii)* implies that $C_1 x$ and $D_{12} u_2$ are orthogonal and there is a nonsingular, normalized ($D_{12}^T D_{12} = I$) penalty on the control. Assumption *iv)* is dual to *iii)* and concerns how the disturbance u_1 enters the plant. These orthogonality conditions correspond to the H_2 (LQG) case when there is no cross weighting between the state and the control. We will have more to say concerning weighting matrices in the sequel.

There are numerous difficulties with this formulation of the H_∞ control problem. First and foremost is that there are few systems that happen to meet all of the assumptions described above. In an effort to deal with these difficulties, Safanov et al. [28] show how the most general form of the controller can be put in DGKF form using loop-shifting techniques using multiple unitary transformations. They also introduce methods using matrix fraction descriptions of the problem to eliminate computational difficulties that sometimes appear in the standard formulation.

The results from DGKF did, however, show a connection between H_∞ controllers and the familiar LQG controllers. Each method has a state-estimator state-feedback structure. Two matrix Ricatti equations are required to generate the state feedback matrix and the output injection matrix (analogous to the Kalman filter gain in LQG). A stable free parameter $\Phi(s)$ with $\|\Phi(s)\|_\infty < \gamma$ generates the family of all stabilizing controllers that produce a closed-loop ∞-norm less than the specified γ. This $\Phi(s)$ is analogous to the Q of the Youla Q-parameterization. And, as we let $\gamma \to \infty$, the H_∞ controller Riccati equations approach the H_2 or LQG controller Riccati equations.

In an amazingly under-cited paper, Glover and Doyle [29], hereafter GD, present proofs to the general H_∞ controller presented in Glover and Doyle [26]; however, they do not indicate that the H_∞ controller equations differ between the two papers. Since an optimal H_∞ controller is not unique, this is admissible, but the differences do not seem to be widely appreciated in the literature. Hvostov [30] shows how the the two different forms of the H_∞ controllers arise in a duality argument, and that as $\gamma \to \infty$, both H_∞ forms approach the LQG controller solution. More details of the behavior of these two H_∞ controller structures will be discussed in the sequel.

Since some of the restrictions required for the DGKF H_∞ controllers are not necessary except for special cases, we will present the general H_∞ controller below. The motivation to repeat the equations here is that many slightly different forms of the H_∞ controller appear in the literature even though these forms can be derived from the general H_∞ controller formulation. Additionally, some papers mix up the required assumptions for a given H_∞ controller formulation. For example, Dailey [7] "requires" condition *i)* be met for the general H_∞ controller formulation when $D_{11} \equiv 0$, when in fact, the weaker conditions listed below are sufficient for a controller to exist. The material below is from Glover and Doyle [26, 29].

We assume the following for the general H_∞ controller:

1) (A, B_2) is stabilizable and (C_2, A) is detectable.

2) D_{12} is full column rank with $\begin{bmatrix} D_{12} & D_\perp \end{bmatrix}$ unitary. $D_\perp$ is any matrix making $[\cdot]$ unitary.

3) D_{21} is full row rank with $\begin{bmatrix} D_{21} \\ \tilde{D}_{\perp} \end{bmatrix}$ unitary. $\tilde{D}_{\perp}$ is any matrix making $[\cdot]$ unitary.

4) $\begin{bmatrix} A - jwI & B_2 \\ C_1 & D_{12} \end{bmatrix}$ has full column rank for all w, (rank $= n + m_2$).

5) $\begin{bmatrix} A - jwI & B_1 \\ C_2 & D_{21} \end{bmatrix}$ has full row rank for all w, (rank $= n + p_2$).

6) $D_{22} = 0$.

Assumption *1)* is required for solutions of the controller to exist. Assumptions *2)* and *3)* include a nonsingular, normalized penalty on the control and disturbance respectively. Assumption *4)* relaxes (C_1, A) detectable and $D_{12}^T C_1 = 0$ and assumption *5)* relaxes (A, B_1) detectable and $B_1 D_{21}^T = 0$. Assumption *6)* is easily lifted using a simple coordinate transformation that yields a system with $D_{22} = 0$.

Before we continue, we need the following definition:

Definition 2.4 *Every algebraic Ricatti equation (ARE)*

$$A^T X + XA - XRX + Q = 0$$

has an associated Hamiltonian Matrix *defined as:*

$$H = \begin{bmatrix} A & -R \\ -Q & -A^T \end{bmatrix}$$

We will use the notation $X = \mathbf{Ric}(H)$ *to denote the positive semidefinite solution of the Ricatti equation such that* $A - RX$ *is stable, and* $X = X^T$.

Because of the form of the optimization problem we are solving (i.e. the $<$ rather than the $\leq$ problem), the *optimal* H_∞ controller is not obtained. Instead of minimizing the ∞-norm of the lower linear fractional transformation of our system: $\|F_l(G,K)\|_\infty$ = minimum, we solve the following suboptimal problem:

Find all controllers (if any exist) such that the closed-loop system is internally stable and the closed-loop transfer function described by the lower linear fractional transformation $F_l(P,K)$, i.e. the transfer function from the disturbance u_1 to the output y_1 satisfies the prescribed norm bound:

$$\|F_l(P,K)\|_\infty < \gamma$$

for some specified $\gamma \in \mathbf{R}$, $\gamma \geq 0$. Once a solution is obtained, γ can be decreased until the solution to one or both of the controller Ricatti equations does not exist; in the limit, the optimal H_∞ controller is approached.

To obtain the H_∞ controller, we need to perform the following operations: first partition the D_{11} matrix as follows:

$$D_{11} \triangleq \begin{bmatrix} D_{1111} & D_{1112} \\ D_{1121} & D_{1122} \end{bmatrix}$$

where, $D_{1111} \in \mathbf{R}^{(p_1-m_2)\times(m_1-p_2)}$, $D_{1112} \in \mathbf{R}^{(p_1-m_2)\times p_2}$, $D_{1121} \in \mathbf{R}^{m_2\times(m_1-p_2)}$, and $D_{1122} \in \mathbf{R}^{m_2\times p_2}$.

Now define,

$$R \triangleq D_{1\cdot}^T D_{1\cdot} - \begin{pmatrix} \gamma^2 I_{m_1} & 0 \\ 0 & 0 \end{pmatrix},$$

where,

$$D_{1\cdot} = \begin{bmatrix} D_{11} & D_{12} \end{bmatrix},$$

and,

$$\tilde{R} \triangleq D_{\cdot 1} D_{\cdot 1}^T - \begin{pmatrix} \gamma^2 I_{p_1} & 0 \\ 0 & 0 \end{pmatrix},$$

where,

$$D_{\cdot 1} = \begin{bmatrix} D_{11} \\ D_{21} \end{bmatrix}.$$

Define X_∞ and Y_∞ as solutions to the following ARE's (recall we are only interested in stabilizing solutions):

$$X_\infty = \mathbf{Ric}\left\{ \begin{pmatrix} A & 0 \\ -C_1^T C_1 & -A^T \end{pmatrix} - \begin{pmatrix} B \\ -C_1^T D_{1\cdot} \end{pmatrix} R^{-1} \begin{bmatrix} D_{1\cdot}^T C_1 & B^T \end{bmatrix} \right\}, \quad (2.14)$$

$$Y_\infty = \mathbf{Ric}\left\{ \begin{pmatrix} A^T & 0 \\ -B_1 B_1^T & -A \end{pmatrix} - \begin{pmatrix} C^T \\ -B_1 D_{\cdot 1}^T \end{pmatrix} \tilde{R}^{-1} \begin{bmatrix} D_{\cdot 1} B_1^T & C^T \end{bmatrix} \right\}, \quad (2.15)$$

and define the "state-feedback" and "output-injection" matrices as

$$F = \begin{pmatrix} F_1 \\ F_2 \end{pmatrix} = -R^{-1}[D_{1\cdot}^T C_1 + B^T X_\infty], \quad (2.16)$$

$$H = \begin{pmatrix} H_1 & H_2 \end{pmatrix} \quad (2.17)$$

$$= -[B_1 D_{\cdot 1}^T + B^T X_\infty]\tilde{R}^{-1}, \quad (2.18)$$

and,

$$F_1 = \begin{pmatrix} F_{11} \\ F_{12} \end{pmatrix} \tag{2.19}$$

$$H_1 = \begin{pmatrix} H_{11} & H_{12} \end{pmatrix} \tag{2.20}$$

where,

$$B = \begin{bmatrix} B_1 & B_2 \end{bmatrix} \tag{2.21}$$

$$C = \begin{bmatrix} C_1 \\ C_2 \end{bmatrix} \tag{2.22}$$

with F_{11}, F_{12}, and F_2 having $m_1 - p_2$, p_2, and m_2 rows, respectively, and H_{11}, H_{12}, and H_2 having $p_1 - m_2$, m_2 and p_2 columns, respectively. Note that based on assumptions *2)* and *3)* we can show that $H_1 D_{12} = H_{12}$ and $D_{21} F_1 = F_{12}$.

The main result is stated in terms of the above matrices:

Theorem 2.2 (General State-Space H_∞ Controller [26]) *For the system described in equations 2.10-2.12 and satisfying assumptions* 1) *through* 6) *on page 21:*

(a) There exists an internally stabilizing controller $K(s)$ such that $\|F_l(G,K)\|_\infty < \gamma$ if and only if:

(i) $\gamma > \max\left(\overline{\sigma}\begin{bmatrix} D_{1111}, & D_{1112} \end{bmatrix}, \overline{\sigma}\begin{bmatrix} D_{1111}^T, & D_{1121}^T \end{bmatrix}\right)$,

(ii) *there exists $X_\infty \geq 0$ and $Y_\infty \geq 0$ satisfying equations 2.14 and 2.15 such that $\rho(X_\infty Y_\infty) < \gamma^2$.*

(b) Given that the conditions of part (a) are satisfied, then all rational, internally

stabilizing controllers $K(s)$ satisfying $\|F_l(G,K)\|_\infty < \gamma$ are given by

$$K = F_l(K_a, \Phi) \text{ for arbitrary } \Phi \in RH_\infty,\ \|\Phi\|_\infty < \gamma,$$

where,

$$K_a \triangleq \left[\begin{array}{c|cc} \hat{A} & \hat{B}_1 & \hat{B}_2 \\ \hline \hat{C}_1 & \hat{D}_{11} & \hat{D}_{12} \\ \hat{C}_2 & \hat{D}_{21} & 0 \end{array}\right]$$

$$\hat{D}_{11} = -D_{1121} D_{1111}^T (\gamma^2 I - D_{1111} D_{1111}^T)^{-1} D_{1112} - D_{1122},$$

and,

$$\hat{D}_{12} \in \mathbf{R}^{m_2 \times m_2}$$
$$\hat{D}_{21} \in \mathbf{R}^{p_2 \times p_2}$$

are any matrices (i.e. Cholesky factors) satisfying:

$$\hat{D}_{12}\hat{D}_{12}^T = I - D_{1121}(\gamma^2 I - D_{1111}^T D_{1111})^{-1} D_{1121}^T,$$
$$\hat{D}_{21}^T\hat{D}_{12} = I - D_{1112}(\gamma^2 I - D_{1111} D_{1111}^T)^{-1} D_{1112}^T,$$

and,

$$\hat{B}_2 = (B_2 + H_{12})\hat{D}_{12},$$
$$\hat{C}_2 = -\hat{D}_{21}(C_2 + F_{12})Z,$$

$$\begin{aligned}
\hat{B}_1 &= -H_2 + \hat{B}_2\hat{D}_{12}^{-1}\hat{D}_{11}, \\
\hat{C}_1 &= F_2 Z + \hat{D}_{11}\hat{D}_{21}^{-1}\hat{C}_2, \\
\hat{A} &= A + HC + \hat{B}_2\hat{D}_{12}^{-1}\hat{C}_1,
\end{aligned}$$

where,

$$Z = (I - \gamma^2 Y_\infty X_\infty)^{-1}. \quad \square$$

The *central* or *maximum entropy* controller is obtained by setting $\Phi \equiv 0$. If we assume $\Phi \equiv 0$ the controller is given by:

$$K = \left[\begin{array}{c|c} \hat{A} & \hat{B}_1 \\ \hline \hat{C}_1 & \hat{D}_{11} \end{array}\right]. \tag{2.23}$$

Notice this controller has the same dimension as the original plant. This is typically the H_∞ controller used since a Φ with dynamics increases the order of the controller (which is undesirable for computational reasons) and does not affect the ∞-norm of the transfer function from u_1 to y_1 as long as $\|\Phi\|_\infty < \gamma$.

Now that we have a general controller, all we need to do is remove assumption *6)*, i.e. assume $D_{22} \neq 0$. First assume that K is a stabilizing controller for the strictly proper plant case ($D_{22} \equiv 0$), and satisfying:

$$\left\| F_l\left(P - \begin{bmatrix} 0 & 0 \\ 0 & D_{22} \end{bmatrix}, K\right)\right\|_\infty < \gamma.$$

Then,

$$F_l(G, K(I + D_{22}K)^{-1}) = G_{11} + G_{12}K(I + D_{22}K - G_{22}K)^{-1}G_{21}$$

$$= F_l\left(G - \begin{bmatrix} 0 & 0 \\ 0 & D_{22} \end{bmatrix}, K\right).$$

Hence, all controllers in this case are given by:

$$\tilde{K} = K(I + D_{22}K)^{-1},$$

which leads to

$$\tilde{K} = F_l(\tilde{K}_a, \Phi) \quad \text{for } \Phi \in RH_\infty,\ \|\Phi\|_\infty < \gamma,$$

where, assuming $\det(I + \hat{D}_{11}D_{22}) \neq 0$,

$$\tilde{K}_a \triangleq \left[\begin{array}{c|c} \hat{A} - \hat{B}(I - M)\hat{D}^{-1}\hat{C} & \hat{B}M \\ \hline \tilde{M}\hat{C} & \hat{D}M \end{array}\right]$$

with

$$M = \left[I + \begin{pmatrix} D_{22} & 0 \\ 0 & 0 \end{pmatrix}\hat{D}\right]^{-1},$$
$$\tilde{M} = \left[I + \hat{D}\begin{pmatrix} D_{22} & 0 \\ 0 & 0 \end{pmatrix}\right]^{-1}.$$

Note that when $D_{22} \neq 0$ there is a possibility of the feedback system becoming ill-posed when

$$\det(I + D_{22}\tilde{K}(\infty)) = 0.$$

This case is obviously excluded.

The results from GD [29] differ from the above controller in the terms $\hat{A}$, $\hat{B}_1$, $\hat{B}_2$, $\hat{C}_1$, and $\hat{C}_2$.

Theorem 2.3 (General State-Space H_∞ Controller [29]) *Same as Glover and Doyle [26] with the following differences:*

$$\begin{aligned}
\hat{B}_2 &= Z(B_2 + H_{12})\hat{D}_{12}, \\
\hat{C}_2 &= -\hat{D}_{21}(C_2 + F_{12}), \\
\hat{B}_1 &= -ZH_2 + \hat{B}_2\hat{D}_{12}^{-1}\hat{D}_{11}, \\
\hat{C}_1 &= F_2 + \hat{D}_{11}\hat{D}_{21}^{-1}\hat{C}_2, \\
\hat{A} &= A + BF + \hat{B}_1\hat{D}_{21}^{-1}\hat{C}_2,
\end{aligned}$$

where,

$$Z = (I - \gamma^2 Y_\infty X_\infty)^{-1}. \quad \square$$

If we assume $D_{11} \equiv 0$, the above equations (we are using the results from GD [29]) simplify considerably. These simplified equations are shown below and are the same as in Dailey [7]

A block diagram of the general H_∞ controller with $D_{11} \equiv 0$ and $D_{22} \equiv 0$ is shown in figure 2.4.

$$X_\infty = \mathbf{Ric}\begin{bmatrix} A - B_2 D_{12}^T C_1 & \gamma^{-2} B_1 B_1^T - B_2 B_2^T \\ -\tilde{C}_1^T \tilde{C}_1 & -(A - B_2 D_{12}^T C_1)^T \end{bmatrix} \tag{2.24}$$

$$Y_\infty = \mathbf{Ric}\begin{bmatrix} (A - B_1 D_{21}^T C_2)^T & \gamma^{-2} C_1^T C_1 - C_2^T C_2 \\ -\tilde{B}_1 \tilde{B}_1^T & -(A - B_1 D_{21}^T C_2) \end{bmatrix} \tag{2.25}$$

$$\tilde{B}_1 = B_1(I - D_{21}^T D_{21}) \tag{2.26}$$

$$\tilde{C}_1 = (I - D_{12} D_{12}^T) C_1 \tag{2.27}$$

$$F_1 = \gamma^{-2} B_1^T X_\infty \tag{2.28}$$

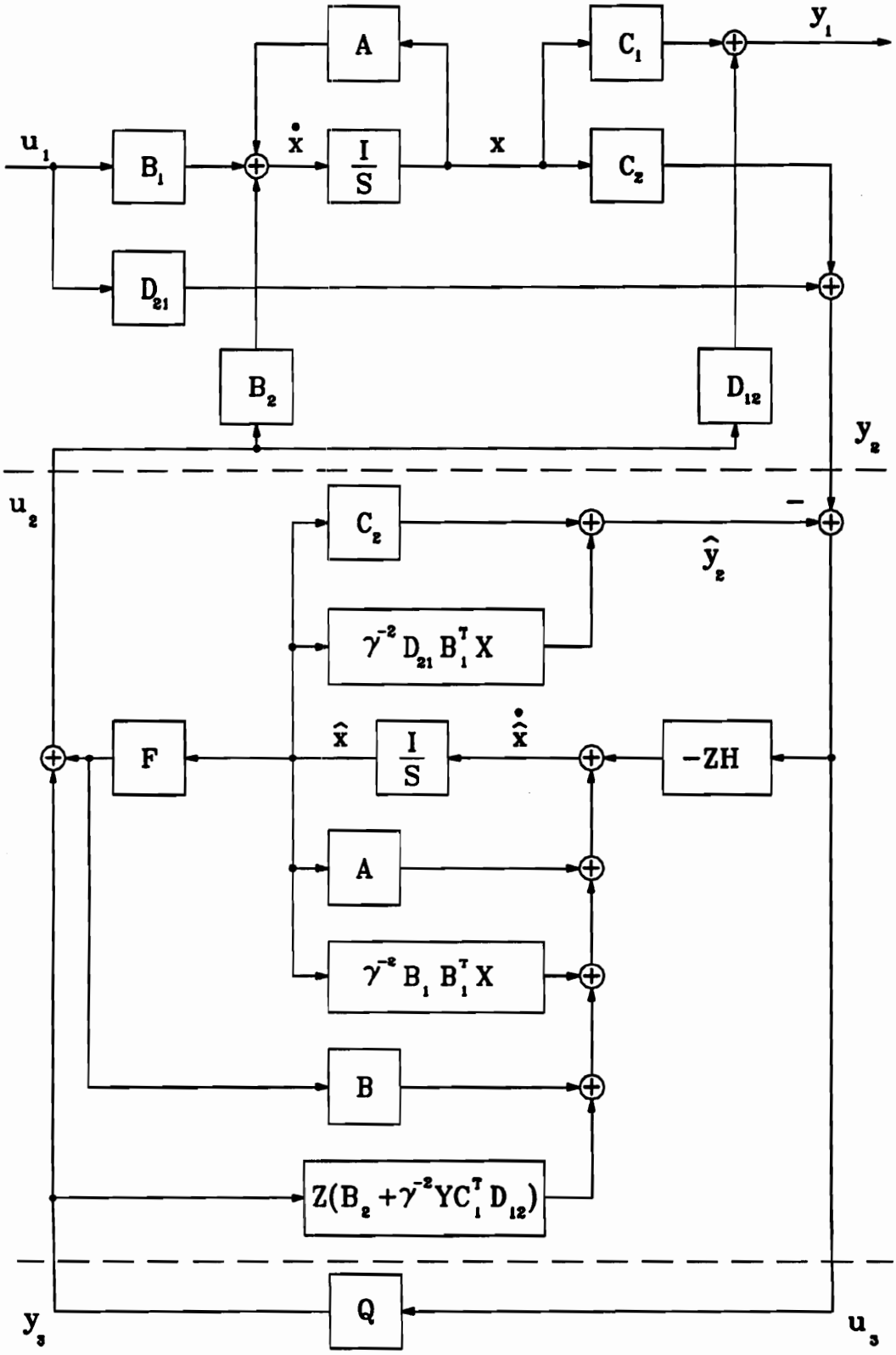

Figure 2.4: The H_∞ Controller Structure

$$F_2 = -(B_2^T X_\infty + D_{12}^T C_1) \tag{2.29}$$

$$H_1 = \gamma^{-2} Y_\infty C_1^T \tag{2.30}$$

$$H_2 = -(Y_\infty C_2^T + B_1 D_{21}^T) \tag{2.31}$$

$$Z = (I - \gamma^{-2} Y_\infty X_\infty)^{-1} \tag{2.32}$$

where $X_\infty \geq 0$, $Y_\infty \geq 0$, $\rho(XY) < \gamma^2$ and X_∞ and Y_∞ exist, i.e. their Hamiltonians have no purely imaginary eigenvalues. Note that the definitions for F_1, F_2, H_1, and H_2 in equations 2.29 and 2.31 have simplified considerably from those in equations 2.16 and 2.18 because of the assumption that $D_{11} \equiv 0$. Unless otherwise mentioned, we will assume F, and H are in the partitioned form immediately above.

Putting the simplified terms back into equation 2.23 yields a closed loop controller of the form:

$$K = \left[\begin{array}{c|c} A + B_1 F_1 + B_2 F_2 + Z H_2 (C_2 + D_{21} F_1) & -Z H_2 \\ \hline F_2 & 0 \end{array}\right] \tag{2.33}$$

Recall that these equations are only for the canonical problem that meets the restrictions *1)* through *6)* mentioned above. For the general case, we can use the loop-shifting methods presented in Safanov et al. [28] to put the system into canonical form. Note the transformations presented below will transform the system into the DGKF form. There are actually simpler transformations to transform the system into GD form. These arise because it is not necessary to zero out the D_{11} terms for the GD form of the controller equations.

The equations shown below are repeated from [7] with typographic errors corrected.

The scalings are used to transform a system so that D_{12}, D_{21}, and D_{22} are in the required form: Also see figure 2.5 for further clarification. We take the "nominal" system which does not meet the conditions required to compute a H_∞ solution and transform it into the "hat" system which does. We compute a controller $\hat{K}$ for the "hat" system and then transform it back to the original basis to obtain a K. Note this "hat" system does not correspond to the "hats" in the preceding theorems.

Step 1: Use the singular value decomposition (SVD) to factor D_{12} and D_{21}:

$$D_{12} = U_1 \begin{bmatrix} 0 \\ \Sigma_1 \end{bmatrix} V_1^T \qquad D_{21} = U_2 \begin{bmatrix} 0 & \Sigma_2 \end{bmatrix} V_2^T$$

Step 2: Scale D_{11} and partition it into a block 2×2 matrix where D_{1122} has the same dimension as D_{22}^T:

$$U_1^T D_{11} V_2 = \begin{bmatrix} D_{1111} & D_{1112} \\ D_{1121} & D_{1122} \end{bmatrix}$$

Step 3: Let $K_\infty = -(D_{1122} + D_{1121}(\gamma^{-2} I - D_{1111}^T D_{1111})^{-1} D_{1111}^T D_{1112})$.

Step 4: Let M and the transformation Θ be given by the following:

$$\begin{aligned} M &= U_1^T D_{11} V_2 + \begin{bmatrix} 0 & 0 \\ 0 & K_\infty \end{bmatrix} = \begin{bmatrix} D_{1111} & D_{1112} \\ D_{1121} & D_{1122} + K_\infty \end{bmatrix} \\ \Theta &= \begin{bmatrix} \theta_{11} & \theta_{12} \\ \theta_{21} & \theta_{22} \end{bmatrix} = \begin{bmatrix} -M & (I - \gamma^{-2} M M^T)^{1/2} \\ (I - \gamma^{-2} M^T M)^{1/2} & \gamma^{-2} M^T \end{bmatrix} \end{aligned}$$

The transformed system is currently as follows:

$$\begin{aligned} \hat{D}_{12} &= (I - \gamma^{-2} M M^T)^{-1/2} \begin{bmatrix} 0 \\ I \end{bmatrix} \\ \hat{D}_{21} &= \begin{bmatrix} 0 & I \end{bmatrix} \gamma^{-2} M^T M)^{-1/2} \end{aligned}$$

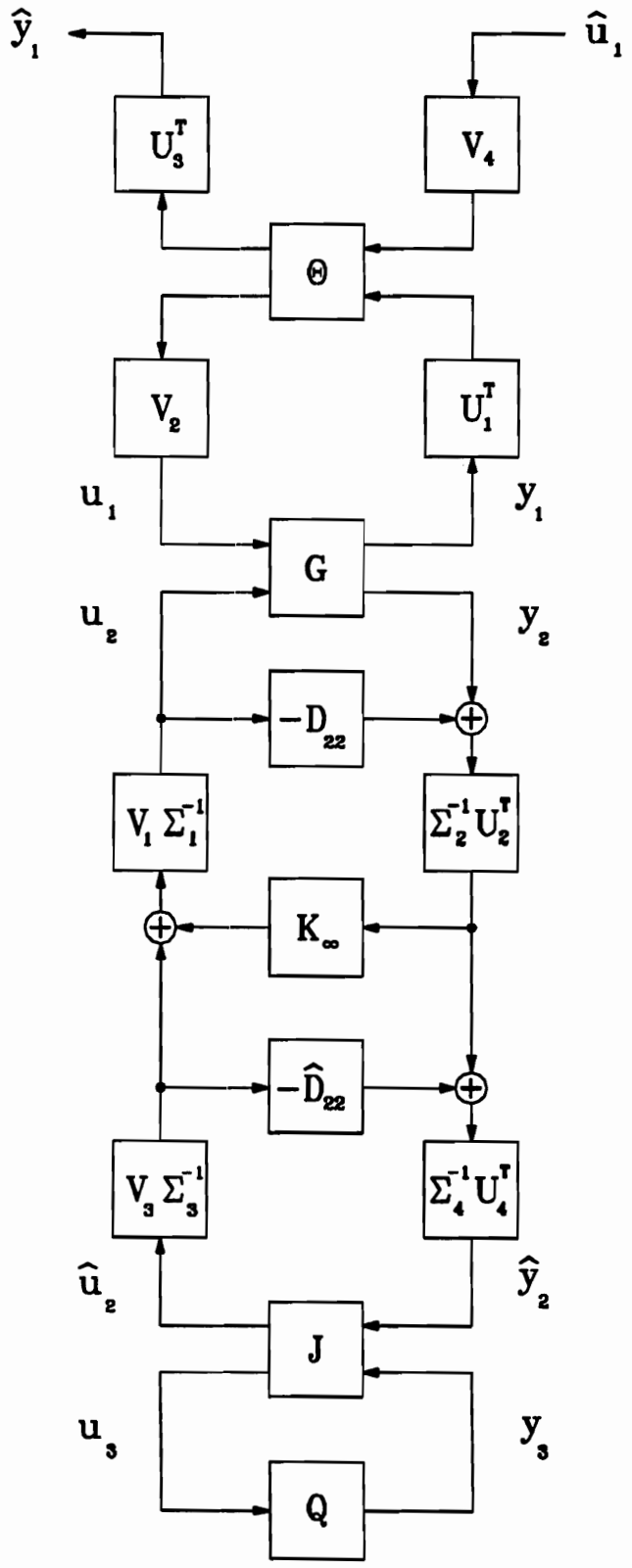

Figure 2.5: Scaling and Loop Shifting Operations for H_∞ Synthesis

$$\hat{D}_{22} = \begin{bmatrix} 0 & I \end{bmatrix} \gamma^{-2} M^T (I - \gamma^{-2} M M^T)^{-1/2} \begin{bmatrix} 0 \\ I \end{bmatrix}$$

Step 5: Use the SVD to factor $\hat{D}_{12}$ and $\hat{D}_{21}$:

$$\hat{D}_{12} = U_3 \begin{bmatrix} 0 \\ \Sigma_3 \end{bmatrix} V_3^T$$
$$\hat{D}_{21} = U_4 \begin{bmatrix} 0 & \Sigma_4 \end{bmatrix} V_4^T$$

Now we have all of the transformations computed. This will transform the "nominal" system to the "hat" system as shown in figure 2.5. We can now group the transformations together to simplify the necessary operations.

The transformation from $\hat{u}_1$ and y_1 to $\hat{y}_1$ and u_1 using the T_1 transformation matrix is given by:

$$\begin{pmatrix} \hat{y}_1 \\ u_1 \end{pmatrix} = \begin{bmatrix} T_{111} & T_{112} \\ T_{121} & T_{122} \end{bmatrix} \begin{pmatrix} \hat{u}_1 \\ y_1 \end{pmatrix} \tag{2.34}$$

where,

$$T_{111} = -U_3^T M V_4 \tag{2.35}$$
$$T_{112} = U_3^T (I - \gamma^{-2} M M^T)^{1/2} U_1^T \tag{2.36}$$
$$T_{121} = V_2 (I - \gamma^{-2} M^T M)^{1/2} V_4 \tag{2.37}$$
$$T_{122} = \gamma^{-2} V_2 M^T U_1^T \tag{2.38}$$

And the transformation from $\hat{u}_2$ and y_2 to $\hat{y}_2$ and u_2 using the T_2 transformation matrix is given by:

$$\begin{pmatrix} u_2 \\ \hat{y}_2 \end{pmatrix} = \begin{bmatrix} T_{211} & T_{212} \\ T_{221} & T_{222} \end{bmatrix} \begin{pmatrix} y_2 \\ \hat{u}_2 \end{pmatrix} \tag{2.39}$$

where,

$$T_{211} = V_1\Sigma_1^{-1}K_\infty\Sigma_2^{-1}U_2^T(I - L_1)^{-1} \tag{2.40}$$

$$T_{212} = V_1\Sigma_1^{-1}(I - L_2)^{-1}V_3\Sigma 3^{-1} \tag{2.41}$$

$$T_{221} = \Sigma_4^{-1}U_4^T\Sigma_2^{-1}U_2^T(I - L_1)^{-1} \tag{2.42}$$

$$T_{222} = -\Sigma_4^{-1}U_4^T[\Sigma_2^{-1}U_2^T D_{22}V_1\Sigma_1^{-1}(I - L_2)^{-1} + \hat{D}_{22}]V_3\Sigma_3^{-1} \tag{2.43}$$

$$L_1 = -D_{22}V_1\Sigma_1^{-1}K_\infty\Sigma_2^{-1}U_2^T \tag{2.44}$$

$$L_2 = -K_\infty\Sigma_2^{-1}U_2^T D_{22}V_1\Sigma_1^{-1} \tag{2.45}$$

One a controller has been found for the "hat" system, we can compute the controller K for the original system by:

$$K = F_l(T_2, \hat{K})$$

Since the advent of these state-space synthesis procedures for H_∞ problems, much of the resent research has been on minor refinements to eliminate numerical difficulties [31, 32], the development of discrete-time synthesis methods [33, 34], mixed H_2 and H_∞ techniques [35, 36, 37], and real-parameter plant perturbations instead of the norm-bounded plant perturbations mentioned previously [38, 39]. Additionally, algebraic derivations of the H_∞ controller equations have also been developed. Zhou et al. [40] gave an algebraic Riccati equation approach for the state feedback case. Sampei et al. [41] extended these results for the output feedback case. What is

noteworthy in this last paper is that the algebraic derivation yields equations that have no rank conditions on either D_{12} or D_{21}. This yields a solution to the input port mixed sensitivity control problem when $D_{21} = 0$. A similar algebraic Riccati equation approach to the non-singular H_∞ problem using many of the results from Zhou and Sampei is presented in [42]. Additionally, assumptions *2)* and *3)* are relaxed from the GD derivation. This formulation will be covered in more detail in the sequel.

There has not been a lot of emphasis on the use of the H_∞ paradigm for disturbance rejection problems. Part of the reluctance to use H_∞ for disturbance rejection problems is the fact that H_∞ treats the worst case rejection rather than the mean-square rejection like the LQG case; however, in the sequel, we will show that in some cases, this behavior is beneficial. Makila [43] shows the results for periodic and almost periodic disturbance signals in an H_∞ setting. Kawatani et al. [44] point out some fundamental properties on the structure of H_∞ controllers with regard to disturbance estimation. They also comment on the relation of the H_∞ controller to LQ game theory cost functions.

There is also a lack of papers that discuss any actual experiments. Fujita et al. [45] also mention the lack of experimental evaluations using H_∞ and cite only three experimental papers in the current literature. Their paper deals with a H_∞ magnetic suspension disturbance attenuation control. Unfortunately, they only treat the case of a step disturbance instead of a Gaussian noise disturbance. Additionally, since an open-loop magnetic suspension makes no sense, they show how various plant perturbations affect the closed-loop stability of their controller.

In one of the other experimental papers, Balas and Doyle [46] analyze performance and robustness tradeoffs for a flexible structure controller. They show that the assumed errors in the plant are critical to stability. In fact, in one set of experiments, five out of six controllers were unstable. They also show the difficulty of using the finite element method to develop a plant model for the control system synthesis even when fitting the model to experimental data.

2.4 Performance and Robustness Using Mu

The previous sections detailed nominal H_∞ controller design. Unfortunately, the "standard" problem formulation makes it difficult to satisfy specified robustness margins simultaneously at the input and the output. We should note that this is also a problem with the LQG/LTR (Linear Quadratic Gaussian with Loop Transfer Recovery) approach. A solution to the problem is to use the H_∞ design procedure to minimize the (weighted) gain from signals injected at both the sensors and actuators to signals measured at both the sensors and actuators. If more than a single block perturbation is used, it is necessary to use μ to perform the stability analysis. A block diagram of a typical plant-controller-perturbation block diagram is shown in Figure 2.6.

The μ-analysis problem is to design a controller, K, so that $\|\mu(F_l(G,K))\|_\infty < 1$. An outline of the μ-synthesis procedure is presented in [7]. We will briefly summarize this material below.

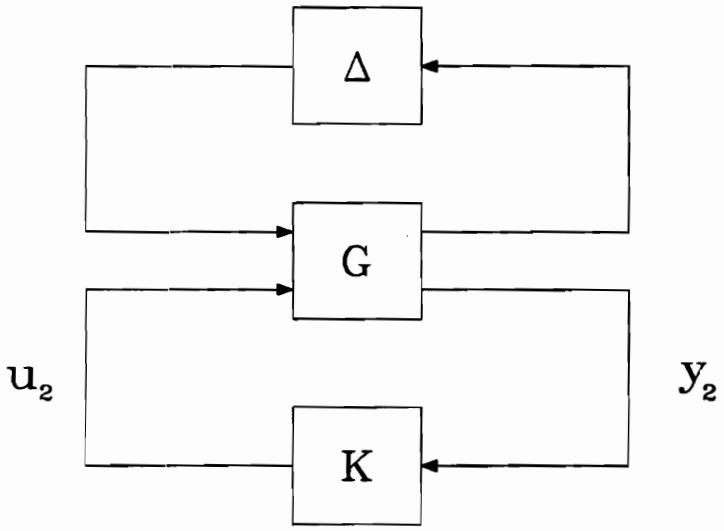

Figure 2.6: Typical Plant-Controller-Perturbation Interconnection Structure

Doyle [23] gave some general theorems on the properties of μ. The most important property for general μ-analysis is that:

$$\mu(M) \leq \overline{\sigma}(D(s)M(s)D^{-1}(s)) \tag{2.46}$$

for any diagonal matrix D that is compatible with the block perturbation $\Delta = \text{diag}(\Delta_1, \ldots, \Delta_n)$. When the scaling matrix D is optimized to minimize $\overline{\sigma}(DMD^{-1})$, the upper bound can be quite tight. In fact, equation 2.46 is an equality when there are three or fewer Δ_i blocks.

The strategy behind μ-synthesis is to pick stable diagonal transfer matrices, $D(s)$, with stable inverses, then to use H_∞-synthesis to compute controllers K which minimize $\|DF_l(G,K)D^{-1}\|_\infty$. The D weighting matrices can be either constants or they may have dynamics. If D matrices are chosen with dynamics, there will be a

corresponding increase in the dimension of the controller.

Mu-synthesis is a two step iterative process called D-K iteration:

Step 1: Pick a diagonal $D(s)$ such that $D(s)$ and $D^{-1}(s)$ are stable and so that the upper bound $\overline{\sigma}(DF_l(G,K)D^{-1})$ is minimized (approximately) over frequency. On the first iteration when K is unknown, choose $D = I$.

Step 2: Use H_∞-synthesis to find a controller $K(s)$ which minimizes the scaled systems ∞-norm $\|DF_l(G,K)D^{-1}\|_\infty$. Go back to step 1 and repeat until $\|\mu(F_l(G,K)\|_\infty < 1$ or until no further reduction in μ is achieved. Note that the D-K iteration is not guaranteed to converge to the global minimum.

There is commercial software now available to solve both the continuous-time H_∞ design and μ-synthesis problems [47]. This toolbox is designed to be used with the MATLAB software package and since the script files are provided, modifications can be made by the user.

Chapter 3

On the Behavior of Optimal State-Space Controllers

The asymptotic and estimation behavior of both H_2 and H_∞ controllers is discussed in this chapter. While the results for the H_2 case are well known, the estimator structure of the H_∞ controllers has not been presented in the literature. We will show that the H_∞ controller is not a state estimator like the H_2 (LQG) controller. Three special cases for the H_∞ controller will be presented in an effort to determine the behavior of the compensator. Some possible interpretations of the behavior of the H_∞ controllers are discussed. In an effort to streamline the discussion of both types of controllers, we will treat both the general H_∞ controller cases and then by letting $\gamma \to \infty$ recover the H_2 case.

We will also discuss the connections of the H_∞ central controllers to Linear Quadratic (LQ) Differential Games and show how some of the common H_∞ terminology can be confusing in terms of the actual behavior of the compensator.

Additionally, we discuss the behavior of systems augmented to account for disturbance dynamics (prefilters). The estimation structure of these systems will be

discussed.

3.1 The Central Controllers

In order to simplify the notation, and since we do not, in general, measure external disturbances, we will assume $D_{11} = 0$. Also, since we want the central controller, we will assume $\Phi = 0$ and without loss of generality (wlog), assume $D_{22} = 0$.

As was mentioned in the previous chapter, there are two different forms for the H_∞ state-space controllers. These two forms arise from a duality argument in terms of the plant formulation [30]. The dual problem used to generate the two different H_∞ controllers is merely to transpose the open-loop plant in a sense to be made clear below. First, define the nominal plant with the above restrictions:

$$G_i \triangleq \left[\begin{array}{c|cc} A & B_1 & B_2 \\ \hline C_1 & 0 & D_{12} \\ C_2 & D_{21} & 0 \end{array}\right] \tag{3.1}$$

and the transpose plant is defined as:

$$G_o \triangleq \left[\begin{array}{c|cc} A^T & C_1^T & C_2^T \\ \hline B_1^T & 0 & D_{21}^T \\ B_2^T & D_{12}^T & 0 \end{array}\right]. \tag{3.2}$$

Using the appropriate transformations, equation 3.1 yields the controller from Glover and Doyle [29], and equation 3.2 yields the controller from Glover and Doyle [26].

The previous H_∞ controller results can be extended slightly by weakening two of the assumptions concerning the form of the plant. In Petersen et al. [42], assumptions

2) and *3)* from GD are relaxed somewhat. Petersen only treats the plant form given in equation 3.1, but the results are easily extended to the plant form in equation 3.2 and are provided below.

The relaxed assumptions pertain to the scaling of the D_{12} and D_{21} matrices and introduce two extra coefficients into the Riccati equations and the H_∞ central controllers. The "relaxed" assumptions obviate the need for some the loop transformations used in Safanov et al. [28]. Both forms of the more general H_∞ compensators are presented below.

The new assumptions on D_{12} and D_{21} are,

2b) $D_{12}^T D_{12} \triangleq E_1 > 0$

3b) $D_{21} D_{21}^T \triangleq E_2 > 0.$

Practically, these rank conditions imply:

1) number of outputs in $y_1 \geq$ number of inputs in u_2

2) number of inputs in $u_1 \geq$ number of outputs in y_2.

The modified Hamiltonian matrices along with the updated controller coefficients are as follows:

$$\begin{aligned} X_\infty &= \mathbf{Ric} \begin{bmatrix} A - B_2 E_1^{-1} D_{12}^T C_1 & \gamma^{-2} B_1 B_1^T - B_2 E_1^{-1} B_2^T \\ -C_1^T (I - D_{12} E_1^{-1} D_{12}^T) C_1 & -(A - B_2 E_1^{-1} D_{12}^T C_1)^T \end{bmatrix} \\ &\triangleq \mathbf{Ric}(H_{X_\infty}) \end{aligned} \tag{3.3}$$

$$Y_\infty = \mathbf{Ric} \begin{bmatrix} (A - B_1 D_{21}^T E_2^{-1} C_2)^T & \gamma^{-2} C_1^T C_1 - C_2^T E_2^{-1} C_2 \\ -B_1 (I - D_{21}^T E_2^{-1} D_{21}) B_1^T & -(A - B_1 D_{21}^T E_2^{-1} C_2) \end{bmatrix}$$

$$\triangleq \mathbf{Ric}(H_{Y_\infty}) \tag{3.4}$$

$$F_1 = \gamma^{-2} B_1^T X_\infty \tag{3.5}$$

$$F_2 = -(B_2^T X_\infty + D_{12}^T C_1) \tag{3.6}$$

$$H_1 = \gamma^{-2} Y_\infty C_1^T \tag{3.7}$$

$$H_2 = -(Y_\infty C_2^T + B_1 D_{21}^T) \tag{3.8}$$

$$Z = (I - \gamma^{-2} Y_\infty X_\infty)^{-1} \tag{3.9}$$

Using the naming convention (which we will show later to be misleading) and the general procedure in Hvostov et al. [30], we define the two H_∞ central controllers in terms of their estimator structure. The *exogenous input* H_∞ controller has the following form:

$$K_i = \left[\begin{array}{c|c} A + B_1 F_1 + B_2 E_1^{-1} F_2 + Z H_2 E_2^{-1}(C_2 + D_{21} F_1) & -Z H_2 E_2^{-1} \\ \hline E_1^{-1} F_2 & 0 \end{array}\right] \tag{3.10}$$

$$\triangleq \left[\begin{array}{c|c} \hat{A}_i & \hat{B}_i \\ \hline \hat{C}_i & 0 \end{array}\right] \tag{3.11}$$

and the *controlled output* H_∞ controller is given by:

$$K_o = \left[\begin{array}{c|c} A + H_1 C_1 + H_2 E_2^{-1} C_2 + (H_1 D_{12} + B_2) E_1^{-1} F_2 Z & -H_2 E_2^{-1} \\ \hline E_1^{-1} F_2 Z & 0 \end{array}\right] \tag{3.12}$$

$$\triangleq \left[\begin{array}{c|c} \hat{A}_o & \hat{B}_o \\ \hline \hat{C}_o & 0 \end{array}\right] \tag{3.13}$$

where F_1, F_2, H_1, and H_2 are from the equations 3.5-3.8 respectively.

The naming convention for the H_∞ controllers becomes more clear if we write the

formulae in a form similar to the LQG optimal controller. For K_i we obtain:

$$\dot{\hat{x}} = A\hat{x} + B_1\hat{u}_1 + B_2u_2 + ZH_2E_2^{-1}(\hat{y}_2 - y_2) \tag{3.14}$$

$$\hat{u}_1 = F_1\hat{x} \tag{3.15}$$

$$u_2 = E_1^{-1}F_2\hat{x} \tag{3.16}$$

$$\hat{y}_1 = 0 \tag{3.17}$$

$$\hat{y}_2 = C_2\hat{x} + D_{21}\hat{u}_1. \tag{3.18}$$

and for K_o we obtain:

$$\dot{\hat{x}} = A\hat{x} + B_2u_2 + \begin{pmatrix} H_1 & H_2E_2^{-1} \end{pmatrix} \left(\begin{bmatrix} \hat{y}_1 \\ \hat{y}_2 \end{bmatrix} - \begin{bmatrix} 0 \\ y_2 \end{bmatrix} \right) \tag{3.19}$$

$$\hat{u}_1 = 0 \tag{3.20}$$

$$u_2 = E_1^{-1}F_2Z\hat{x} \tag{3.21}$$

$$\hat{y}_1 = C_1\hat{x} + D_{12}u_2 \tag{3.22}$$

$$\hat{y}_2 = C_2\hat{x} \tag{3.23}$$

From this, we can see that the estimator structure for each H_∞ controller is different. In some sense, the *exogenous input* controller generates an "estimate" of the exogenous plant input, $\hat{u}_1$, based on the knowledge of the "plant state estimate," $\hat{x}$. The *controlled output* controller functions in a dual manner to the controller above in that the controlled output, $\hat{y}_1$, is "estimated" from the knowledge of the "plant state estimate".

The reason $\hat{u}_1 = F_1\hat{x}$ is called an "estimate" of the external disturbance, u_1, is because of the relation of the H_∞ controller to Linear Quadratic (LQ) differential

game theory. It turns out that calling $\hat{u}_1$ an estimate of the exogenous input and $\hat{y}_1$ an estimate of the controlled outputs is really a misnomer. We will touch on this in more detail below.

We put "plant state estimate" in quotation marks in the above section because the H_∞ controller does not really estimate the plant states like the LQG controller (we will show this below). Also, most (if not all) of the literature treats the controller states as estimates of the plant states. The literature also contains references to the separation structure of the H_∞ controllers as being analogous to the LQG controller; however, the separation occurs in a transformed (affine) coordinate system that merely preserves the infinity-norm of the closed-loop system. These subtleties do not seem to be widely appreciated in the literature.

Before we proceed to show that the H_∞ controllers are not state estimators, we need the following lemmas.

Lemma 3.1 (Petersen et al. [42]) *The matrix $A + ZH_2E_2^{-1}C_2$ is a stability matrix.*

Lemma 3.2 (Petersen et al. [42]) *The matrix $A + H_2E_2^{-1}C_2$ is a stability matrix.*

Proposition 3.3 *Both forms of the H_∞ controllers do not yield plant state estimates.*

Proof:

Case 1: *Exogenous input "estimation", K_i:*

Define the error between the plant and the controller states to be $e \triangleq x - \hat{x}$. *The plant and controller equations are as follows:*

$$\dot{x} = Ax + B_1 u_1 + B_2 u_2 \tag{3.24}$$

$$y_2 = C_2 x + D_{21} u_1 \tag{3.25}$$

$$\dot{\hat{x}} = \left[A + B_1 F_1 + B_2 F_2 + Z H_2 E_2^{-1}(C_2 + D_{21} F_1)\right] \hat{x} - Z H_2 E_2^{-1} y_2 \tag{3.26}$$

$$u_2 = E_1^{-1} F_2 \hat{x} \tag{3.27}$$

Solving the above equations for $\dot{e}$ *yields:*

$$\dot{e} = (A + Z H_2 E_2^{-1} C_2) e + (B_1 + Z H_2 E_2^{-1} D_{21})(u_1 - \hat{u}_1).$$

If we set the external disturbance $u_1 \equiv 0$ *we find:*

$$\dot{e} = (A + Z H_2 E_2^{-1} C_2) e - (B_1 + Z H_2 E_2^{-1} D_{21}) \hat{u}_1.$$

From Lemma 3.1 we see that the error is asymptotically stable. We can also see that if

$$x \equiv \hat{x} \neq 0 \;\Rightarrow\; \dot{e} \neq 0$$

$$\Rightarrow\; x \neq \hat{x}$$

unless $x = \hat{x} \equiv 0 \quad \forall\, t$. *This clearly indicates that the* H_∞ *compensator does not yield state estimates.*

The forcing function for the error dynamics is proportional to the magnitude of the

controller states, $\hat{x}$. We cannot make any general statements about the magnitude of the coefficient of $\hat{u}_1$, so we cannot, in general, conclude that the forcing term on the error equation is small.

Another way to look at the error dynamics in an effort to understand the behavior of the H_∞ controller is to look at the closed loop system. The closed-loop system can be shown to be:

$$\begin{pmatrix} \dot{x} \\ \dot{\hat{x}} \end{pmatrix} = \begin{bmatrix} A & B_2\hat{C}_i \\ \hat{B}_iC_2 & \hat{A}_i \end{bmatrix} \begin{pmatrix} x \\ \hat{x} \end{pmatrix} + \begin{bmatrix} B_1 \\ \hat{B}_iD_{21} \end{bmatrix} u_1 \tag{3.28}$$

$$y_1 = \begin{bmatrix} C_1 & D_{12}\hat{C}_i \end{bmatrix} \begin{pmatrix} x \\ \hat{x} \end{pmatrix} \tag{3.29}$$

where the terms are as previously defined.

If we use the error, $e \triangleq x - \hat{x}$, as a change of variables for the closed-loop system, we obtain:

$$\begin{aligned} \begin{pmatrix} \dot{x} \\ \dot{e} \end{pmatrix} &= \begin{bmatrix} A + B_2\hat{C}_i & -B_2\hat{C}_i \\ A - \hat{A}_i + \hat{B}_iC_2 - \hat{B}_iC_2 & \hat{A}_i - B_2\hat{C}_i \end{bmatrix} \begin{pmatrix} x \\ e \end{pmatrix} \\ &\quad + \begin{bmatrix} B_1 \\ B_1 - \hat{B}_iD_{21} \end{bmatrix} u_1 \end{aligned} \tag{3.30}$$

$$y_1 = \begin{bmatrix} C_1 + D_{12}\hat{C}_i & -D_{12}\hat{C}_i \end{bmatrix} \begin{pmatrix} x \\ e \end{pmatrix}. \tag{3.31}$$

Setting $u_1 \equiv 0$ as before and using the results from Petersen et al. [42] that show both closed-loop forms are asymptotically stable, we see that the plant states and the estimator error are asymptotically stable, but the previous analysis shows that they are not stable at the same rate.

Case 2: *Controlled Output "Estimation", K_o:*

The plant and controller equations are as follows:

$$\dot{x} = Ax + B_1u_1 + B_2u_2 \tag{3.32}$$

$$y_2 = C_2x + D_{21}u_1 \tag{3.33}$$

$$\dot{\hat{x}} = [A + H_1C_1 + H_2E_2^{-1}C_2 + (H_1D_{12} + B_2)E_1^{-1}F_2Z]\hat{x} - H_2E_2^{-1}y_2 \tag{3.34}$$

$$u_2 = E_1^{-1}F_2Z\hat{x} \tag{3.35}$$

Solving the above equations for $\dot{e}$ yields:

$$\dot{e} = (A + H_2E_2^{-1}C_2)e + (B_1 + H_2E_2^{-1}D_{21})u_1 + H_1\hat{y}_1. \tag{3.36}$$

If we set $u_1 \equiv 0$ we find:

$$\dot{e} = (A + H_2E_2^{-1}C_2)e - H_1\hat{y}_1. \tag{3.37}$$

Using Lemma 3.2 and the previous arguments from case 1, we see that the error is asymptotically stable and that this form of the H_∞ compensator does not yield state-estimates. □

We should also note that the error dynamics differ for each form of the H_∞ compensator.

To show that we can recover the LQG controller from both H_∞ formulations, we let

$\gamma \to \infty$. We can easily see that:

$$\lim_{\gamma\to\infty} F_1 = 0 \tag{3.38}$$

$$\lim_{\gamma\to\infty} H_1 = 0 \tag{3.39}$$

$$\lim_{\gamma\to\infty} Z = I \tag{3.40}$$

$$\lim_{\gamma\to\infty} \hat{y}_1 = 0 \tag{3.41}$$

$$\lim_{\gamma\to\infty} \hat{u}_1 = 0 \tag{3.42}$$

and the controller becomes

$$K_{H_2} = \left[\begin{array}{c|c} A + B_2E_1^{-1}F_2 + H_2E_2^{-1}C_2 & -H_2E_2^{-1} \\ \hline E_1^{-1}F_2 & 0 \end{array}\right] \tag{3.43}$$

and the error dynamics are given by

$$\dot{e} = (A + H_2E_2^{-1}C_2)e + (B_1 + H_2E_2^{-1}D_{21})u_1 \tag{3.44}$$

which when we assume no external disturbance, i.e. $u_1 \equiv 0$, the error is asymptotically stable and shows the controller states are estimates of the plant states which is the expected result. The non-standard, extra E_1^{-1} and E_2^{-1} terms appear in the LQG result because of the assumed scaling on D_{21}. Without loss of generality, we can let $E_1^{-1} = I$, $E_2^{-1} = I$ and recover the standard LQG formulation. Note that the error equation for the LQG case has the same dynamics as the output estimation H_∞ compensator.

What is also interesting to note is that the LQG compensator and its dual (in terms of the transpose problem posed above) are identical. This indicates there is an

asymmetry to the H_∞ compensators, i.e. K_i attempts to construct an "estimate" (in a sense to be made clear below) of the external disturbance, and K_o attempts to "estimate" the controlled output. Since the H_2 controller has access to entire plant output, y_1 and y_2, because of the trivial embedding of the the measurement, y_2, in the performance index, the H_2 controller does not attempt to reconstruct an estimate of the exogenous input. Hvostov treats the Z term as a "penalty" of the incomplete knowledge of the system outputs when compared to the complete output knowledge in the H_2 case. The special cases presented below attempt to explain this behavior in a limited context.

We notice that both H_∞ controllers satisfy the frequency domain constraint:

$$\|T_{u_1 y_1}\|_\infty < \gamma$$

where $T_{u_1 y_1}$ is the closed loop transfer function from u_1 to y_1. What is not clear is how the time domain behavior of each H_∞ formulation differs. Since we have shown that the H_∞ controllers do not estimate the plant states, it is difficult to extrapolate some assumed behavior based on the behavior of the LQG controller.

3.2 Special Cases

This section deals with three special cases of the central controllers discussed by Hvostov that yield some interesting closed-loop behavior. By assuming the plant has a particular form, we can simplify the closed-loop system and make some inferences on the behavior of the H_∞ controller. Before we proceed, we require the following

lemmas.

Lemma 3.4 (Hvostov et al. [30]) *Assume that D_{21}^{-1} exists and that $A - B_1 D_{21}^{-1} C_2$ is a stability matrix. Then the output injection Hamiltonian matrix H_{Y_∞} is upper block triangular and $Y_\infty \equiv 0$.*

Lemma 3.5 (Hvostov et al. [30]) *Assume that D_{12}^{-1} exists and that $A - B_2 D_{12}^{-1} C_1$ is a stability matrix. Then the state feedback Hamiltonian matrix H_{X_∞} is upper block triangular and $X_\infty \equiv 0$.*

Case 1: Assume D_{21}^{-1} exists. We can assume, wlog, that $D_{21} = I$, $E_1 = I$, $E_2 = I$, and, since D_{21} is invertible, we can solve for the unmeasurable disturbance, u_1, in terms of known quantities:

$$y_2 = C_2 x + D_{21} u_1 \quad \Rightarrow \quad u_1 = D_{21}^{-1} y_2 - D_{21}^{-1} C_2 x.$$

We can now plug u_1 into the original plant equation and we get:

$$\begin{aligned} \dot{x} &= (A - B_1 D_{21}^{-1} C_2) x - B_1 D_{21}^{-1} y_2 + B_2 u_2 \\ &= (A - B_1 C_2) x - B_1 y_2 + B_2 u_2. \end{aligned}$$

From Lemma 3.4, the controller coefficients simplify to:

$$\begin{aligned} Y_\infty &= 0 \\ H_1 &= 0 \\ H_2 &= -B_1 \\ Z &= I \end{aligned}$$

and both forms of the H_∞ controllers simplify under the previous assumptions to the following:

$$\begin{aligned}\dot{\hat{x}} &= (A + B_2F_2 + H_2C_2)\hat{x} - H_2y_2 \\ &= (A + B_2F_2 - B_1C_2)\hat{x} - B_1y_2\end{aligned}$$

If we now solve for the error, we get:

$$\dot{e} = (A - B_1C_2)e$$

which under the conditions of Lemma 3.1 is asymptotically stable and yields a state estimate. Note that Lemmas 3.1 and 3.2 are identical under the assumptions above ($Z = I$). One thing interesting about the error dynamics above is that we have made no assumptions on the external disturbance, u_1. There is no forcing term on the error dynamics in this case.

The invertibility of D_{21} gives us complete information of the plant output and disturbance based only on the measurement, y_2. In terms of the previous controllers, the weighting on $\hat{y}_1$ is zero, and the controller makes no attempt to "estimate" the disturbance input, $\hat{u}_1 = 0$.

We should note that this case corresponds to the Disturbance Feedforward case presented in Doyle et al. [27].

Case 2: Assume D_{12}^{-1} exists. We can again assume, wlog, that $D_{12} = I$, $E_1 = I$, $E_2 = I$, and, since D_{12} is invertible, we can solve for a control input, u_2 from the controlled output equation:

$$u_2 = D_{12}^{-1}(y_1 - C_1 x).$$

We choose $y_1 \equiv 0$ since we want to minimize the controlled output, and since we don't know x, we can use $\hat{x}$ even though we have shown it is not, in general, a state estimate. This yields

$$u_2 = -C_1 \hat{x}.$$

We can now plug u_2 and $y_1 = 0$ into the original plant equation and we get:

$$\begin{aligned} \dot{x} &= Ax + B_1 u_1 - B_2 D_{12}^{-1} C_1 \hat{x} \\ &= Ax + B_1 u_1 - B_2 C_1 \hat{x} \end{aligned}$$

Under the assumptions of Lemma 3.5, the controller coefficients simplify to:

$$\begin{aligned} X_\infty &= 0 \\ F_1 &= 0 \\ F_2 &= -C_1 \\ Z &= I \end{aligned}$$

and both forms of the H_∞ controllers simplify under the previous assumptions to the following:

$$\begin{aligned}\dot{\hat{x}} &= (A + B_2F_2 + H_2C_2)\hat{x} - H_2y_2 \\ &= (A + B_2F_2 - B_1C_2)\hat{x} + B_1(C_2x + D_{21}u_1).\end{aligned}$$

If we now solve for the error, we get:

$$\dot{e} = (A - B_1C_2)e + (B_1 - B_1D_{21})u_1$$

which under the conditions of Lemma 3.1 is asymptotically stable and gives state estimates. Note that the error in this case has a forcing function proportional to u_1. Also, we have "forced" the controlled output to be exactly 0 in this case, independent of any external disturbance. That is given any arbitrary forcing function, $u_1 \neq 0$, we obtain $y_1 \equiv 0$.

The invertibility of D_{12} lets us choose a control signal to zero the controlled output; however, since we do not know the state, we can only use the best approximation, $\hat{x}$. Fortunately, under the assumed conditions, we do have a state estimator. In terms of the previous controllers, $\hat{u}_1 \equiv 0$, that is the controller makes no attempt to "estimate" the disturbance input, and the "estimate" of the controlled output is trivially cancelled.

Note that this case corresponds to the Doyle et al. [27] Output Estimation case.

Case 3: Suppose both Lemma 3.4 and Lemma 3.5 hold. In this case, both the disturbance and control can be obtained from the measurement. Assuming that $D_{12} = I$, $D_{21} = I$, and $y_1 = 0$ as presented above, we obtain:

$$\begin{aligned} y_1 = C_1 x + D_{12} u_2 \quad &\Rightarrow \quad u_2 = -C_1 x \\ y_2 = C_2 x + D_{21} u_1 \quad &\Rightarrow \quad u_1 = y_2 - C_2 x. \end{aligned}$$

Now, both $X_\infty = 0$ and $Y_\infty = 0$ gives the controller coefficients:

$$\begin{aligned} X_\infty &= 0 \\ Y_\infty &= 0 \\ F_1 &= 0 \\ H_1 &= 0 \\ F_2 &= -C_1 \\ H_2 &= -B_1 \\ Z &= I \end{aligned}$$

Plugging into the plant equation yields:

$$\dot{x} = (A - B_1 C_2)x + B_1 y_2 - B_2 C_1 \hat{x}$$

and the controller becomes:

$$\begin{aligned} \dot{\hat{x}} &= (A - B_2 C_1 - B_1 C_2)\hat{x} + B_1 y_2 \\ &= (A - B_2 C_1 - B_1 C_2)\hat{x} + B_1 (C_2 + D_{21} u_1). \end{aligned}$$

Solving for the error gives:

$$\dot{e} = (A - B_1 C_2)e.$$

which from Lemma 3.1 is asymptotically stable.

Based on the assumptions for this case, we see that we obtain asymptotic error behavior regardless of disturbance, u_1, and $y_1 \equiv 0$ which implies that $\|T_{u_1 y_1}\|_\infty \equiv 0$ which says we can cancel any external disturbance exactly.

Based on the literature, it would seem that the H_∞ compensators try to "estimate" either the exogenous input or the controlled output and are penalized by Z on the incomplete knowledge of the system behavior. Perhaps a more realistic way to look at the controller behavior is to think of what it is trying to accomplish. The H_∞ controller minimizes the maximum singular value of the closed-loop transfer function from u_1 to y_1. The way it does this is to increase the singular value of the closed-loop transfer function where it is has a small magnitude and decrease it where it is large. This gives the characteristic "flat" singular value response of the closed-loop system. The so called exogenous input and controlled output "estimates" are just the extra terms the closed loop dynamics need to cause this flat singular value response. Stating that the compensator "estimates" certain quantities when clearly, it does not is merely misleading. This is discussed in more detail in the section below.

3.3 Some Comments on LQ Game Theory and the H_∞ Central Controllers

In this section we discuss the connections between the H_∞ central controllers and LQ game theory. The discussion is somewhat brief and ignores many of the details. We want to use the LQ game theory results to show that we can obtain arbitrarily poor estimates of the exogenous input from the H_∞ central controller formulation.

Consider a zero-sum differential game with plant dynamics

$$\dot{x} = Ax + B_1 u_1 + B_2 u_2 \tag{3.45}$$

and a value function (cost function):

$$J(u_1, u_2) = \int_{-\infty}^{\infty} \left(\|y_1\|_2^2 + \|u_2\|_2^2 - \|u_1\|_2^2 \right) \, dt.$$

The minimizing player chooses a strategy u_2 and the maximizing player chooses strategy u_1. We can show [48] that the optimal strategies (denoted uppercase ^{o}) satisfy:

$$J(u_1, u_2^o) \leq J(u_1^o, u_2^o) \leq J(u_1^o, u_2)$$

and

$$J(u_1^o, u_2^o) \equiv 0$$

where each strategy pair (u_1, u_2) defines unique solutions to the plant equation, 3.45

and to the H_∞ central controller(s):

$$K = \left[\begin{array}{c|c} \hat{A}_i & \hat{B}_i \\ \hline \hat{C}_i & 0 \end{array}\right] \quad \text{or} \quad K = \left[\begin{array}{c|c} \hat{A}_o & \hat{B}_o \\ \hline \hat{C}_o & 0 \end{array}\right]$$

Doyle [27] shows (in a somewhat less than general case):

$$\begin{aligned} \|y_1\|_2^2 - \gamma^2\|u_1\|_2^2 &= \|u_2 + B_2^T X_\infty x\|_2^2 - \gamma^2\|u_1 - \gamma^{-2}B_1^T X_\infty x\|_2^2 \qquad (3.46) \\ &\triangleq \|v\|_2^2 - \gamma^2\|r\|_2^2. \qquad (3.47) \end{aligned}$$

If we choose $u_1 = \gamma^{-2}B_1^T X_\infty x$, we see that this value maximizes the value in equation 3.46 for the minimizing value of $u_2 = -B_2^T X_\infty x$. That is, the u_1 making $r = 0$ and the u_2 making $v = 0$ satisfy the saddle-point condition of the LQ game problem. The difficulty in an H_∞ control setting is that we do not get to pick the disturbance like the maximizing player in the LQ game problem. This fact motivates the description in the literature of $\hat{u}_1 = \gamma^{-2}B_1^T X_\infty \hat{x}$ as the worst case disturbance estimate.

To show that this description is misleading, we pose the following problem. Suppose we choose, for the general H_∞ control problem, an external disturbance $u_1 = Fcos(wt) + \gamma^{-2}B_1^T X_\infty x$ for some $w, F \in \mathbf{R}$, with $w, F > 0$. Clearly, $\hat{u}_1 = \gamma^{-2}B_1^T X_\infty \hat{x}$ is in no sense an estimate of u_1 as the naming convention would imply. Additionally, since we do not in general have a state estimate, the saddle point condition is not satisfied even for the LQ game problem.

Using the more general results of Uchida [48], we can view the same problem in a slightly different manner. If we partition the external disturbance matrix into

disturbance and measurement noise,

$$u_1 \triangleq \begin{pmatrix} u_{1d} \\ u_{1m} \end{pmatrix}$$

the maximizing player's strategy has the form:

$$u_1^o = \begin{pmatrix} B_1^T X_\infty^{-1}(x - \hat{x}) \\ -C_2(x - \hat{x}) + C_2 X_\infty (X_\infty^{-1} - Y_\infty)^{-1}\hat{x} \end{pmatrix}$$

and the minimizing player uses the strategy:

$$u_2^o = -B_2^T (X_\infty^{-1} - Y_\infty)^{-1}\hat{x}$$

which shows that in order to satisfy the saddle-point condition, the disturbance and measurement noise must be functions of the plant and controller states.

Now, we can use a simple *gedanken* to show that we can get arbitrarily poor estimates of the exogenous input from the H_∞ central controller.

Suppose we have a single spring-mass-damper system driven by a sinusoidal disturbance. By varying the frequency of the disturbance sinusoid, we can choose any phase (between 0 and 180 degrees) between the sinusoidal disturbance and the position of the mass. We would expect that because of this behavior, we could selectively choose a disturbance frequency that would give arbitrarily bad disturbance "estimates". This point is argued in more detail below.

The "estimated" disturbance is defined to be $\hat{u}_1 = \gamma^{-2} B_1^T X_\infty \hat{x}$. We have shown that the error dynamics of the H_∞ compensator do not estimate the states and the

forcing function for the error dynamics is proportional to $\hat{x}$. If we look at equation 3.28 we see we can choose an arbitrary phase angle between the disturbance input and the closed-loop system states x, and $\hat{x}$ just by varying the disturbance frequency. We can see the same behavior in equation 3.30 where the states are x, and $e = x - \hat{x}$. Thus, merely by varying the disturbance frequency, we see we can get arbitrarily poor "estimates" of the external disturbance, i.e. the H_∞ controller does not attempt to estimate either the exogenous input signal or the controlled output.

3.4 Disturbance Dynamics and Optimal Controllers

In this section, we use a plant augmentation approach to deal with non-white (colored) disturbance dynamics and with output smoothing filters. We will show that the augmented H_∞ compensators have an estimator structure that mimics both the LQG and H_∞ results from above. In an effort to streamline the discussion, only the GD H_∞ controller formulation will be augmented; the dual controller can similarly be extended with minimal effort.

The LQG paradigm assumes the plant disturbance and measurement noise are zero-mean, white, and Gaussian. In order to accommodate disturbance dynamics such as narrowband, wideband, etc. in the standard LQG formulation, additional dynamics must be augmented to the nominal plant to account for the actual disturbance spectrum. Two methods of performing this augmentation are the Disturbance Modelling (DM), and the Frequency Shaped Cost Functional (FSCF). These two techniques

are described in [49, 50] respectively, and are shown to be equivalent through a duality argument. In this section, we will restrict ourselves to the DM technique where the disturbance dynamics are augmented to the nominal plant model.

Recall that the H_∞ formulation makes no assumptions about the statistics of the disturbance and noise measurements other than the assumption of signals being in the unit ball. In order to deal with disturbance dynamics in an H_∞ context, we can use the same plant augmentation approach used in the LQG case, however, we can think of it as a weighting envelope rather than some statistical model.

3.4.1 Augmenting Disturbance Dynamics to the Nominal Plant

In terms of overall system dynamics, plant disturbance dynamics usually appear as a prefilter to the plant. Since the standard H_∞ formulation includes both the plant disturbance and the measurement noise in the disturbance term u_1, we will explicitly carry along each term to clarify the derivation to follow. We define:

$$u_1 \triangleq \begin{pmatrix} u_{1d} \\ u_{1m} \end{pmatrix}$$

where, u_{1d} is the plant disturbance, and u_{1m} is the measurement noise. We also need to define the terms affected by u_1:

$$\begin{aligned} B_1 &\triangleq \begin{bmatrix} B_{1d} & B_{1m} \end{bmatrix} \\ D_{11} &\triangleq \begin{bmatrix} D_{11d} & D_{11m} \end{bmatrix} \\ D_{21} &\triangleq \begin{bmatrix} D_{21d} & D_{21m} \end{bmatrix} \end{aligned}$$

The standard plant formulation with explicit disturbance and measurement terms is defined as:

$$\dot{x} = Ax + \begin{bmatrix} B_{1d} & B_{1m} \end{bmatrix} \begin{pmatrix} u_{1d} \\ u_{1m} \end{pmatrix} + B_2 u_2 \tag{3.48}$$

$$y_1 = C_1 x + \begin{bmatrix} D_{11d} & D_{11m} \end{bmatrix} \begin{pmatrix} u_{1d} \\ u_{1m} \end{pmatrix} + D_{12} u_2 \tag{3.49}$$

$$y_2 = C_2 x + \begin{bmatrix} D_{21d} & D_{21m} \end{bmatrix} \begin{pmatrix} u_{1d} \\ u_{1m} \end{pmatrix} \tag{3.50}$$

We will make some assumptions on the general form of the B, and D matrices that are typical of most systems. We assume that there is no coupling between the measurement noise and the plant dynamics. Additionally, we assume that the measurement noise does not appear in the controlled output. Thus,

$$\begin{aligned} B_1 &= \begin{bmatrix} B_{1d} & 0 \end{bmatrix} \\ D_{11} &= \begin{bmatrix} D_{11d} & 0 \end{bmatrix} \end{aligned}$$

We assume the disturbance dynamics have the form:

$$\dot{x}_f = A_f x_f + B_f \nu \tag{3.51}$$

$$y_f \triangleq u_{1d} = C_f x_f \tag{3.52}$$

where $x_f \in \mathbf{R}^m$, and ν is zero-mean, white Gaussian noise. When we append the disturbance dynamics to the plant, we obtain the following augmented system:

$$\begin{pmatrix} \dot{x} \\ \dot{x}_f \end{pmatrix} = \begin{bmatrix} A & B_{1d} C_f \\ 0 & A_f \end{bmatrix} \begin{pmatrix} x \\ x_f \end{pmatrix} + \begin{bmatrix} 0 & 0 \\ B_f & 0 \end{bmatrix} \begin{pmatrix} \nu \\ u_{1m} \end{pmatrix} + \begin{bmatrix} B_2 \\ 0 \end{bmatrix} u_2 \tag{3.53}$$

$$y_1 = \begin{bmatrix} C_1 & D_{11d}C_f \end{bmatrix} \begin{pmatrix} x \\ x_f \end{pmatrix} + \begin{bmatrix} 0 & 0 \end{bmatrix} \begin{pmatrix} \nu \\ u_{1m} \end{pmatrix} + D_{12}u_2 \quad (3.54)$$

$$y_2 = \begin{bmatrix} C_2 & D_{21d}C_f \end{bmatrix} \begin{pmatrix} x \\ x_f \end{pmatrix} + \begin{bmatrix} 0 & D_{21m} \end{bmatrix} \begin{pmatrix} \nu \\ u_{1m} \end{pmatrix} + D_{22}u_2. \quad (3.55)$$

Note that the feedthrough terms from D_{11d} and D_{21d} get "absorbed" into the C_1 and C_2 matrices respectively. The implication for this is the following: if D_{11d} and/or D_{21d} is non-zero, this implies that we can measure the disturbance; however, if we cannot measure the disturbance, we can estimate it (in a way to be made clear below) by augmenting the disturbance dynamics to the nominal plant. The corresponding entries in the D_1 and D_2 matrices are now zero.

3.4.2 Augmented System H_∞ Controllers

Now that we have an augmented plant, we need to design an H_∞ controller for it. In this section, we will present the GD H_∞ controller for the augmented system given above. In order to streamline the presentation, we will assume wlog that $E_1 = I$, $E_2 = I$, and $\gamma = 1$.

The augmented system is assumed to be $(n+m)$-dimensional and we partition the solution to the state-feedback and output-injection Riccati equations as

$$X_\infty \triangleq \begin{pmatrix} X_{11} & X_{12} \\ X_{21} & X_{22} \end{pmatrix}$$

$$Y_\infty \triangleq \begin{pmatrix} Y_{11} & Y_{12} \\ Y_{21} & Y_{22} \end{pmatrix}$$

respectively, and the augmented Z matrix is partitioned as

$$Z_\infty \triangleq \begin{pmatrix} Z_{11} & Z_{12} \\ Z_{21} & Z_{22} \end{pmatrix}$$

where the terms $(\cdot)_{11} \in \mathbf{R}^{n\times n}$, $(\cdot)_{12} \in \mathbf{R}^{n\times m}$, $(\cdot)_{21} \in \mathbf{R}^{m\times n}$, and $(\cdot)_{22} \in \mathbf{R}^{m\times m}$.

If we plug the augmented system matrices into the H_∞ controller formulation given in equation 3.11 the symbolic result is quite messy, so, in the interest of clarity, we will present the controller coefficients term-by-term. This also gives additional insight into the behavior of the H_∞ compensator.

$$B_1F_1 = \begin{bmatrix} 0 & 0 \\ B_fB_f^TX_{21} & B_fB_f^TX_{22} \end{bmatrix} \tag{3.56}$$

$$B_2F_2 = -\begin{bmatrix} B_2(B_2^TX_{11} + D_{12}^TC_1) & B_2(B_2^TX_{12} + D_{12}^TD_{11d}C_f) \\ 0 & 0 \end{bmatrix} \tag{3.57}$$

We need the following partial computation to simplify the results:

$$\begin{aligned} ZH_2 &= -\begin{bmatrix} Z_{11}(Y_{11}C_2^T + Y_{12}C_f^TD_{21d}^T) + Z_{12}(Y_{21}C_2^T + Y_{22}C_f^TD_{21d}^T) \\ Z_{21}(Y_{11}C_2^T + Y_{12}C_f^TD_{21d}^T) + Z_{22}(Y_{21}C_2^T + Y_{22}C_f^TD_{21d}^T) \end{bmatrix} \\ &\triangleq -\begin{bmatrix} Z_{H1} \\ Z_{H2} \end{bmatrix} \end{aligned}$$

Using the above shorthand, we obtain:

$$ZH_2C_2 = -\begin{bmatrix} Z_{H1}C_2 & Z_{H1}D_{11d}C_f \\ Z_{H2}C_2 & Z_{H2}D_{11d}C_f \end{bmatrix} \tag{3.58}$$

$$ZH_2D_{21}F_1 = \begin{bmatrix} 0 & 0 \\ 0 & 0 \end{bmatrix} \tag{3.59}$$

Notice that we get *no* contribution from the $\gamma^{-2}ZH_2D_{21}B_1^TX_\infty$ term when there is no direct disturbance feedthrough. It is also interesting that the B_1F_1 term has no effect on the plant dynamics and correspondingly, the B_2F_2 term has no effect on the disturbance dynamics.

3.4.3 Estimation Behavior of the Augmented Controller

In this section we will look at the estimation structure of the augmented H_∞ controller. We will perform the same type of analysis used above when discussing the dual *exogenous input* and *controlled output* H_∞ controllers.

Define the error of the augmented system to be:

$$e \triangleq x_a - \hat{x}_a = \begin{pmatrix} x \\ x_f \end{pmatrix} - \begin{pmatrix} \hat{x} \\ \hat{x}_f \end{pmatrix}$$

where $(\cdot)_a$ signifies the augmented plant.

Proposition 3.6 *When disturbance dynamics are appended to the H_∞ controller in the form presented above:*

(i) *the plant states are estimated,*

(ii) *the disturbance states are not estimated.*

Proof:

Solving for the error dynamics we get:

$$\dot{e}_a \triangleq \begin{pmatrix} \dot{e}_x \\ \dot{e}_{x_f} \end{pmatrix} = [A + ZH_2C_2] \begin{pmatrix} e_x \\ e_{x_f} \end{pmatrix} - \gamma^{-2} \begin{bmatrix} 0 & 0 \\ B_f B_f^T X_{21} & B_f B_f^T X_{22} \end{bmatrix} \begin{pmatrix} \hat{x} \\ \hat{x}_f \end{pmatrix} + \begin{bmatrix} 0 & Z_{H1} D_{21m} \\ B_f & Z_{H2} D_{21m} \end{bmatrix} \begin{pmatrix} \nu \\ u_{1d} \end{pmatrix} \tag{3.60}$$

From lemma 3.1 the error is asymptotically stable, and if we let $\nu = 0$ *and* $u_{1d} = 0$, *we see that the plant error dynamics,* e_x, *are only a function of the plant and disturbance error dynamics while the disturbance error dynamics have a forcing term proportional to the plant and disturbance states.* □

Chapter 4

Controlled Output Equations for Disturbance Rejection

One difficulty when designing optimal controllers is that both the LQG and H_∞ controllers are optimal with respect to a controlled output equation or equivalently, are optimal with respect to some weighting matrices. Typically the controlled output is chosen in an ad hoc fashion and the relation of minimizing the H_2-norm or the H_∞-norm of the controlled output to the actual system measurement is not clear.

In this chapter, we first present the connections of the time-domain LQG cost function to the frequency domain H_2 problem. Then, we present a new method of choosing a controlled output equation for disturbance rejection based on the physics of the open-loop plant using the knowledge of the relation between the time-domain and frequency-domain representations of the controlled output equations. We use a "minimum acceleration" cost function to generate a controlled output equation. This new approach yields penalties on the augmented (and uncontrollable) disturbance estimator states which typically are not penalized [49, 50]. The utility of penalizing uncontrollable states is not clear if only a time-domain cost approach is used. It is the connection of the most general time-domain and frequency-domain

LQG cost function that yields the penalties on the uncontrollable augmented states. The controlled output equation obtained using this approach can be used for both LQG and H_∞ disturbance rejection controllers. Additionally, the effect of adding an output smoothing filter (used on digital control systems to get rid of the "staircase" control signal) on the selection of a controlled output equation will be discussed.

In an effort to clarify the theoretical discussion above, simulations of narrowband disturbance rejection on a single spring-mass-damper (SMD) system will be presented before proceeding with the simply-supported plate experiment in the next chapter. These simulations will show in a quantitative manner the effect of some ad hoc controlled output designs versus the new minimum acceleration design procedure.

4.1 Time-Domain and Frequency-Domain Connections in LQG Cost Functions

In this section we show the connections between the standard LQG time-domain cost functional and the frequency domain H_2 controlled output equation. The LQG results are presented without a great deal of explanation, for full details see [52]. The LQG controller minimizes the average time-domain cost functional:

$$J_{LQG} = \min_{u_2 \in U} \left\{ \lim_{t_f \to \infty} \frac{1}{2} E \left[\int_0^{t_f} \begin{pmatrix} x^T & u_2^T \end{pmatrix} \begin{bmatrix} Q & W \\ W^T & R \end{bmatrix} \begin{pmatrix} x \\ u_2 \end{pmatrix} dt \right] \right\} \quad (4.1)$$

where, $Q \geq 0$, $R > 0$ and W are weighting matrices with,

$$\begin{bmatrix} Q & W \\ W^T & R \end{bmatrix} \geq 0,$$

and U is the set of admissible controls.

Also we assume the noise (disturbance and measurement) statistics satisfy:

$$\begin{aligned} E[u_1] &= 0 && (4.2) \\ E[u_1(t)u_1(\tau)^T] &= E\left[\begin{pmatrix} u_{1d}(t) \\ u_{1m}(t) \end{pmatrix} \begin{pmatrix} u_{1d}^T(\tau) & u_{1m}^T(\tau) \end{pmatrix}\right] && (4.3) \\ &= E\begin{bmatrix} u_{1d}(t)u_{1d}^T(\tau) & u_{1d}(t)u_{1m}^T(\tau) \\ u_{1m}(t)u_{1d}^T(\tau) & u_{1m}(t)u_{1m}^T(\tau) \end{bmatrix} && (4.4) \\ &= \begin{bmatrix} \Xi & \Upsilon \\ \Upsilon^T & \Lambda \end{bmatrix} \delta(t-\tau) && (4.5) \end{aligned}$$

Typically, the cross terms between the state and control are assumed to be zero, $W = 0$, and there is no correlation between the disturbance and measurement noise, $\Upsilon = 0$. We will show in the sequel that the cross weights between the state and control can be important for disturbance rejection.

Taking advantage of the separation structure of the LQG controller, e.g. the state-feedback (LQR) gains can be specified separately from the estimator (Kalman Filter) gains, we will show how the plant dynamics can be used to generate the appropriate controlled output equation.

Recall that the standard H_∞ problem minimizes the infinity-norm from u_1 to y_1. If we use the 2-norm instead and choose the appropriate controlled output, we can

show that the LQG cost function is satisfied. The general measurement equation is defined as:

$$y_1 = C_1 x + D_{11} u_1 + D_{12} u_2 \tag{4.6}$$

$$= C_1 x + \begin{bmatrix} D_{11d} & D_{11m} \end{bmatrix} \begin{pmatrix} u_{1d} \\ u_{1m} \end{pmatrix} + D_{21} u_2. \tag{4.7}$$

We will assume throughout this section that there is no disturbance feedthrough, i.e. $D_{11} \equiv 0$.

If we compute the 2-norm of of the controlled output, y_1, we get

$$\|y_1\|_2^2 = \int_0^\infty y_1^T y_1 \, dt \tag{4.8}$$

$$= \int_0^\infty \left\{ \begin{pmatrix} x^T & u_2^T \end{pmatrix} \begin{bmatrix} C_1^T C_1 & C_1^T D_{12} \\ D_{12}^T C_1 & D_{12}^T D_{12} \end{bmatrix} \begin{pmatrix} x \\ u_2 \end{pmatrix} \right\} dt \tag{4.9}$$

and if we define

$$\begin{aligned} C_1 &\triangleq Q^{\frac{1}{2}} \\ C_1^T &\triangleq (Q^{\frac{1}{2}})^T \\ D_{12} &\triangleq R^{\frac{1}{2}} \\ D_{12}^T &\triangleq (R^{\frac{1}{2}})^T \end{aligned}$$

and let

$$\begin{aligned} Q &= (Q^{\frac{1}{2}})^T Q^{\frac{1}{2}} = C_1^T C_1 \\ R &= (R^{\frac{1}{2}})^T R^{\frac{1}{2}} = D_{12}^T D_{12} \\ W &= (Q^{\frac{1}{2}})^T R^{\frac{1}{2}} = C_1^T D_{12} \end{aligned}$$

and assuming the previous definiteness conditions are met, we can see the connection between the time-domain cost and the frequency domain cost functions.

This is important because it provides a method of picking the quadratic weights based on the physics of the problem. If we wish to minimize the norm of the measurements of the system, the above method provides a natural solution to that problem by using the system parameters (C_1 and D_{12}) as a basis for the cost function.

In a sample problem to be shown below, we will find that merely using the system measurement may not provide adequate disturbance rejection if we measure position or velocity and use that to computing the quadratic weights or controlled output equation. In fact, regardless of the quantity measured, using a "minimum acceleration" cost function seems to provide the most disturbance rejection. That is, we compute the quadratic weights and controlled output equation based on the acceleration of the system even if we measure position and/or velocity.

If we consider the less general "standard" LQR case when there are no cross terms between the state and control, the corresponding frequency domain cost can be derived if we let the controlled output be:

$$y_1 = \begin{pmatrix} C_1 \\ 0 \end{pmatrix} x + \begin{pmatrix} 0 \\ D_{12} \end{pmatrix} u_2 \tag{4.10}$$

which we will denote for brevity for both the H_∞ and H_2 controllers as:

$$y_1 = \begin{pmatrix} C_1 x \\ D_{12} u_2 \end{pmatrix}. \tag{4.11}$$

If we solve the H_2 problem for this we find:

$$\|y_1\|_2^2 = \int_0^\infty y_1^T y_1 \, dt \tag{4.12}$$

$$= \int_0^\infty \left[x^T C_1^T C_1 x + u_2^T D_{12}^T D_{12} u_2 \right] \, dt \tag{4.13}$$

and if we let

$$\begin{aligned} Q &\triangleq C_1^T C_1 \\ R &\triangleq D_{12}^T D_{12} \\ W &= 0 \end{aligned}$$

we recover the standard LQR cost function with no cross weights, i.e. $W \equiv 0$.

We have shown how to use the physics of the problem to determine the LQR weights; now we must see how the noise statistics enter the Kalman Filter problem. We assume that the disturbance and measurement noise are uncorrelated ($\Upsilon = 0$) for the initial development. If we look at the "transformed" system equations where $D_{11} = 0$ and $D_{22} = 0$, we have:

$$\dot{x} = Ax + B_1 u_1 + B_2 u_2 \tag{4.14}$$

$$y_1 = C_1 x + D_{12} u_2 \tag{4.15}$$

$$y_2 = C_2 x + D_{21} u_1 \tag{4.16}$$

and if we look at how the disturbance enters through B_1, and D_{21} in terms of the previously defined statistics we find that

$$\begin{aligned} E[(B_{1d}u_{1d})(B_{1d}u_{1d})^T] &= E[B_{1d}u_{1d}u_{1d}^T B_{1d}^T] && (4.17)\\ &= B_{1d}E[u_{1d}u_{1d}^T]B_{1d}^T && (4.18)\\ &= B_{1d}\Xi B_{1d}^T\,\delta(t-\tau) && (4.19) \end{aligned}$$

and

$$\begin{aligned} E[(D_{21m}u_{1m})(D_{21m}u_{1m})^T] &= E[D_{21m}u_{1m}u_{1m}^T D_{21m}^T] && (4.20)\\ &= D_{21m}E[u_{1m}u_{1m}^T]D_{21m}^T && (4.21)\\ &= D_{21m}\Lambda D_{21m}^T\,\delta(t-\tau). && (4.22) \end{aligned}$$

Using the controlled output approach of H_∞ or H_2 instead of the quadratic weights approach of LQG, we see that there we require an additional plant scaling required to take into account how the disturbance and measurement covariances enter the plant and measurement respectively. The necessity of this scaling is clear if we recall that without the additional weights, the unscaled system assumes the noise is zero mean with standard deviation one, denoted $N(0,1)$, for the H_2 case or the noise is in the unit ball for the H_∞ case. If we include these additional noise weights in the plant and measurement equations, the equations for a disturbance rejection controller design become:

$$\begin{aligned} \dot{x} &= Ax + \begin{bmatrix} B_{1d}(\Xi)^{\frac{1}{2}} & 0 \end{bmatrix}\begin{pmatrix} u_{1d} \\ u_{1m} \end{pmatrix} + B_2u_2 && (4.23)\\ y_1 &= C_1x + D_{12}u_2 && (4.24) \end{aligned}$$

$$y_2 = C_2 x + \left[\begin{array}{cc} D_{21d} & D_{21m}(\Lambda)^{\frac{1}{2}} \end{array} \right] \left(\begin{array}{c} u_{1d} \\ u_{1m} \end{array} \right) \tag{4.25}$$

If we admit correlation between the disturbance and measurement noise we obtain the following, general form:

$$\dot{x} = Ax + \left[\begin{array}{cc} B_{1d}(\Xi)^{\frac{1}{2}} & B_{1m}(\Upsilon)^{\frac{1}{2}} \end{array} \right] \left(\begin{array}{c} u_{1d} \\ u_{1m} \end{array} \right) + B_2 u_2 \tag{4.26}$$

$$y_1 = C_1 x + D_{12} u_2 \tag{4.27}$$

$$y_2 = C_2 x + \left[\begin{array}{cc} D_{21d}(\Xi)^{\frac{1}{2}} & D_{21m}(\Lambda)^{\frac{1}{2}} \end{array} \right] \left(\begin{array}{c} u_{1d} \\ u_{1m} \end{array} \right) \tag{4.28}$$

If we look at the general noise covariance of u_1 as defined above, we get:

$$E[(B_1 u_1)(B_1 u_1)^T] = B_1 E[u_1 u_1^T] B_1^T \tag{4.29}$$

$$= \left[\begin{array}{cc} B_{1d}(\Xi)^{\frac{1}{2}} & B_{1M}(\Upsilon)^{\frac{1}{2}} \end{array} \right] \left(\begin{array}{c} (\Xi^{\frac{1}{2}})^T B_{1d}^T \\ (\Upsilon^{\frac{1}{2}})^T B_{1m}^T \end{array} \right) \delta(t-\tau) \tag{4.30}$$

$$= \left[\begin{array}{cc} B_{1d} \Xi B_{1d}^T & B_{1m}(\Upsilon^{\frac{1}{2}})(\Xi^{\frac{1}{2}})^T B_{1d}^T \\ B_{1d}(\Xi^{\frac{1}{2}})(\Upsilon^{\frac{1}{2}})^T B_{1m}^T & B_{1m} \Lambda B_{1m}^T \end{array} \right] \delta(\cdot) \tag{4.31}$$

which if we redefine the covariance terms above we see is equivalent to the form given in equation 4.5 for the standard LQG problem. We can also introduce an additional scaling on the cross-terms if necessary to treat the most general case.

4.2 Controlled Output Equations for Systems with Feedthrough

In this section we show how to select a controlled output equation for systems with disturbance and measurement feedthrough. Since we have feedthrough, we will

assume the plant equations have not been transformed into the standard form. The general form of the system equations is:

$$\dot{x} = Ax + \begin{bmatrix} B_{1d}(\Xi)^{\frac{1}{2}} & 0 \end{bmatrix} \begin{pmatrix} u_{1d} \\ u_{1m} \end{pmatrix} + B_2 u_2 \tag{4.32}$$

$$y_1 = C_1 x + D_{11} u_1 + D_{12} u_2 \tag{4.33}$$

$$y_2 = C_2 x + \begin{bmatrix} D_{21d}(\Xi)^{\frac{1}{2}} & D_{21m}(\Lambda)^{\frac{1}{2}} \end{bmatrix} \begin{pmatrix} u_{1d} \\ u_{1m} \end{pmatrix} + D_{22} u_2 \tag{4.34}$$

Now, we would like to set $y1 = y2 -$ "measurement noise". But, we do not want the additional noise covariance weights to be in our controlled output. We want (as close as is practicable) the controlled output equation to be actual unweighted measurements. If we use the weights here, we are not minimizing the "correct" cost, i.e. the actual measurements. Thus, for the y_1 controlled output equation, we will not have Ξ or Λ terms.

One difficulty is that we do not have access (in general) to the disturbance. We can circumvent this difficulty by using the system augmented with disturbance dynamics as presented in Chapter 3. If we do this, the required disturbance measurement $D_{11} \neq 0$ turns into a disturbance estimate and the augmented system has no disturbance feedthrough. The resulting equations are identical to equations 3.53- 3.55.

We can easily set $y1 = y2 - D_{21m} u_{1m}$. If we do this, our controlled output equation is:

$$y_1 = \begin{bmatrix} C_2 & D_{21d} C_f \end{bmatrix} \begin{pmatrix} x \\ x_f \end{pmatrix} + \begin{bmatrix} 0 & 0 \end{bmatrix} \begin{pmatrix} \nu \\ u_{1m} \end{pmatrix} + D_{22} u_2. \tag{4.35}$$

If we choose the controlled output as shown above, there are some interesting impli-

cations with respect to the usual methods of choosing LQR weights for augmented systems. Let us compute the 2-norm of y_1:

$$\|y_1\|_2^2 = \int_0^\infty (y_1^T y_1)\, dt \tag{4.36}$$

$$= \int_0^\infty \left\{ \left[\begin{pmatrix} x^T & x_f^T \end{pmatrix} \begin{bmatrix} C_2^T \\ C_f^T D_{21d}^T \end{bmatrix} + u_2^T D_{22}^T \right] \left[\begin{bmatrix} C_1 & D_{21d} C_f \end{bmatrix} \begin{pmatrix} x \\ x_f \end{pmatrix} + D_{22} u_2 \right] \right\} dt \tag{4.37}$$

$$= \int_0^\infty \begin{pmatrix} x^T & x_f^T & u_2^T \end{pmatrix} \begin{bmatrix} Q & W \\ W^T & R \end{bmatrix} \begin{pmatrix} x \\ x_f \\ u_2 \end{pmatrix} dt \tag{4.38}$$

where

$$\left[\begin{array}{cc} Q & W \\ W^T & R \end{array} \right] \triangleq \left[\begin{array}{cc|c} C_1^T C_1 & C_1^T D_{21d} C_f & C_1^T D_{22} \\ C_f D_{21d}^T C_1 & C_f^T D_{21d}^T D_{21d} C_f & C_f^T D_{21d}^T D_{22} \\ \hline D_{22}^T C_1 & D_{22}^T D_{21d} C_f & D_{22}^T D_{22} \end{array} \right] \tag{4.39}$$

and the notation used above is to denote the partitioning of the matrices.

There are two important items in equation 4.39 worth noting. The first is that there are weights on the uncontrollable disturbance states. Much of the literature discussing LQG disturbance rejection penalizes the only the unaugmented plant states, for example [49, 50]. The motivation for not penalizing the disturbance estimates is that since they are uncontrollable, penalizing them does nothing except increase the time-domain cost. The other item worth noting is there are cross-weights between the plant states and the control. These are normally assumed to be zero in the literature.

The only reference found where the augmented disturbance states were weighted is

Jones [51]. What is interesting to note, however, is how the weights on the disturbance states arise. Jones first computes a control signal that will cancel the external disturbance, and then solves the inverse optimal control problem to get a set of Q, W, and R matrices. The weighting matrices obtained only penalize the augmented plant states. In order to add transient suppression (damping), minimum modal energy weights are added to the inverse LQ problem weights, and these new Q, R, and W matrices are used to compute an LQG controller. Interestingly, the weights obtained in this fashion contain cross terms between the state, x, and the control, u_2 but no cross terms between the states. That is, Q is diagonal, and $W \neq 0$. Jones also failed to notice the connection of penalizing the uncontrollable augmented disturbance states with the time-domain cost.

The same controlled output equation also can be used for the H_∞ controller. The only difference is that the ∞-norm is minimized instead of the 2-norm. A comparison of the nominal LQG and H_∞ results is given for a simple spring-mass-damper system. Before we present the example, we will discuss systems with no disturbance feedthrough.

4.3 Controlled Output Equations for Systems with No Feedthrough

In this section, we discuss systems with no disturbance feedthrough. We will see that this makes the selection of an appropriate controlled output equation more difficult. For the assumption of no feedthrough, the term D_{21d} is zero in the measurement equation, y_2, and we must assume some measurement noise for the problem to be

well defined. The system equations for a plant with no disturbance feedthrough is given below:

$$\dot{x} = Ax + \begin{bmatrix} B_{1d}(\Xi)^{\frac{1}{2}} & 0 \end{bmatrix} \begin{pmatrix} u_{1d} \\ u_{1m} \end{pmatrix} + B_2 u_2 \tag{4.40}$$

$$y_1 = C_1 x + D_{11} u_1 + D_{12} u_2 \tag{4.41}$$

$$y_2 = C_2 x + \begin{bmatrix} 0 & D_{21m}(\Lambda)^{\frac{1}{2}} \end{bmatrix} \begin{pmatrix} u_{1d} \\ u_{1m} \end{pmatrix} + [0] u_2 \tag{4.42}$$

If we augment the system to model the disturbance dynamics as we did previously, we find:

$$y_2 = \begin{bmatrix} C_2 & 0 \end{bmatrix} \begin{pmatrix} x \\ x_f \end{pmatrix} + \begin{bmatrix} 0 & D_{21m} \end{bmatrix} \begin{pmatrix} \nu \\ u_{1m} \end{pmatrix} + [0] u_2. \tag{4.43}$$

We can try to set $y1 = y2 -$ "measurement noise" as in the previous case; however, without a feedthrough term the problem is ill posed. The most obvious solution is to use the "orthogonal" weights from the H_2 section above. If we do this we get,

$$y_1 = \left(\begin{bmatrix} C_2 & 0 \end{bmatrix} \begin{pmatrix} x \\ x_f \end{pmatrix} + \begin{bmatrix} 0 & 0 \end{bmatrix} \begin{pmatrix} \nu \\ u_{1m} \end{pmatrix} + [0] u_2 \right) \tag{4.44}$$

$$\underset{\Psi u_2}{} = \begin{pmatrix} C_2 x \\ \Psi u_2 \end{pmatrix}. \tag{4.45}$$

where $\Psi > 0$ is some arbitrary weight for the control inputs u_2.

Note the H_2-norm of y_1 in equation 4.45 is identical to equation 4.13 except $D_{12}^T D_{12}$ has been replaced by the arbitrary weight $\Psi^T \Psi$.

4.4 Output Smoothing Filters and Controlled Output Equations

We often find it necessary to use output analog smoothing filters on digital control systems to get rid of the high frequency information introduced by the sampling process. We must account for the filter dynamics in the control system design; otherwise the unmodelled phase and magnitude can drive the closed-loop system unstable.

We can model the smoothing filter dynamics as

$$\begin{aligned} \dot{x}_s &= A_s x_s + B_s u_2 \\ y_s &\triangleq u_s = C_s x_s \end{aligned}$$

where u_2 is the output from the digital controller and u_s is the "smoothed" control signal to be input to the plant.

If we form the augmented system using the nominal plant model, we get:

$$\begin{aligned} \begin{pmatrix} \dot{x} \\ \dot{x}_s \end{pmatrix} &= \begin{bmatrix} A & B_2 C_s \\ 0 & A_s \end{bmatrix} \begin{pmatrix} x \\ x_s \end{pmatrix} + \begin{pmatrix} B_1 \\ 0 \end{pmatrix} u_1 + \begin{pmatrix} 0 \\ B_s \end{pmatrix} u_2 \\ y_2 &= \begin{bmatrix} C_2 & D_{22} C_s \end{bmatrix} \begin{pmatrix} x \\ x_s \end{pmatrix} + D_{21} u_1 \\ &\triangleq C_{2_a} x_a + D_{21} u_1. \end{aligned}$$

Note that we no longer have a controller feedthrough term. We now have the difficulty of choosing a controlled output equation since the method of using the 2-norm of the measurement is ill posed when there is no feedthrough. The most obvious

approach is to choose weights based on the previously presented no feedthrough costs, i.e.

$$y_1 = \begin{pmatrix} C_{2_a} x_a \\ \Psi u_2 \end{pmatrix}.$$

If we use the general augmented system with disturbance dynamics and a smoothing filter, we can show that:

$$\begin{pmatrix} \dot{x} \\ \dot{x}_f \\ \dot{x}_s \end{pmatrix} = \begin{bmatrix} A & B_{1d}C_f & B_2 C_s \\ 0 & A_f & 0 \\ 0 & 0 & A_s \end{bmatrix} \begin{pmatrix} x \\ x_f \\ x_s \end{pmatrix} + \begin{bmatrix} 0 & 0 \\ B_f & 0 \\ 0 & 0 \end{bmatrix} \begin{pmatrix} \nu \\ u_{1m} \end{pmatrix} + \begin{pmatrix} 0 \\ 0 \\ B_s \end{pmatrix} u_2$$

$$y_2 = \begin{bmatrix} C_2 & D_{21d}C_f & D_{22}C_s \end{bmatrix} \begin{pmatrix} x \\ x_f \\ x_s \end{pmatrix} + \begin{bmatrix} 0 & D_{21m} \end{bmatrix} \begin{pmatrix} \nu \\ u_{1m} \end{pmatrix} + [0]u_2$$

and we can use the same form of the controlled output equation as presented above.

4.5 Example Narrowband Disturbance Rejection Problem

We will present a simple example problem in this section to show how the design procedure presented above is used. This is not meant to be an exhaustive study; it is only meant to highlight some of the results of the proposed design approach in a qualitative rather than quantitative manner. Also keep in mind that any data presented cannot validate the proposed approach; it is only suggestive of possible general closed-loop behavior.

The system we will attempt to control is a single degree-of-freedom spring-mass-damper (SMD) system excited by a narrowband disturbance. The undamped natu-

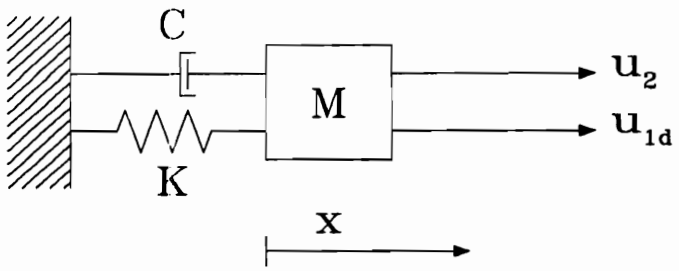

Figure 4.1: Example problem schematic

ral frequency of the spring-mass system is 50 Hz and the narrowband disturbance is centered at 60 Hz. We assume that the proportional damping is 0.01 percent critical damping. A diagram of the system is shown in figure 4.1.

The SMD dynamics are given by:

$$m\ddot{x} + c\dot{x} + kx = u_{1d} + u_2 \tag{4.46}$$

and we will have three different measurement cases to design controllers for: position, velocity, and acceleration. These three measurement equations are, respectively:

$$y_{2p} = x + u_{1m} \tag{4.47}$$

$$y_{2v} = \dot{x} + u_{1m} \tag{4.48}$$

$$y_{2a} = \ddot{x} = \frac{1}{m}(u_{1d} + u_2 - c\dot{x} - kx) + u_{1m} \tag{4.49}$$

If we put the system in standard first-order form we obtain:

$$\begin{pmatrix} \dot{x}_1 \\ \dot{x}_2 \end{pmatrix} = \begin{bmatrix} 0 & 1 \\ -\frac{k}{m} & -\frac{c}{m} \end{bmatrix} \begin{pmatrix} x_1 \\ x_2 \end{pmatrix} + \begin{pmatrix} 0 \\ \frac{1}{m} \end{pmatrix} u_{1d} + \begin{pmatrix} 0 \\ \frac{1}{m} \end{pmatrix} u_2 \tag{4.50}$$

$$y_{2p} = \begin{bmatrix} 1 & 0 \end{bmatrix} \begin{pmatrix} x_1 \\ x_2 \end{pmatrix} + u_{1m} \tag{4.51}$$

$$y_{2v} = \begin{bmatrix} 0 & 1 \end{bmatrix} \begin{pmatrix} x_1 \\ x_2 \end{pmatrix} + u_{1m} \tag{4.52}$$

$$y_{2a} = \begin{bmatrix} -\frac{k}{m} & -\frac{c}{m} \end{bmatrix} \begin{pmatrix} x_1 \\ x_2 \end{pmatrix} + u_{1m} + \frac{1}{m} u_2. \tag{4.53}$$

We assume the narrowband noise is modelled by Gaussian noise, $\nu(t) = N(0,1)$, and is filtered by the following dynamics:

$$\frac{u_{1d}(s)}{\nu(s)} = \frac{\xi s}{s^2 + 2\zeta w_n s + w_n^2} \tag{4.54}$$

where ζ is the damping of the filter, assumed for this case to be 0.01,and w_n is the undamped natural frequency of the filter, assumed to be 60 Hz. If we put the filter in standard first-order form, we obtain:

$$\begin{pmatrix} \dot{x}_3 \\ \dot{x}_4 \end{pmatrix} = \begin{bmatrix} 0 & 1 \\ -w_n^2 & -2\zeta w_n \end{bmatrix} \begin{pmatrix} x_3 \\ x_4 \end{pmatrix} + \begin{pmatrix} 0 \\ \xi \end{pmatrix} \nu \tag{4.55}$$

$$u_{1d} = \begin{bmatrix} 0 & 1 \end{bmatrix} \begin{pmatrix} x_3 \\ x_4 \end{pmatrix}. \tag{4.56}$$

Collecting both the nominal plant and the disturbance dynamics we get the following augmented system:

$$\begin{pmatrix} \dot{x}_1 \\ \dot{x}_2 \\ \dot{x}_3 \\ \dot{x}_4 \end{pmatrix} = \begin{bmatrix} 0 & 1 & 0 & 0 \\ -\frac{1}{m}k & -\frac{1}{m}c & 0 & \frac{1}{m} \\ 0 & 0 & 0 & 1 \\ 0 & 0 & -w_n^2 & -2\zeta w_n \end{bmatrix} \begin{pmatrix} x_1 \\ x_2 \\ x_3 \\ x_4 \end{pmatrix} + \begin{bmatrix} 0 & 0 \\ 0 & 0 \\ 0 & 0 \\ \xi & 0 \end{bmatrix} \begin{pmatrix} \nu \\ u_{1m} \end{pmatrix} + \begin{bmatrix} 0 \\ \frac{1}{m} \\ 0 \\ 0 \end{bmatrix} u_2 \tag{4.57}$$

$$y_{2p} = \begin{bmatrix} 1 & 0 & 0 & 0 \end{bmatrix} \begin{pmatrix} x_1 \\ x_2 \\ x_3 \\ x_4 \end{pmatrix} + \begin{bmatrix} 0 & 1 \end{bmatrix} \begin{pmatrix} \nu \\ u_{1m} \end{pmatrix} \tag{4.58}$$

$$y_{2v} = \begin{bmatrix} 0 & 1 & 0 & 0 \end{bmatrix} \begin{pmatrix} x_1 \\ x_2 \\ x_3 \\ x_4 \end{pmatrix} + \begin{bmatrix} 0 & 1 \end{bmatrix} \begin{pmatrix} \nu \\ u_{1m} \end{pmatrix} \tag{4.59}$$

$$y_{2a} = \begin{bmatrix} -\frac{k}{m} & -\frac{c}{m} & 0 & \frac{1}{m} \end{bmatrix} \begin{pmatrix} x_1 \\ x_2 \\ x_3 \\ x_4 \end{pmatrix} + \begin{bmatrix} 0 & 1 \end{bmatrix} \begin{pmatrix} \nu \\ u_{1m} \end{pmatrix} + \frac{1}{m} u_2. \tag{4.60}$$

The first case we will compute a controller for is the disturbance feedthrough case, i.e. when we measure acceleration. If we let

$$y_1 = y_{2a} - u_{1m} \tag{4.61}$$

$$= \begin{bmatrix} -\frac{k}{m} & -\frac{c}{m} & 0 & \frac{1}{m} \end{bmatrix} \begin{pmatrix} x_1 \\ x_2 \\ x_3 \\ x_4 \end{pmatrix} + \begin{bmatrix} 0 & 0 \end{bmatrix} \begin{pmatrix} \nu \\ u_{1m} \end{pmatrix} + \frac{1}{m} u_2 \tag{4.62}$$

and if we compute the 2-norm of y_1 we get:

$$\|y_1\|_2^2 = \int_0^\infty \left\{ \frac{1}{m^2} X^T \begin{bmatrix} k^2 & kc & 0 & -k & -k \\ kc & c^2 & 0 & -c & -c \\ 0 & 0 & 0 & 0 & 0 \\ -k & -c & 0 & 1 & 1 \\ -k & -c & 0 & 1 & 1 \end{bmatrix} X \right\} dt \tag{4.63}$$

where

$$X \triangleq \begin{pmatrix} x_1 \\ x_2 \\ x_3 \\ x_4 \\ u_2 \end{pmatrix}$$

Note the order of the terms in the state weighting matrix, i.e., the weight on x_1 is proportional to the undamped natural frequency raised to the fourth power, etc. which is not a normally used set of state weightings.

There is one immediate problem when assuming that y_1 is in the form above. Condition *4* for the GD controller is violated at $w = 0$. When this necessary condition is violated, the Hamiltonian has eigenvalues on the jw-axis and correspondingly, the output injection Riccati equation has no solution.

For our example, we find,

$$\left[\begin{array}{cc} A - jwI & B_2 \\ C_1 & D_{12} \end{array}\right]\Bigg|_{w=0} = \left[\begin{array}{ccccc} 0 & 1 & 0 & 0 & 0 \\ -\frac{k}{m} & -\frac{c}{m} & 0 & \frac{1}{m} & \frac{1}{m} \\ 0 & 0 & 0 & 1 & 0 \\ 0 & 0 & -w_n^2 & -2\zeta w_n & 0 \\ -\frac{k}{m} & -\frac{c}{m} & 0 & \frac{1}{m} & \frac{1}{m} \end{array}\right]. \qquad (4.64)$$

We can clearly see that the second row and the fifth row are identical and the necessary rank condition is violated. In order to circumvent this difficulty, we can add a term to the C_1 matrix. If we let $C_1 = \left[\begin{array}{cccc} -\frac{k}{m} + 1 & -\frac{c}{m} & 0 & \frac{1}{m} \end{array}\right]$ the rank condition is satisfied and we can compute a controller. The "correction" we chose was completely ad hoc; it was based on the size of the terms in C_1. If the terms in C_1 are "large", a "large" correction is needed or else the numerical accuracy of the computation will still cause the failure of the rank condition.

Note that this condition also shows there is a transmission zero at $w = 0$. This is easy to explain physically because we can not measure DC with accelerometers. It is not clear if there is any connection between this transmission zero and the form

of the Hamiltonian.

In general, this rank deficiency does not occur. One manifestation of the rank condition occurs when accelerations are measured using collocated sensors and actuators. There may also be other examples where this condition arises.

Up to this point, we have not included the output smoothing filter in the system model. We choose the smoothing filter to be a unity-gain Sallen-Key filter since it is an easily realizable filter. The filter is modelled as:

$$\begin{pmatrix} \dot{x}_5 \\ \dot{x}_6 \end{pmatrix} = \begin{bmatrix} 0 & 1 \\ -w_{sf}^2 & -2\zeta_{sf}w_{sf} \end{bmatrix} \begin{pmatrix} x_5 \\ x_6 \end{pmatrix} + \begin{pmatrix} 0 \\ w_{sf}^2 \end{pmatrix} u_2 \tag{4.65}$$

$$u_s = \begin{bmatrix} 1 & 0 \end{bmatrix} \begin{pmatrix} x_5 \\ x_6 \end{pmatrix}. \tag{4.66}$$

If we append this to the previous system dynamics, we obtain the following augmented system:

$$\begin{pmatrix} \dot{x}_1 \\ \dot{x}_2 \\ \dot{x}_3 \\ \dot{x}_4 \\ \dot{x}_5 \\ \dot{x}_6 \end{pmatrix} = \begin{bmatrix} 0 & 1 & 0 & 0 & 0 & 0 \\ -\frac{1}{m}k & -\frac{1}{m}c & 0 & \frac{1}{m} & \frac{1}{m} & 0 \\ 0 & 0 & 0 & 1 & 0 & 0 \\ 0 & 0 & -w_n^2 & -2\zeta w_n & 0 & 0 \\ 0 & 0 & 0 & 0 & 0 & 1 \\ 0 & 0 & 0 & 0 & -w_{sf}^2 & -2\zeta_{sf}w_{sf} \end{bmatrix} \begin{pmatrix} x_1 \\ x_2 \\ x_3 \\ x_4 \\ x_5 \\ x_6 \end{pmatrix}$$
$$+ \begin{bmatrix} 0 & 0 \\ 0 & 0 \\ 0 & 0 \\ \xi & 0 \\ 0 & 0 \\ 0 & 0 \end{bmatrix} \begin{pmatrix} \nu \\ u_{1m} \end{pmatrix} + \begin{bmatrix} 0 \\ 0 \\ 0 \\ 0 \\ 0 \\ w_{sf}^2 \end{bmatrix} u_2 \tag{4.67}$$

$$y_{2p} = \begin{bmatrix} 1 & 0 & 0 & 0 & 0 & 0 \end{bmatrix} \begin{pmatrix} x_1 \\ x_2 \\ x_3 \\ x_4 \\ x_5 \\ x_6 \end{pmatrix} + \begin{bmatrix} 0 & 1 \end{bmatrix} \begin{pmatrix} \nu \\ u_{1m} \end{pmatrix} \tag{4.68}$$

$$y_{2v} = \begin{bmatrix} 0 & 1 & 0 & 0 & 0 & 0 \end{bmatrix} \begin{pmatrix} x_1 \\ x_2 \\ x_3 \\ x_4 \\ x_5 \\ x_6 \end{pmatrix} + \begin{bmatrix} 0 & 1 \end{bmatrix} \begin{pmatrix} \nu \\ u_{1m} \end{pmatrix} \tag{4.69}$$

$$y_{2a} = \begin{bmatrix} -\frac{k}{m} & -\frac{c}{m} & 0 & \frac{1}{m} & \frac{1}{m} & 0 \end{bmatrix} \begin{pmatrix} x_1 \\ x_2 \\ x_3 \\ x_4 \\ x_5 \\ x_6 \end{pmatrix} + \begin{bmatrix} 0 & 1 \end{bmatrix} \begin{pmatrix} \nu \\ u_{1m} \end{pmatrix}. \tag{4.70}$$

We can clearly see that the acceleration measurement case no longer has any disturbance feedthrough so we must treat it the same as any system without any feedthrough.

In order to streamline the presentation of the simulation results, we will present results for the following controlled output (weighting matrices) cases:

- Without output smoothing filter:

  1. Acceleration measurement:

     (a) Acceleration cost, $y_1^T y_1$, where $y_1 \triangleq y_2 - D_{21m} u_{1m}$

     (b) $y_1 = \begin{pmatrix} \begin{bmatrix} 1 & 0 & 0 & 0 \\ 0 & 1 & 0 & 0 \\ 0 & 0 & 0 & 0 \end{bmatrix} \begin{pmatrix} x_1 \\ x_2 \\ x_3 \\ x_4 \end{pmatrix} \\ \Psi u_2 \end{pmatrix}$

2. Velocity measurement:

   (a) $y_1 = \begin{pmatrix} \begin{bmatrix} 1 & 0 & 0 & 0 \\ 0 & 1 & 0 & 0 \\ 0 & 0 & 0 & 0 \end{bmatrix} \begin{pmatrix} x_1 \\ x_2 \\ x_3 \\ x_4 \end{pmatrix} \\ \Psi u_2 \end{pmatrix}$

   (b) acceleration cost

3. Position Measurement:

   (a) $y_1 = \begin{pmatrix} \begin{bmatrix} 1 & 0 & 0 & 0 \\ 0 & 1 & 0 & 0 \\ 0 & 0 & 0 & 0 \end{bmatrix} \begin{pmatrix} x_1 \\ x_2 \\ x_3 \\ x_4 \end{pmatrix} \\ \Psi u_2 \end{pmatrix}$

   (b) acceleration cost

- With a smoothing filter

1. Acceleration measurement:

   (a) "Pseudo acceleration" weights, $y_1 = \begin{pmatrix} C_2 x \\ \Psi u_2 \end{pmatrix}$

   (b) $y_1 = \begin{pmatrix} \begin{bmatrix} 1 & 0 & 0 & 0 \\ 0 & 1 & 0 & 0 \\ 0 & 0 & 0 & 0 \end{bmatrix} \begin{pmatrix} x_1 \\ x_2 \\ x_3 \\ x_4 \end{pmatrix} \\ \Psi u_2 \end{pmatrix}$

where, $\Psi = 10^{-4}$ unless otherwise noted.

Intuitively, we should (hopefully) be able to get the same degree of disturbance rejection on the simple SMD system regardless of the measurement we use; the difficulty when using an optimal control approach is in the selection of the controlled output equation to obtain the "best" disturbance rejection. The results for the cases with no output smoothing filter are shown in figures 4.2- 4.4. The transfer functions

shown are from force-to-acceleration, force-to-velocity, or force-to-position depending on the system measurement.

We should note that we can achieve some degree disturbance rejection at the disturbance frequency for all cases presented above. What is interesting to note is the increase in the low-frequency response of the H_∞ controller for the position and velocity cases. Additionally, both of the position and velocity LQR and H_∞ controller designs require a larger ratio for the disturbance/measurement covariance to obtain any rejection; when accelerations are measured, lower ratios will generate the desired notch.

When we add the output smoothing filter, we see the same types of behavior as the previous cases when there is no feedthrough except for the LQG case where only additional damping was provided instead of a notch. The results for the SMD system augmented with disturbance dynamics and the output smoothing filter are shown in figure 4.5. The notch generated using the cost from part a), i.e., in this case using $C_2'C_2$ and an orthogonal control weight is deeper than the notch using the ad hoc approach. Additionally, the disturbance/noise covariance ratio must be increased to obtain any performance with the addition of the smoothing filter.

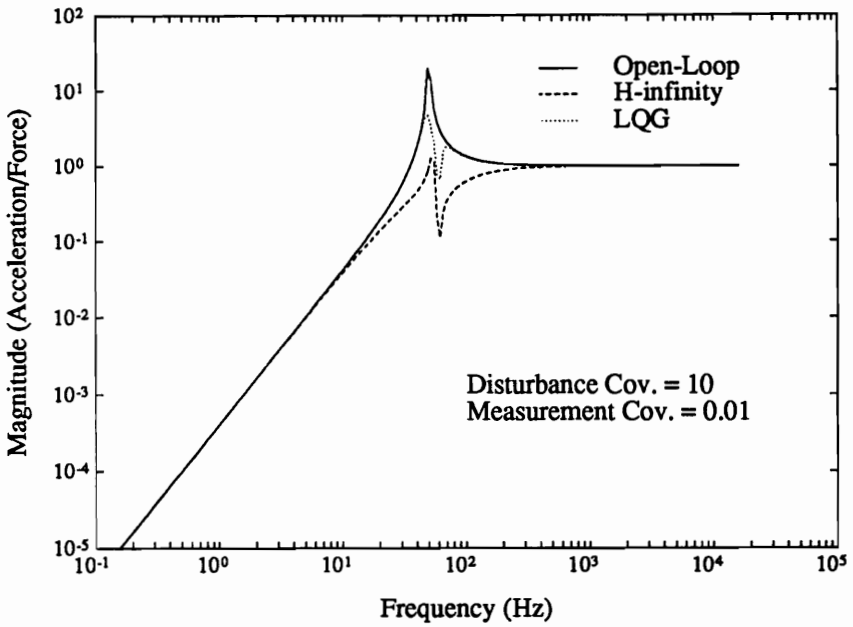

a) acceleration weights

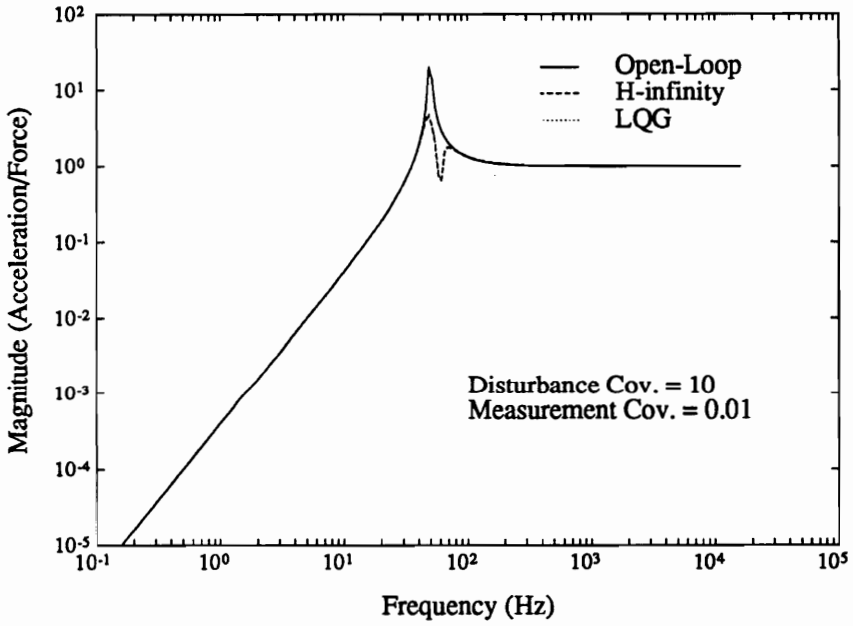

b) position and velocity weights

Figure 4.2: Force-to-acceleration transfer function for SMD example problem.

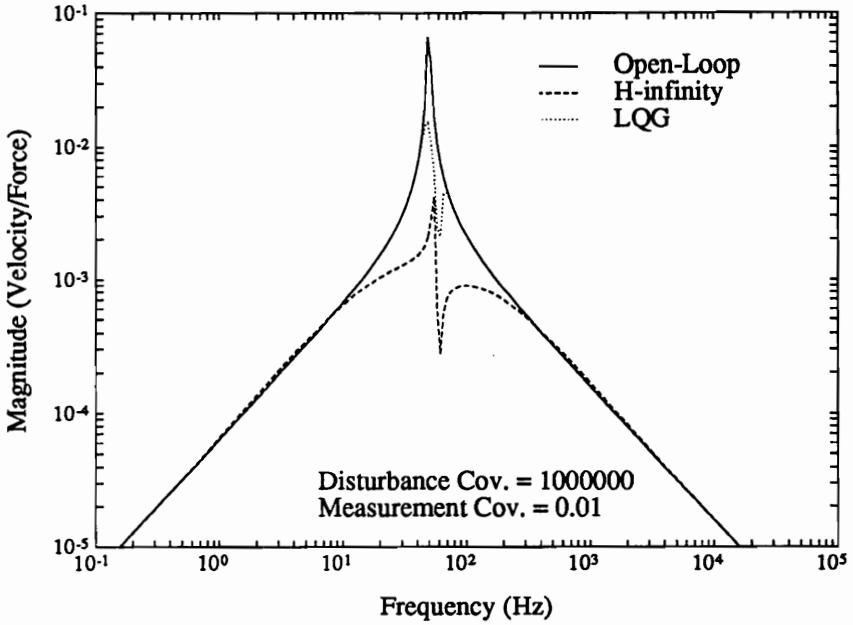

a) position and velocity weights

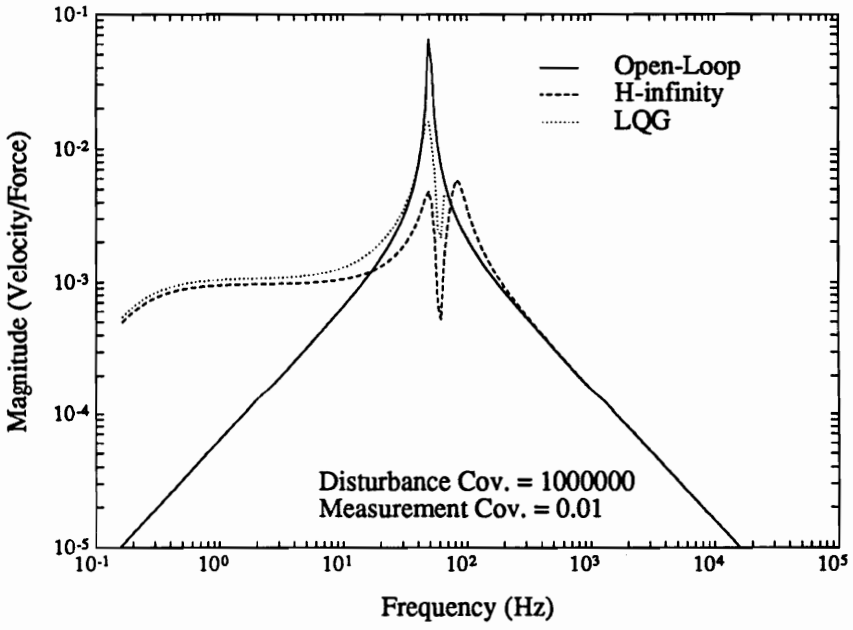

b) acceleration weights

Figure 4.3: Force-to-velocity transfer function for SMD example problem.

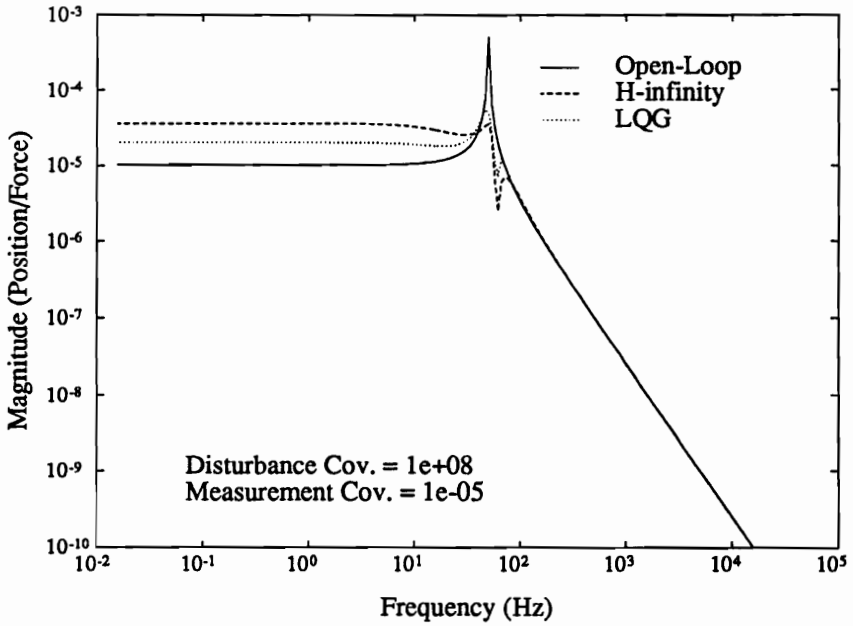

a) position and velocity weights

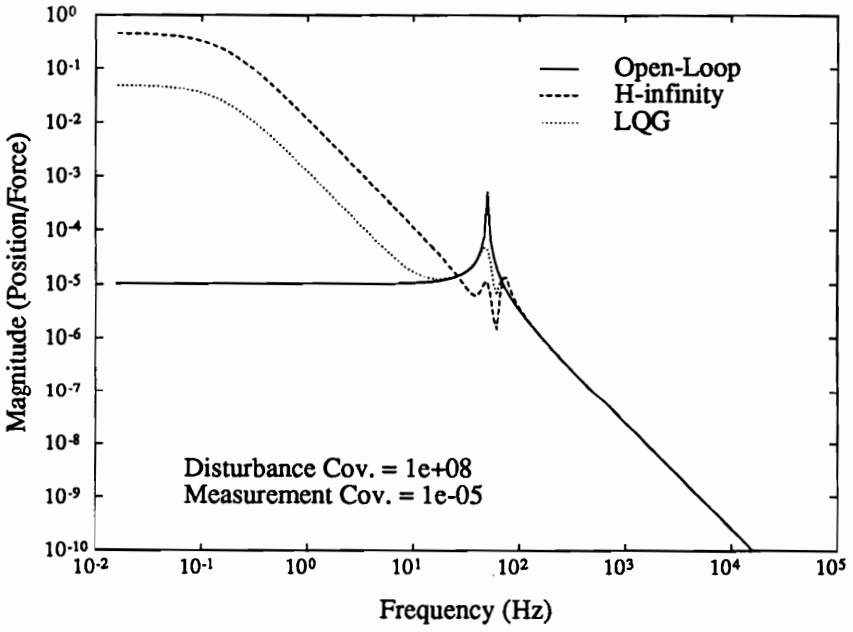

b) acceleration weights, $\Psi = 10^{-3}$

Figure 4.4: Force-to-position transfer function for SMD example problem.

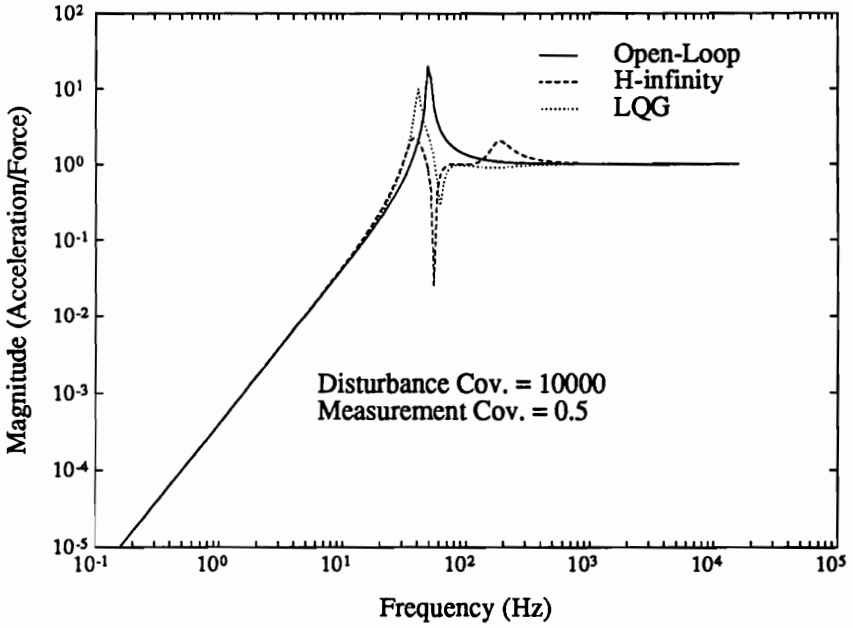

a) pseudo acceleration weights, $\Psi = 1$

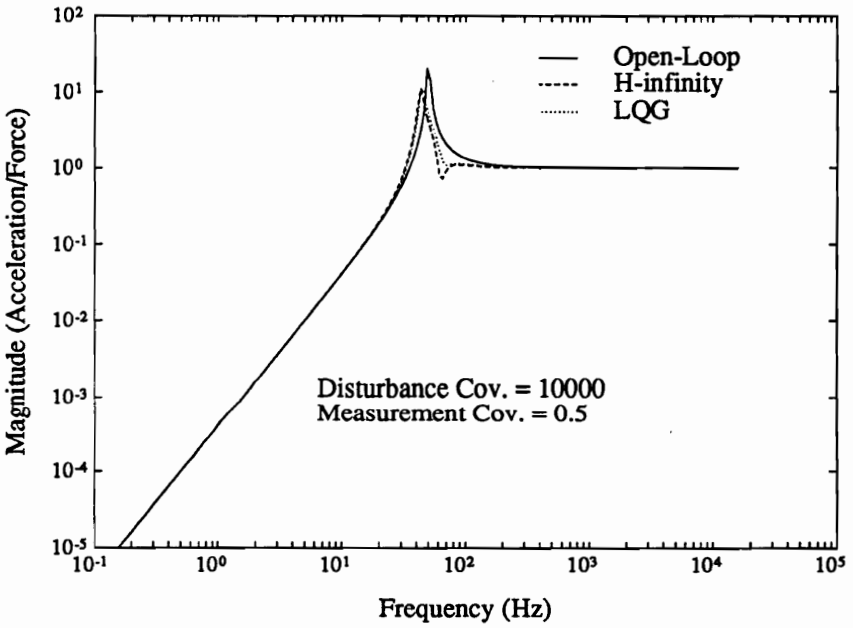

b) position and velocity weights, $\Psi = 10^{-7}$

Figure 4.5: Force-to-acceleration transfer function for SMD example problem with output smoothing filter.

Chapter 5

Disturbance Rejection on a Simply-Supported Plate: Simulation and Experiment

In this chapter, we perform both simulations and experiments for the disturbance rejection problem on a simply-supported plate using the new minimum acceleration design procedure presented in the previous chapter. We are specifically concerned with sinusoidal and narrowband Gaussian disturbance rejection for both H_2 (LQG), and H_∞ controllers. We will design controllers using the following three approaches:

1. Discrete LQG controller (DLQG),
2. Continuous LQG controller transformed via a bilinear transformation to discrete time,
3. Continuous H_∞ controller transformed via a bilinear transformation to discrete time.

We will also compare the open- and closed-loop impulse response for the plate to show the increased damping that both the LQG and H_∞ provide in addition to the

direct disturbance cancellation.

We use the discrete LQG approach because this models the effect of the sampling process of the digital controller correctly. The continuous-time H_∞ controller that has been transformed to discrete is used because the Mu Tools software package only solves the continuous time H_∞ control problem. We use the continuous-time transformed-to-discrete LQG controller for a comparison to the H_∞ and the DLQG to see what type of performance we loose using the continuous-to-discrete approximation approach.

Time-domain results are presented for each individual controller first, and then a comparison of the performance of each controller is given in the frequency domain. The experimental impulse response using each controller is then presented to show the additional damping provided for each case. Much of the data presented here is compared to the results presented in Rubenstein [53]. We do this since he was the first to implement an LQG controller on the simply-supported plate and this gives us a basis for determining whether or not the "minimum acceleration" design approach has merit.

5.1 Experimental Apparatus and Control Hardware

We will briefly discuss the simply-supported plate and associated control hardware that is used for the experiments in this section. The full details of the apparatus are presented in Rubenstein [53].

The plate is a rectangular, 0.5m × 0.6m × 2.9mm cold-rolled steel plate that is approximately simply-supported by the radial mounting of the edges of the plate with soft shim-stock to a heavy steel frame. There is an array of twelve accelerometers on the front of the plate arranged so the first twelve modes of the plate are observable. There are two electromagnetic shakers attached to the back side of the plate that are collocated with two of the accelerometers. One shaker is used to provide the (unmeasured) disturbance, and the other shaker is used for the control force. The shakers are positioned so they can affect the first two modes of the plate and are also located near the nodal lines for the third and fourth mode in an effort to minimize possible spillover effects.

The controller consists of a parallel processing system based on transputers (a microprocessor designed for parallel processing) hosted by a PC compatible system. The controller has sixteen channels of analog-to-digital, 12-bit inputs with simultaneous sample/hold capability and sixteen channels of 12-bit digital-to-analog outputs. The maximum sample rate is 100Khz for one channel on the input (sample rate for more channels is 100Khz/number of channels) and 100KHz per channel on the outputs. More information on the data acquisition and control system can be found in Ellis [54].

5.2 Control System Design

This section contains the development of the analytical model used for the control system design for all three cases mentioned above. Since we only have one control

actuator, and to simplify the experiments, a two-plate-mode controller was used for all cases.

Rubenstein [53] performed both finite element and modal analyses of the simply-supported plate in order to develop a state-space model for the control system design. The state-space model for the plate is given by:

$$\dot{x} = Ax + B_1 u_{1d} + B_2 u_2 \tag{5.1}$$

$$y_2 = C_2 x + D_{21d} u_{1d} + D_{21m} u_{1m} + D_{22} u_2. \tag{5.2}$$

or, if we expand the equations above using the plate modal model, we find:

$$\begin{aligned} \frac{d}{dt}\begin{pmatrix} x_p \\ x_v \end{pmatrix} &= \begin{bmatrix} 0 & I \\ -\Omega^2 & -2Z\Omega \end{bmatrix}\begin{pmatrix} x_p \\ x_v \end{pmatrix} + \begin{bmatrix} 0 & 0 \\ Q_{u_1} & 0 \end{bmatrix}\begin{pmatrix} u_{1d} \\ u_{1m} \end{pmatrix} \\ &\quad + \begin{bmatrix} 0 \\ Q_{u_2} \end{bmatrix} u_2 \end{aligned} \tag{5.3}$$

$$\begin{aligned} y_2 &= \begin{bmatrix} -\Omega^2 & -2Z\Omega \end{bmatrix}\begin{pmatrix} x_p \\ x_v \end{pmatrix} + \begin{bmatrix} Q_{u_1} & D_{21m} \end{bmatrix}\begin{pmatrix} u_{1d} \\ u_{1m} \end{pmatrix} \\ &\quad + Q_{u_2} u_2 \end{aligned} \tag{5.4}$$

where the variables and their dimensions are defined as follows:

$x_p \in R^{n_m} \triangleq$ modal position

$x_v \in R^{n_m} \triangleq$ modal velocity

$u_{1d} \in R^p \triangleq$ disturbance input

$u_{1m} \in R^l \triangleq$ measurement (sensor) noise

$u_2 \in R^m \triangleq$ control input

$y_2 \in R^l \triangleq$ measurement, modal acceleration.

Since we have one external disturbance and one control actuator, $m = n = 1$ and since we are using a two-plate-mode controller, $n_m = 2$.

The modal frequencies, Ω, and the modal damping ratios, Z are defined to be:

$$\begin{aligned} \Omega &\triangleq \text{diag}\{w_1, w_2, \ldots, w_{n_m}\} \\ &= 2\pi \cdot \text{diag}\{f_1, f_2, \ldots, f_{n_m}\} \\ Z &\triangleq \text{diag}\{\zeta_1, \zeta_2, \ldots, \zeta_{n_m}\}. \end{aligned}$$

The first nine modal frequencies and damping ratios for the plate are shown in table 5.1.

Table 5.1: Natural Frequencies and Damping Ratios for the Simply-Supported Plate.

Mode Number	Frequency (Hz)	Damping Ratio
1	49.45	0.0077228
2	108.96	0.0171460
3	130.25	0.0083185
4	188.53	0.0027311
5	203.25	0.0027250
6	265.62	0.0023876
7	285.78	0.0012244
8	326.08	0.0013216
9	338.30	0.0022209

The two terms Q_{u_1} and Q_{u_2} are the eigenvectors corresponding to the disturbance and control inputs respectively. They can be extracted from the 12×9 experimental eigenvector matrix since the disturbance and control shakers are each collocated with one of the plate accelerometers. The disturbance coefficients correspond with the

5^{th} row of Q and the control coefficients correspond with the 8^{th} row of Q. That is,

$$Q_{u_1} = q_5^T, \text{ and } Q_{u_2} = q_8^T$$

where $q_i \triangleq$ the i^{th} row of Q.

The 12 $\times$ 9 experimental eigenvector matrix Q is shown below:

$$\begin{bmatrix}
0.2068 & -0.5350 & 0.4716 & -0.6245 & -0.4200 & -0.3708 & -0.5257 & -0.6133 & -0.2620 \\
0.4290 & -0.7181 & 0.1104 & -0.1516 & -0.6814 & 0.4496 & -0.0798 & 0.6420 & -0.4180 \\
0.3072 & -0.4771 & -0.5241 & 0.6138 & -0.4607 & -0.3951 & 0.4640 & -0.6078 & -0.2086 \\
0.4001 & -0.2333 & 0.8233 & -0.1619 & 0.3468 & -0.6213 & 0.5346 & -0.2604 & 0.4473 \\
0.7033 & -0.3062 & 0.1353 & -0.0554 & 0.5246 & 0.6389 & 0.1319 & 0.3292 & 0.6070 \\
0.4829 & -0.1404 & -0.9120 & 0.4227 & 0.3599 & -0.6038 & -0.6515 & -0.2957 & 0.3680 \\
0.4468 & 0.2215 & 0.7428 & 0.6210 & 0.3438 & -0.6273 & 0.6039 & 0.3454 & -0.3710 \\
0.7033 & 0.3664 & 0.1091 & 0.2185 & 0.5573 & 0.6715 & 0.1343 & -0.4100 & -0.5521 \\
0.4480 & 0.2853 & -0.8733 & -0.4771 & 0.3848 & -0.6201 & -0.6411 & 0.3428 & -0.3926 \\
0.2803 & 0.4538 & 0.5085 & 1.0755 & -0.5294 & -0.3369 & -0.7840 & 0.6357 & 0.1768 \\
0.4365 & 0.7018 & 0.0766 & 0.2210 & -0.7149 & 0.4368 & -0.1769 & -0.8063 & 0.3551 \\
0.1884 & 0.4729 & -0.5331 & -1.0680 & -0.4109 & -0.3970 & 0.7980 & 0.5814 & 0.1820
\end{bmatrix}$$

Even though we have twelve accelerometers, we only have nine usable modes from the experimental system identification, so $l = 9$. We use a least-squares transformation to map from the twelve-mode space to a nine-mode space. Even though we are using only a two-mode controller in this case, we truncate the nine-mode space to two-modes rather than perform a least-squares projection from twelve-modes to two-modes. Retaining the nine modes and truncating to the desired number of modes decreases the opportunity for modal spillover because of the non-orthogonality of the least-squares projection and the original basis. We call the operation of transforming from the measurement space to the modal acceleration space *modal filtering.*

Since we use a digital controller, the control signal consists of a series of step func-

tions. To decrease the high-frequency content of the control signal, it is passed through a second order, unity gain Sallen-Key low-pass filter with a 120 Hz cutoff frequency to smooth the control signal before it is fed to the amplifier and then the control actuator. The Sallen-Key filter was chosen because it is easily realizable. The Sallen-Key smoothing filter is modelled as:

$$\dot{x}_s = A_s x_s + B_s u_s \tag{5.5}$$

$$y_s \triangleq u_s = C_s x_s \tag{5.6}$$

where u_2 is the output from the digital controller and u_s is the smoothed control signal to be input to the control shaker on the plate. The coefficients for the smoothing filter are as follows:

$$A_s = \begin{bmatrix} 0 & 1 \\ -\omega_s^2 & -2\zeta_s\omega_s \end{bmatrix}$$

$$B_s = \begin{bmatrix} 0 \\ w_s^2 \end{bmatrix}$$

$$C_s = \begin{bmatrix} 1 & 0 \end{bmatrix}$$

where, $w_s = 2\pi \cdot 120$, and $\zeta_s = 0.707$.

We also need to include the assumed disturbance dynamics to the nominal model since we are assuming a narrowband disturbance input. The model is the same as presented in Chapter 4 and in state-space form is given by

$$\dot{x}_f = A_f x_f + B_f \nu \tag{5.7}$$

$$y_f \triangleq u_{1d} = C_f x_f \tag{5.8}$$

where ν is a Gaussian white noise source, $N(0,1)$. The nominal coefficients for the disturbance dynamics are as follows:

$$\begin{aligned} A_f &= \begin{bmatrix} 0 & 1 \\ -\omega_f^2 & -2\zeta_f\omega_f \end{bmatrix} \\ B_f &= \begin{bmatrix} 0 \\ 1 \end{bmatrix} \\ C_f &= \begin{bmatrix} 0 & 1 \end{bmatrix} \end{aligned}$$

where, $w_f = 2\pi \cdot 55$, and $\zeta_s = 0.1$.

The reason that we said that the disturbance filter specifications presented above are nominal is that the damping ratio, ζ_s can be used as a tuning parameter in the control system design. This will be discussed below.

If we bundle all of these subsystems together and also put it in the standard H_∞ state-space form we have

$$\begin{aligned} \begin{pmatrix} \dot{x} \\ \dot{x}_f \\ \dot{x}_s \end{pmatrix} &= \begin{bmatrix} A & B_{1_d}C_f & B_2C_s \\ 0 & A_f & 0 \\ 0 & 0 & A_s \end{bmatrix} \begin{pmatrix} x \\ x_f \\ x_s \end{pmatrix} + \begin{bmatrix} 0 & 0 \\ B_f & 0 \\ 0 & 0 \end{bmatrix} \begin{pmatrix} \nu \\ u_{1m} \end{pmatrix} \\ &\quad + \begin{pmatrix} 0 \\ 0 \\ B_s \end{pmatrix} u_2 \qquad (5.9) \\ &\triangleq A_a x_a + B_{1_a} u_1 + B_{2_a} u_2 \qquad (5.10) \\ y_2 &= \begin{bmatrix} C_2 & D_{21_d}C_f & D_{22}C_s \end{bmatrix} \begin{pmatrix} x \\ x_f \\ x_s \end{pmatrix} + \begin{bmatrix} 0 & D_{21_m} \end{bmatrix} \begin{pmatrix} \nu \\ u_{1m} \end{pmatrix} \\ &\quad + [0]u_2 \qquad (5.11) \\ &\triangleq C_a x_a + D_{21_a} u_1 + D_{22_a} u_2 \qquad (5.12) \end{aligned}$$

The external disturbance can either be a sine wave or a narrowband Gaussian disturbance. The sine wave is generated using a precision signal generator and the narrowband Gaussian is generated on a separate transputer system so the disturbance dynamics can be precisely controlled. This digitally generated narrowband disturbance contains undesired high frequency components due to sampling just like the control signal, so it is also smoothed using a low-pass filter. Notice that as long as the smoothing filter does not affect the disturbance in its pass-band, we do not need to include its effects in our disturbance model.

5.2.1 Discrete LQG Controller

The discrete-time LQG controller accounts directly for the sampling behavior of the digital controller and is implemented as a predictor-corrector to account for the implicit delay in the closed-loop control. The controller is implemented as a Kalman filter state-estimator and a state-feedback LQR controller. The real-time implementation is as follows:

$$\begin{aligned}
\hat{x}_{k|k-1} &= A_a \hat{x}_{k-1|k-1} + B_a u_{2_{k-1}} \\
u_{2_k} &= -C_{lq} \hat{x}_{k|k-1} \\
\hat{y}_k &= C_a \hat{x}_{k|k-1} + D_a u_{2_k} \\
\hat{x}_{k|k} &= \hat{x}_{k|k-1} + K_f (y_k - \hat{y}_k)
\end{aligned}$$

where A_a, B_a, C_a , D_a are the augmented system matrices; C_{lq} and K_f are the state-feedback and Kalman filter gains respectively; $\hat{y}_k$ is an estimate of the measurement y_k (modal accelerations after transformation); and the notation $\hat{x}_{k|k-1}$ means the

estimated value of $\hat{x}$ at the k^{th} time step given measurements up to the $(k-1)^{st}$ time step. More details on the discrete Kalman filter and LQG control can be found in Chui [55] and Stengel [52] respectively.

Since the augmented plant dynamics include a smoothing filter, we must use a cost function with a separate weight on the control signal. We assume the cost function has the form:

$$y_1 = \begin{pmatrix} C_a x_a \\ \rho u_2 \end{pmatrix}.$$

where ρ is a scalar weight since we only have one actuator, and C_a is from the augmented plant model above.

In order to get quadratic weighting matrices for use in the DLQG computation, we must compute $y_1^T y_1$. We must also account for the effect of the external disturbance and measurement noise covariances in the augmented plant model since we do not normally have $N(0,1)$ Gaussian signals. The system equations are modified as discussed in Chapter 4 yielding the following equations that are used in the controller design:

$$\dot{x}_a = A_a x_a + B_{1_a}(\Xi)^{\frac{1}{2}} u_1 + B_{2_a} u_2 \tag{5.13}$$

$$y_2 = C_a x_a + D_{21_a}(\Lambda)^{\frac{1}{2}} u_1 + D_{22_a} u_2 \tag{5.14}$$

where Ξ and Λ are the disturbance and measurement noise covariances respectively. At this point, values for ρ and ζ_f must be selected and the closed-loop system simulated in order to determine the effect of the controller.

Linear systems theory tells us that we can use as high a gain set as we would like to obtain the desired performance. Reality tells us that with system nonlinearities like actuator saturation and unmodelled effects that can cause modal spillover to deal with, we must strike a careful balance between performance and stability. Also, since we are concerned with maximum possible performance for each controller, we do not normalize the controllers such that they each use the same control energy or power. Each controller is optimized for the maximum possible disturbance rejection.

After several trials and tribulations, the following parameters were determined to be the "best" in terms of closed-loop disturbance rejection and closed-loop stability. The word "best" here means that in a non-rigorous sense, no other set of design parameters provides more closed-loop rejection of the persistent disturbance and a stable closed-loop system than the ones presented here. For example, if the control penalty is lowered, the actuator will saturate and the closed-loop system will go unstable. The values used for both the harmonic and narrowband disturbance rejection problems are shown in table 5.2.

The implications of the differences in the design parameters between the harmonic and the narrowband cases will be discussed after the results for all three controllers has been presented.

Table 5.2: Design Parameters for the DLQG Controller.

	Harmonic Disturbance	Narrowband Disturbance
Control Weight, ρ	0.6	0.2
Disturbance Filter Damping ζ_f	0.01	0.1
Disturbance Covariance Ξ	500	500
Measurement Covariance Λ	25	25

DLQG Harmonic Disturbance Rejection Results

The 55Hz harmonic disturbance was scaled so that the peak mode-one acceleration was approximately 12 $\text{kg}^{\frac{1}{2}}\frac{\text{m}}{\text{s}^2}$ to match the peak accelerations presented in Rubenstein. Lower values of peak acceleration would tolerate a higher gain setting (lower control penalty) before an unstable closed-loop controller resulted, so in the interest of fair comparisons, the same disturbance magnitude was used in this study also.

The time histories for mode-one simulation and experimental results and mode-two simulation and experimental results are shown in figures 5.1 and 5.2 respectively. We see that when the controller is activated, the modal acceleration for mode one achieves steady-state values in approximately 0.1 seconds and mode two in approximately 0.2 seconds. The external disturbance is not completely eliminated from

mode one; however, there is about a 20dB reduction in the mode one response from the open-loop to closed-loop. Notice also that there is an increase in the second mode response. This is due to the control actuator location and the relative phasing of modes one and two.

The agreement between experimental and simulated mode one response is exceptional. There is just a slight "glitch" in the experimental data during the turn-on transient when compared to the simulation. Additionally, the closed-loop amplitude matches to within a few percent. Mode two data does not look quite as good in terms of amplitude. Part of the reason may be that the simulated mode two response was not given adequate time to reach steady-state before the loop was closed. Another reason may be that the modal spillover and unmodelled effects are "contaminating" the modal filter for mode two. The amplitude discrepancy for the mode two simulation and experiment is probably due to the experimental system identification. The system identification for the plate matches the simulation around mode one but there is some question as to the accuracy of the mode two since the analytical and experimental modal amplitudes differ by approximately a factor of two.

DLQG Narrowband Disturbance Rejection Results

The narrowband disturbance was scaled so that peak accelerations were again approximately 12 $\text{kg}\frac{1}{2}\frac{\text{m}}{\text{s}^2}$ for mode one. Because of the difficulty of duplicating the same random signal for both the simulation and experiment, the time-domain results for the narrowband case are difficult to compare. A frequency domain comparison of all controllers will be presented in section 5.2.4 below which will give a better idea as

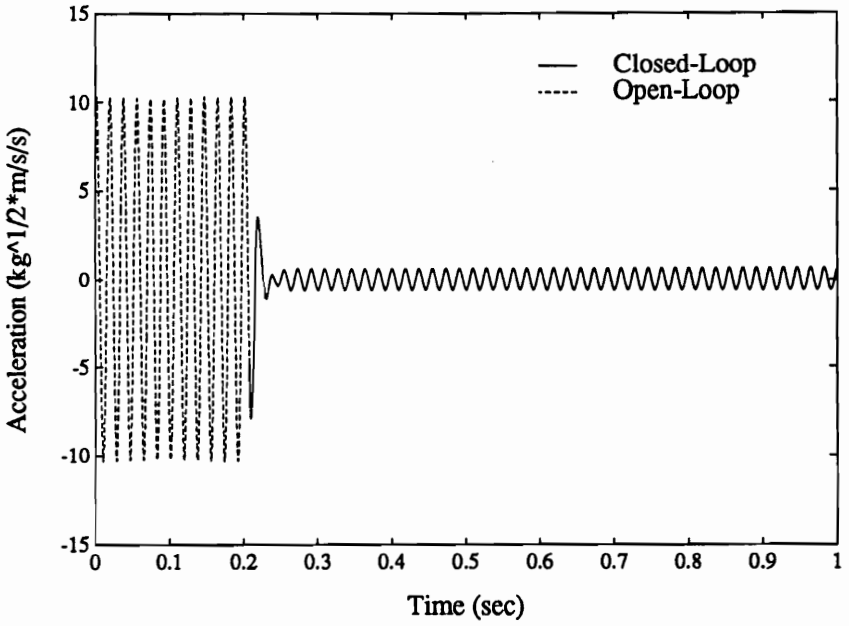

a) simulated data

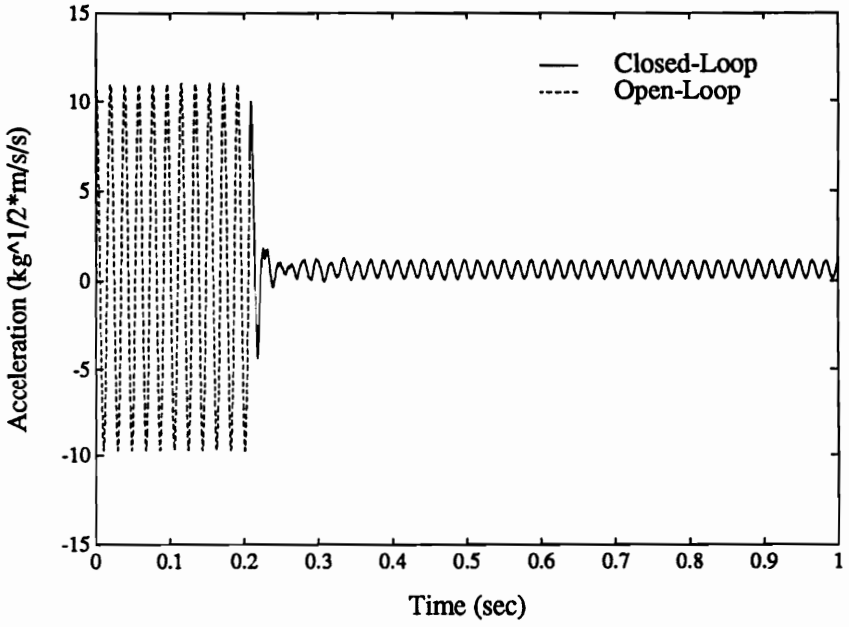

b) experimental data

Figure 5.1: DLQG Harmonic Disturbance Rejection: Mode 1

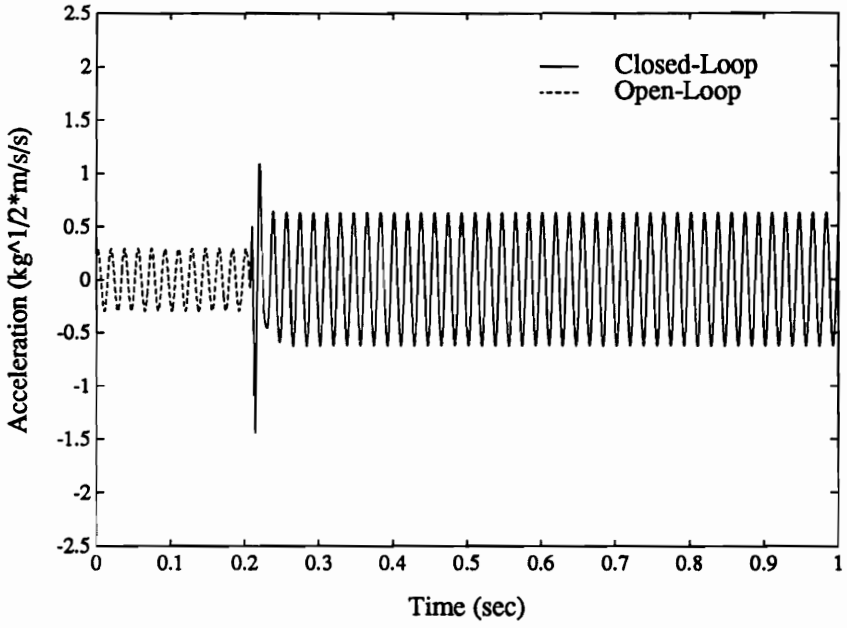

a) simulated data

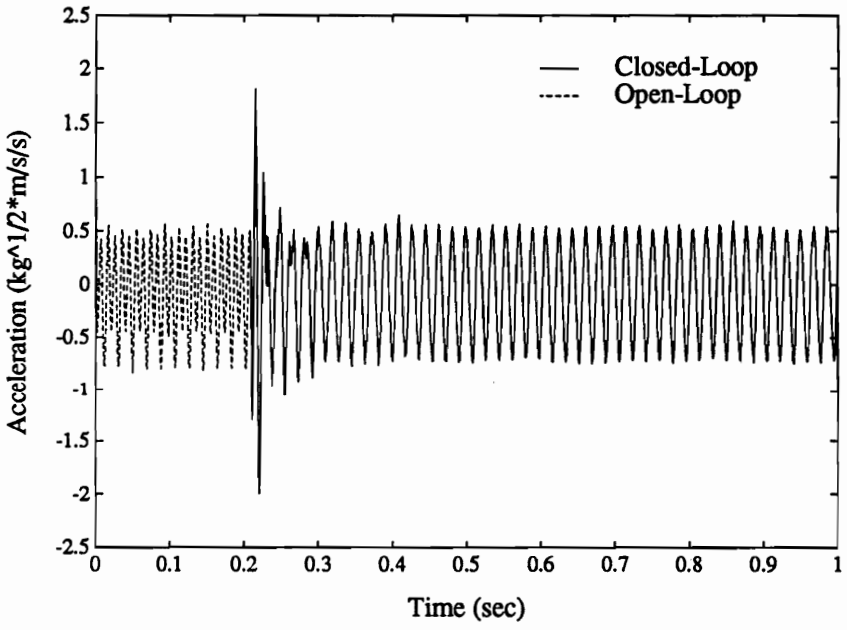

b) experimental data

Figure 5.2: DLQG Harmonic Disturbance Rejection: Mode 2

to the actual performance of the DLQG narrowband controller. The time-domain results for the narrowband DLQG controller are given in figures 5.3 and 5.4.

5.2.2 Continuous LQG Controller

The continuous controller design differs slightly from its discrete-time counterpart in that it does not have the predictor-corrector form. The continuous time LQG controller can be expressed as a strictly-proper transfer function. Using our earlier notation, we have,

$$K_{lqg} = \left[\begin{array}{c|c} \hat{A} & \hat{B} \\ \hline \hat{C} & 0 \end{array}\right]$$

or in the time domain,

$$\begin{aligned} \dot{\hat{x}} &= \hat{A}\hat{x} + \hat{B}y_2 \\ u_2 &= \hat{C}\hat{x}. \end{aligned}$$

If we use the following bilinear transformation to map our controller from the left-half-plane to the unit disk (from the s-plane to the z-plane),

$$z = \frac{1 + \left(\frac{T}{2}\right)s}{1 - \left(\frac{T}{2}\right)s}$$

where T is the sample period, we end up with the following discrete-time proper controller:

$$\begin{aligned} \tilde{x}_{k+1} &= \tilde{A}\tilde{x}_k + \tilde{B}y_{2_k} \\ u_{2_{k+1}} &= \tilde{C}\tilde{x}_k + \tilde{D}y_{2_k} \end{aligned}$$

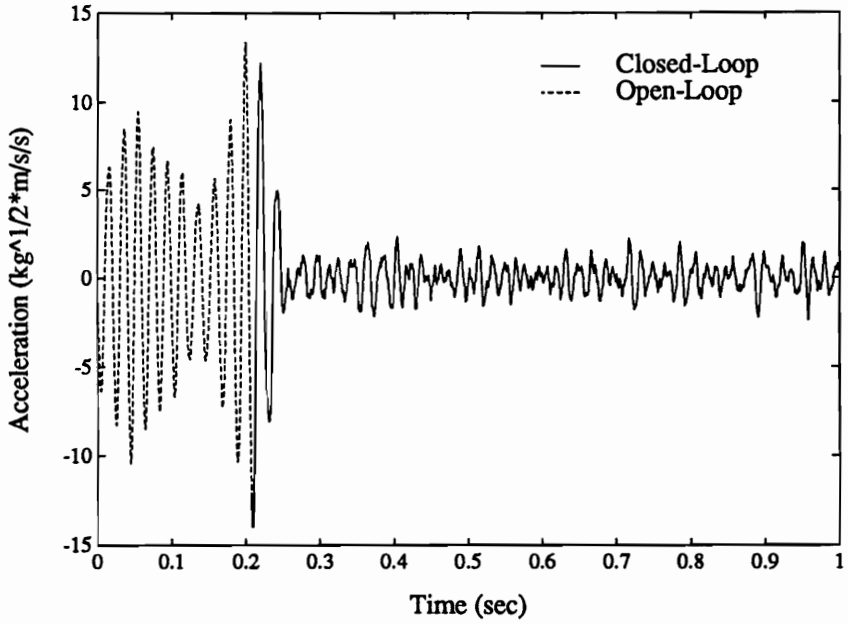

a) simulated data

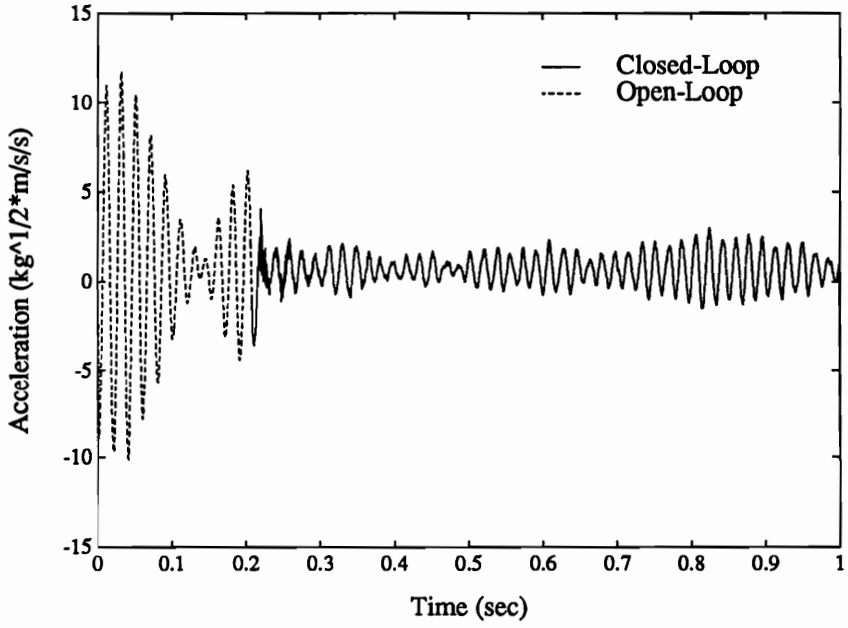

b) experimental data

Figure 5.3: DLQG Narrowband Disturbance Rejection: Mode 1

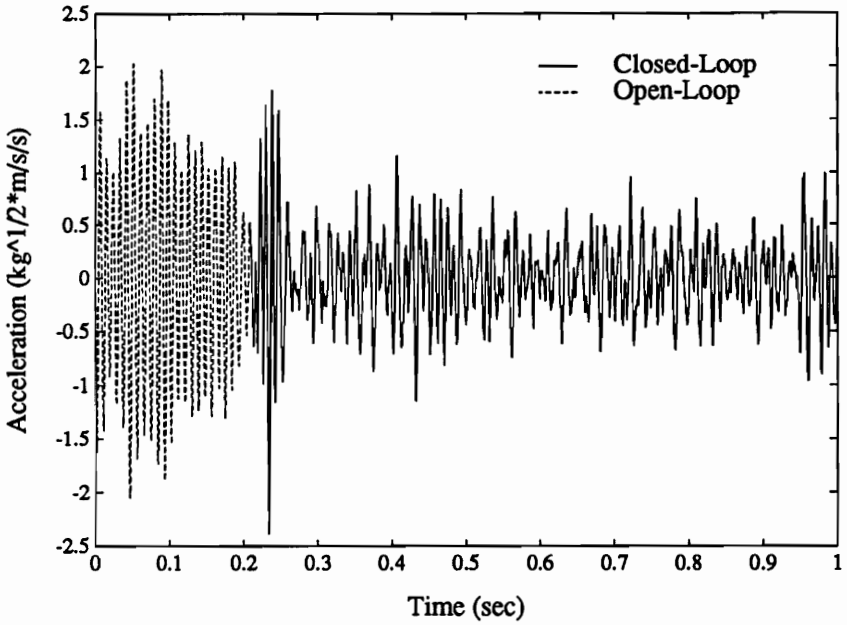

a) simulated data

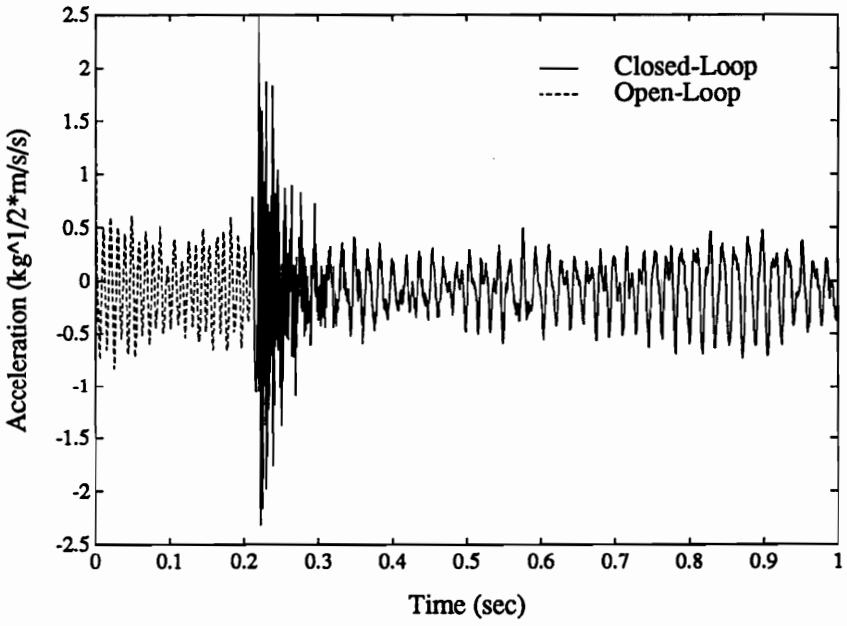

b) experimental data

Figure 5.4: DLQG Narrowband Disturbance Rejection: Mode 2

In addition from obtaining a non-zero D term (proper versus strictly proper transfer function) we loose the sparseness of the original system matrices when we perform the bilinear transformation which may degrade attainable sample rate due to the additional computations required for a non-sparse matrix multiplication.

We have also not accounted for the inherent delay in a sampled data controller when we perform the continuous-to-discrete transformation. One method of doing this is to use a Padé approximation for the delay and append these extra dynamics to the controller to account for the delay.

The first order Padé approximation for the delay is:

$$e^{-sT} \approx \frac{1 - \left(\frac{T}{2}\right) s}{1 + \left(\frac{T}{2}\right) s}.$$

LQG controllers with and without the delay modelled were tested. Since the sample rate for the closed-loop LQG controller without the delay approximated is 2600Hz and the controller only uses information up to the second modal frequency at 109Hz, the difference between modelling the delay and not modelling the delay is insignificant. Correspondingly, we will use the controller approximation without the delay.

We choose the controller design parameters for the LQG controller in the same manner as the DLQG case for both the harmonic and narrowband controllers: maximum disturbance rejection and closed-loop stability. These design weights are summarized in table 5.3. Note that the design parameters are significantly different than the ones obtained for the DLQG controller.

Table 5.3: Design Parameters for the LQG Controller.

	Harmonic Disturbance	Narrowband Disturbance
Control Weight, ρ	0.6	0.05
Disturbance Filter Damping ζ_f	0.05	0.1
Disturbance Covariance Ξ	500	500
Measurement Covariance Λ	0.5	0.2

Initially, the DLQG design weights were used as a "first guess;" however, these weights did not provide any closed-loop performance due to low control signals levels being commanded. Investigation into the lack of closed-loop performance showed that the output injection gains, $\hat{B}$, were so low that the controller dynamics were not effectively driven. Lowering the measurement noise covariance to decrease the "penalty" on the measurement process provided the necessary increase in $\hat{B}$ to allow the control system dynamics to function properly.

LQG Harmonic Disturbance Rejection Results

The simulation and experimental data for the 55Hz harmonic disturbance case are shown in figures 5.5 and 5.6.

The LQG results show the same trends as the DLQG results; however, the disturbance rejection obtained using the continuous LQG design and then converting to discrete-time does not provide the same degree of disturbance rejection available as the discrete-time design procedure. Given the relatively high sample rates achieved, this lack of performance when compared to the DLQG is surprising. One possible explanation for this result is that the DLQG control signal is based on a one-step prediction of the future state of the plate while the LQG is based on measured values. Another explanation is the error introduced by approximating the discrete controller with a bilinear-transformed continuous system. Unfortunately, we can not compare the two differently formulated controllers directly since their forms differ. The discrete design yields a controller with a strictly-proper transfer function while the continuous-to-discrete approach yields a proper controller.

LQG Narrowband Disturbance Rejection Results

The LQG narrowband time-domain results are shown in figures 5.7 and 5.8. Again, it is difficult to make any general conclusions about the performance of the closed-loop controllers with this type of time-domain data since the disturbance inputs differ; but, the general attenuation achieved can be seen.

5.2.3 H_∞ Controller

The continuous-time H_∞ controller is developed using exactly the same approach as the LQG controller presented above except we solve the infinity-norm problem

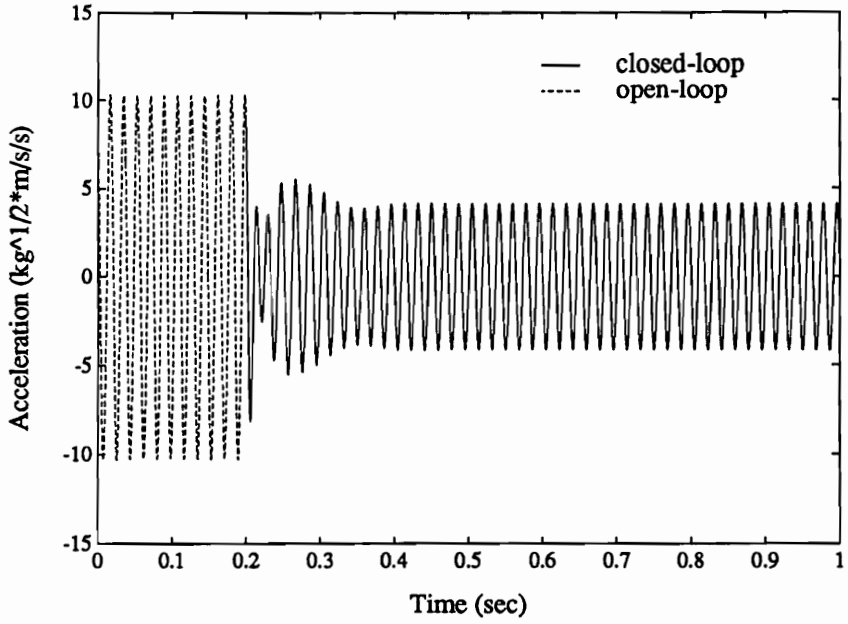

a) simulated data

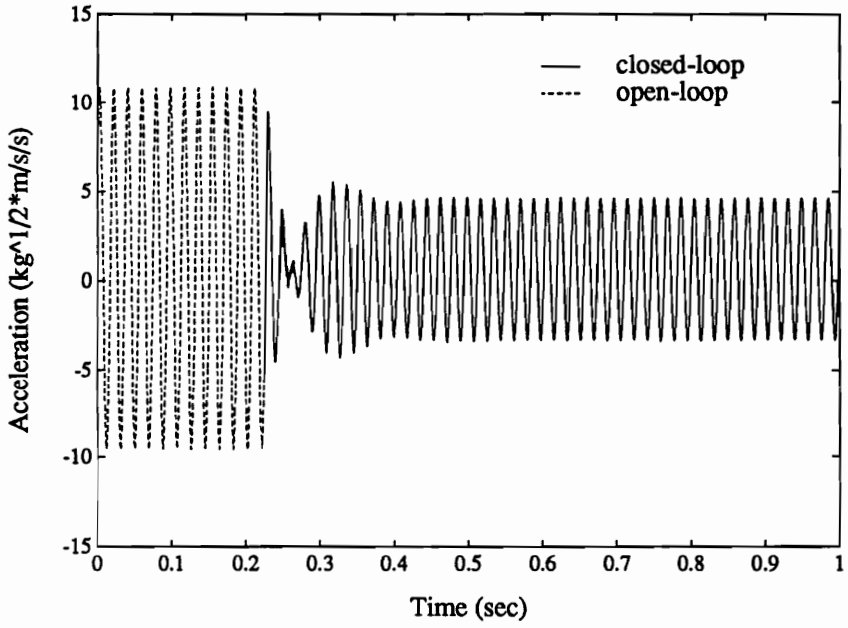

b) experimental data

Figure 5.5: LQG Harmonic Disturbance Rejection: Mode 1

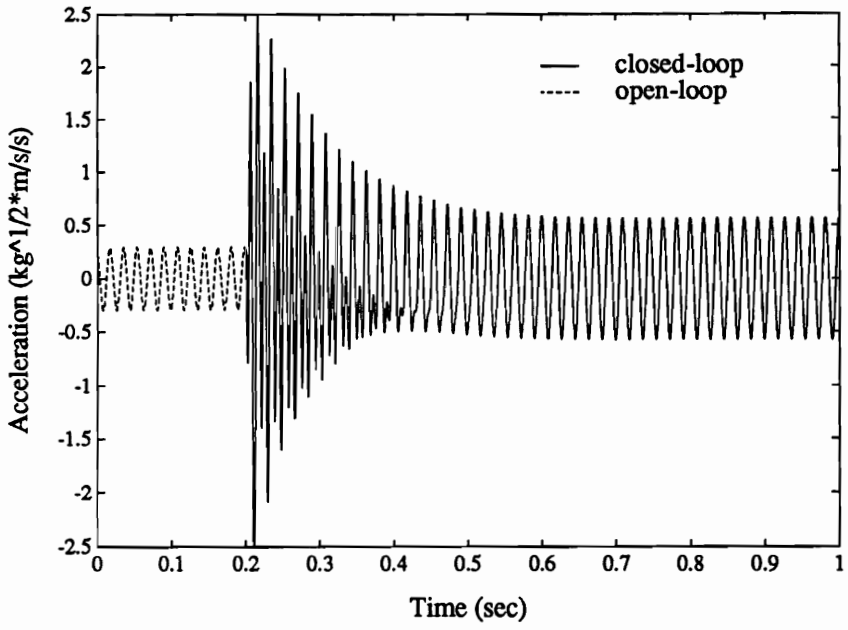

a) simulated data

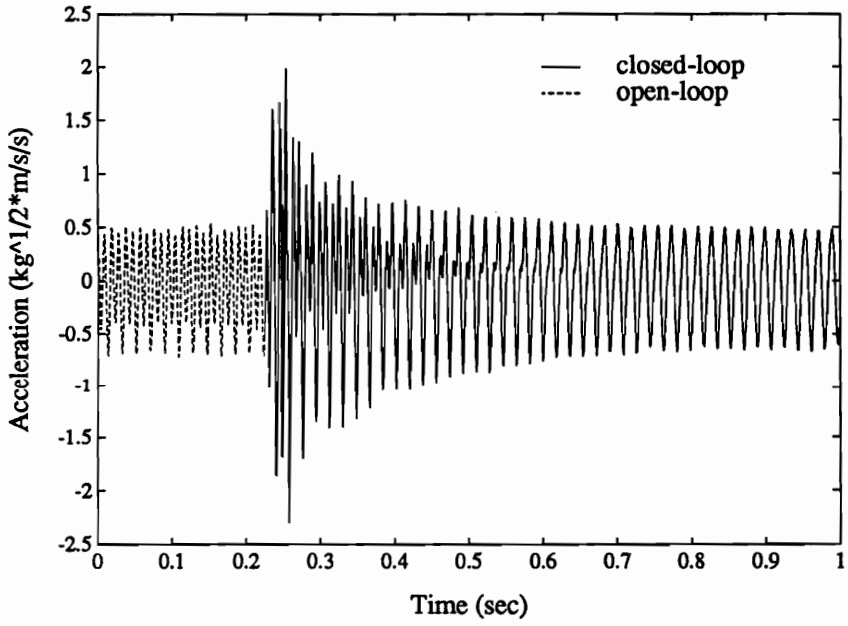

b) experimental data

Figure 5.6: LQG Harmonic Disturbance Rejection: Mode 2

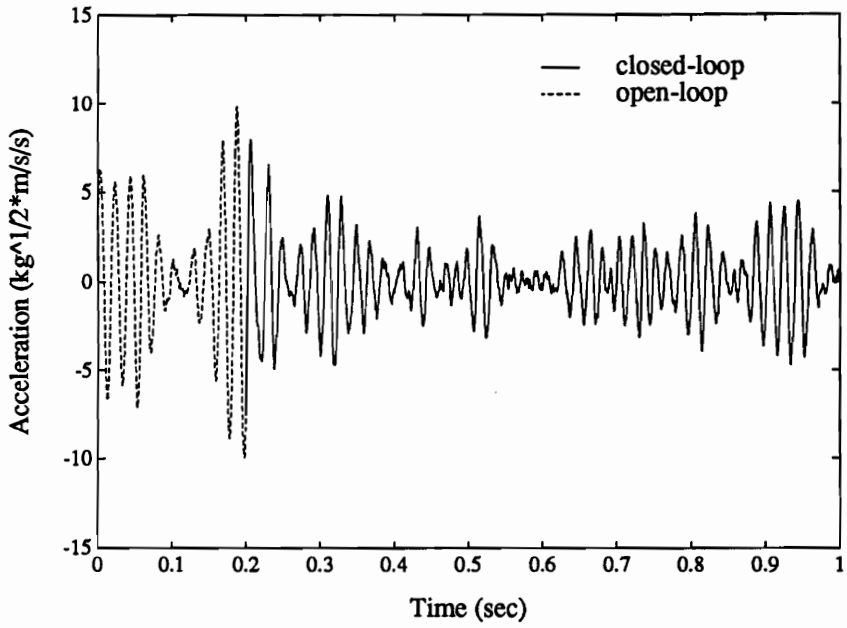

a) simulated data

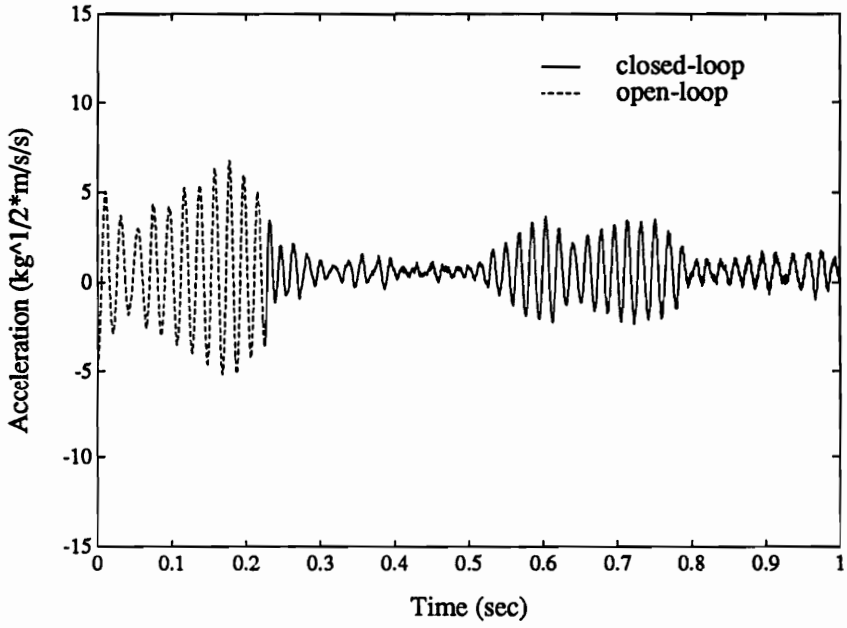

b) experimental data

Figure 5.7: LQG Narrowband Disturbance Rejection: Mode 1

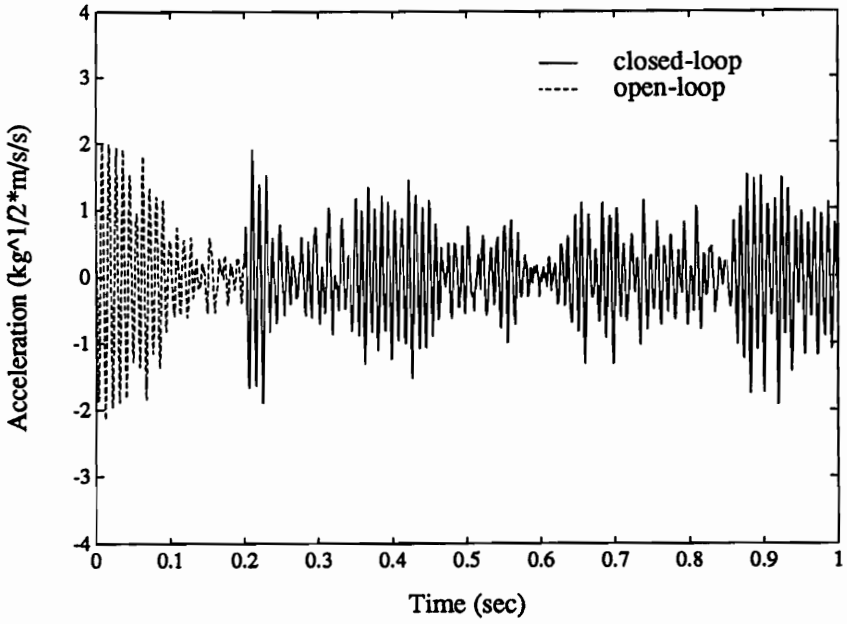

a) simulated data

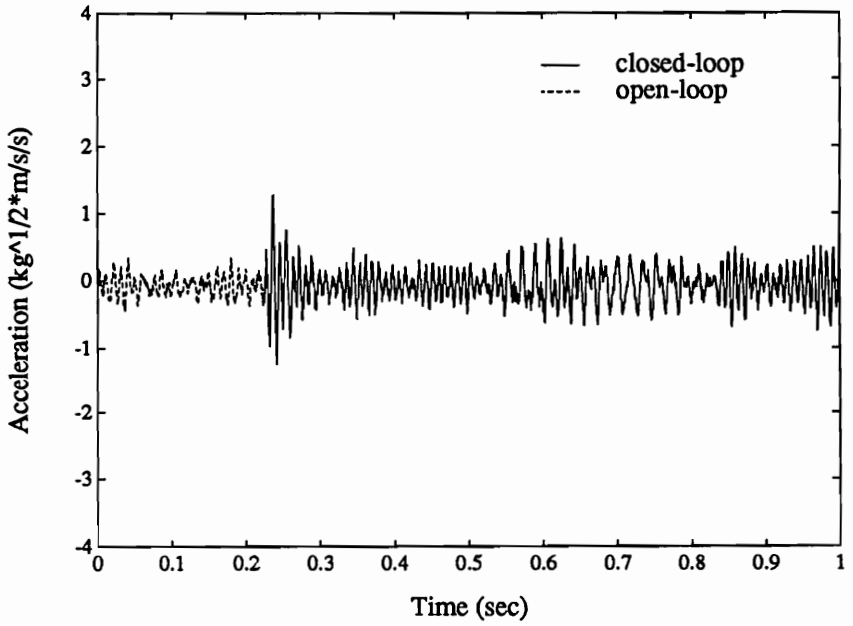

b) experimental data

Figure 5.8: LQG Narrowband Disturbance Rejection: Mode 2

instead of the 2-norm problem. The results are similar to the LQG case except we are able to obtain slightly more disturbance rejection than the LQG controller and not as much as the DLQG controller. Quantitative results will be presented below in the frequency domain section.

The same comparisons are made here that were made above: 55Hz harmonic and narrowband experiment and simulation. The design parameters used for the H_∞ controller are shown in table 5.4. Initially, the same weights as the LQG case were used, but because of the higher loop gains obtained when using the H_∞ approach, the design weights had to be decreased to obtain a stable controller. This is because the H_∞ controller is effectively trying to minimize the maximum singular value of the closed-loop transfer function. In this problem, this occurs at the disturbance frequency and there are correspondingly higher gains at that frequency with H_∞ than with LQG with the same design weights.

The experimental and simulation results for the H_∞ controller are shown in figures 5.9 through 5.12.

5.2.4 Frequency Domain Comparison of the Different Controllers

Unfortunately, the time-domain results presented above are not adequate to determine quantitatively the performance of each controller. This is especially true for the narrowband time-domain data. In an attempt to ascertain the performance of each narrowband controller, two different frequency domain tests were performed.

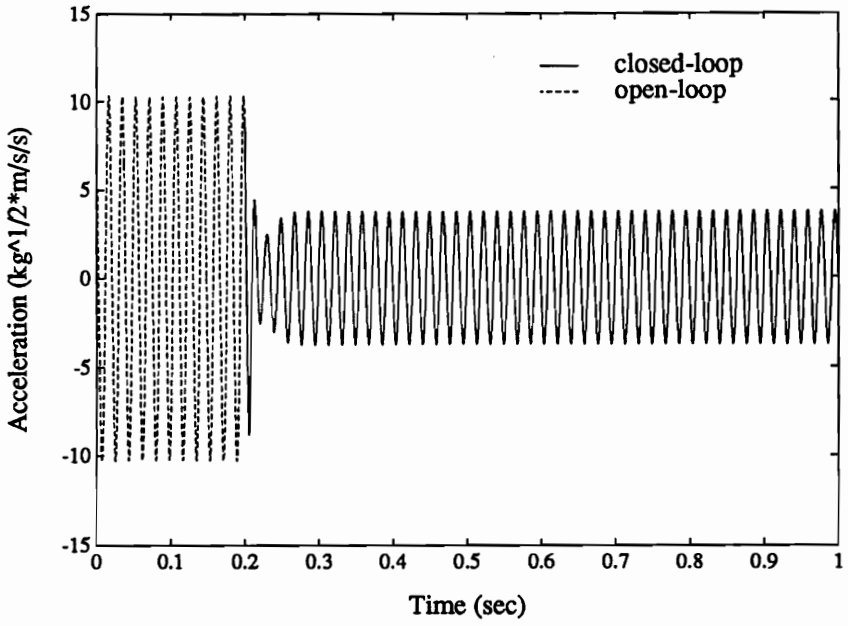

a) simulated data

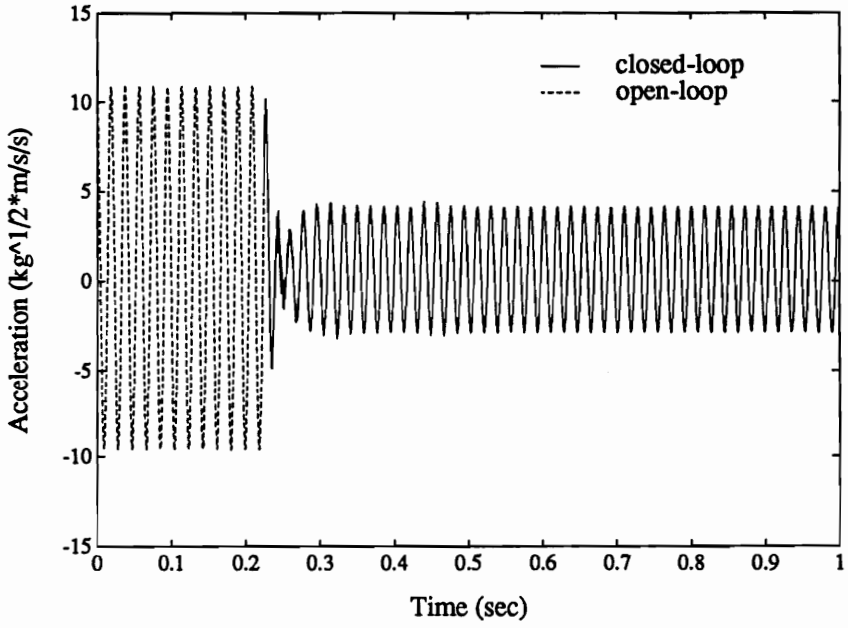

b) experimental data

Figure 5.9: H_∞ Harmonic Disturbance Rejection: Mode 1

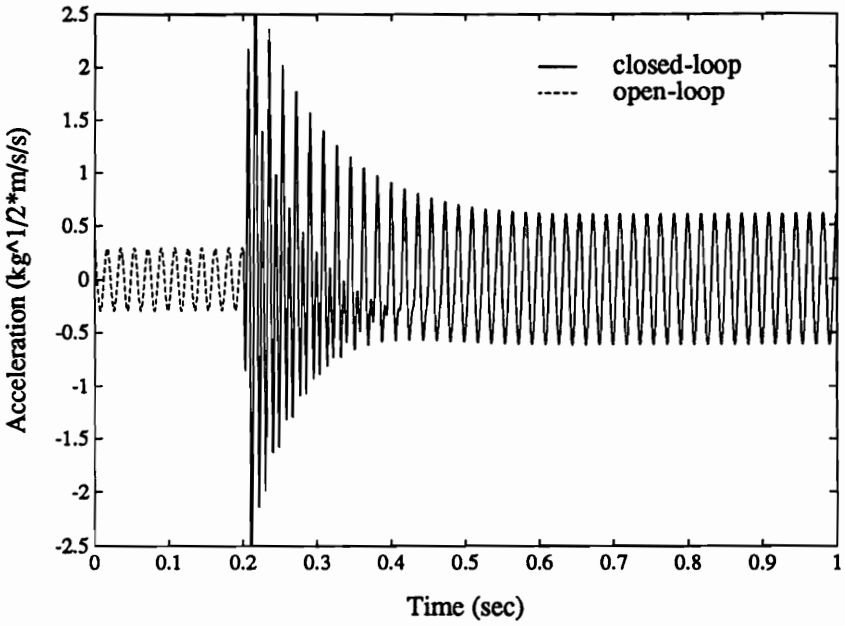

a) simulated data

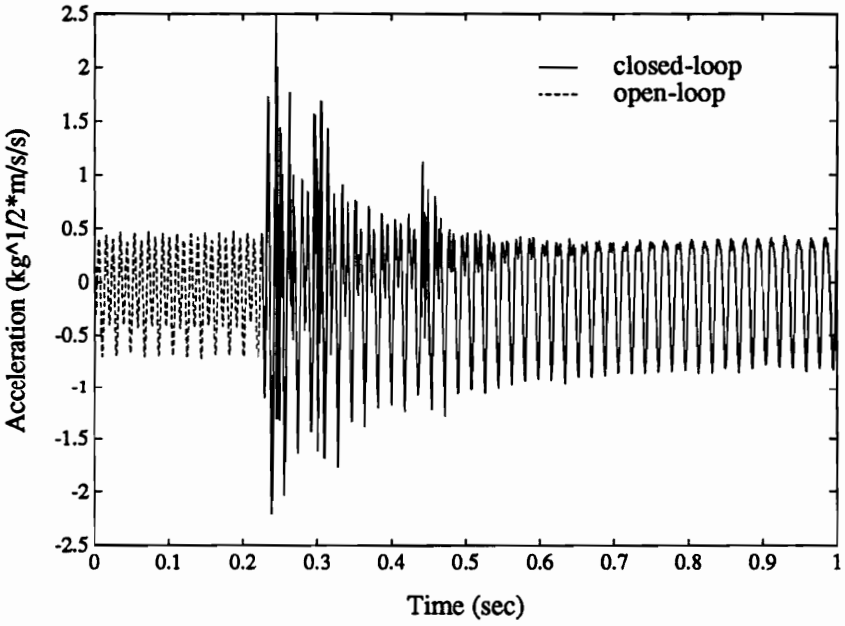

b) experimental data

Figure 5.10: H_∞ Harmonic Disturbance Rejection: Mode 2

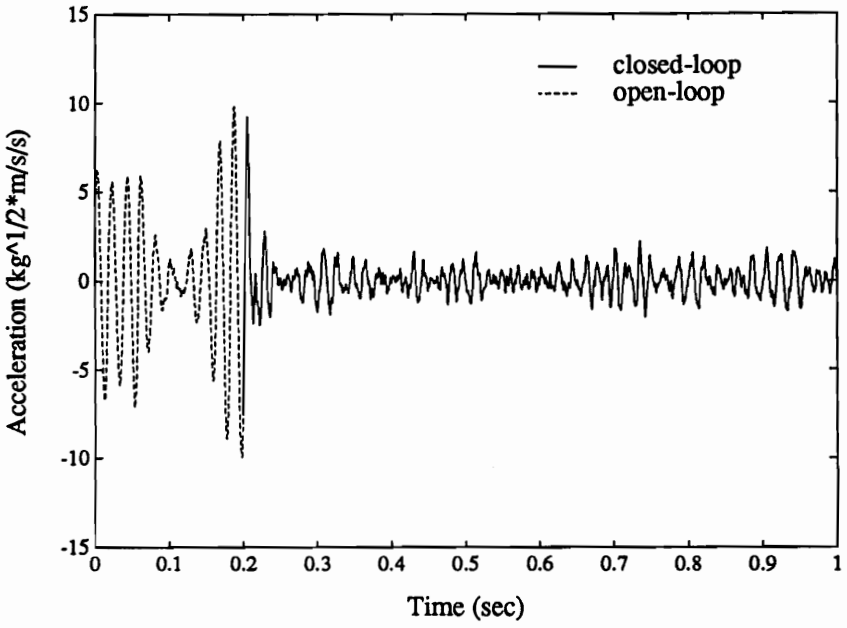

a) simulated data

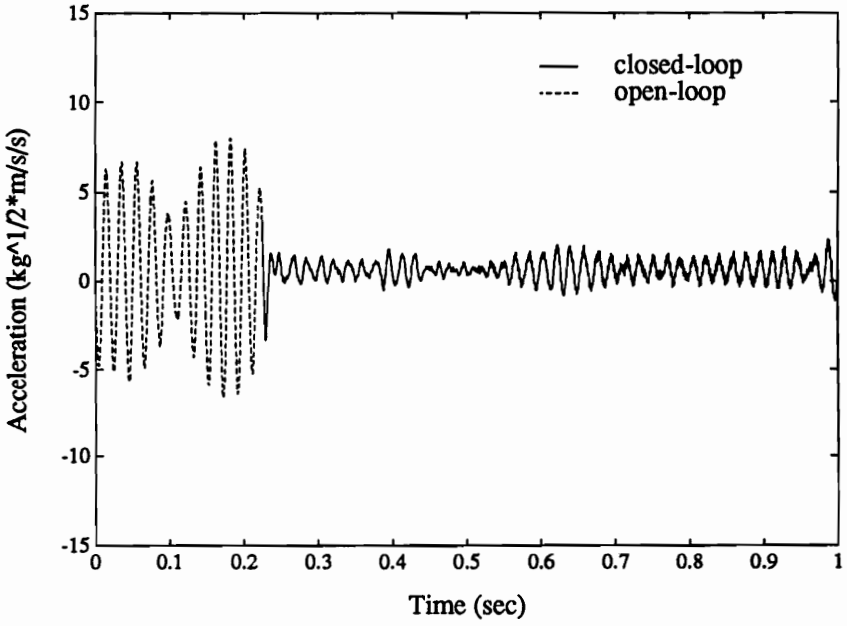

b) experimental data

Figure 5.11: H_∞ Narrowband Disturbance Rejection: Mode 1

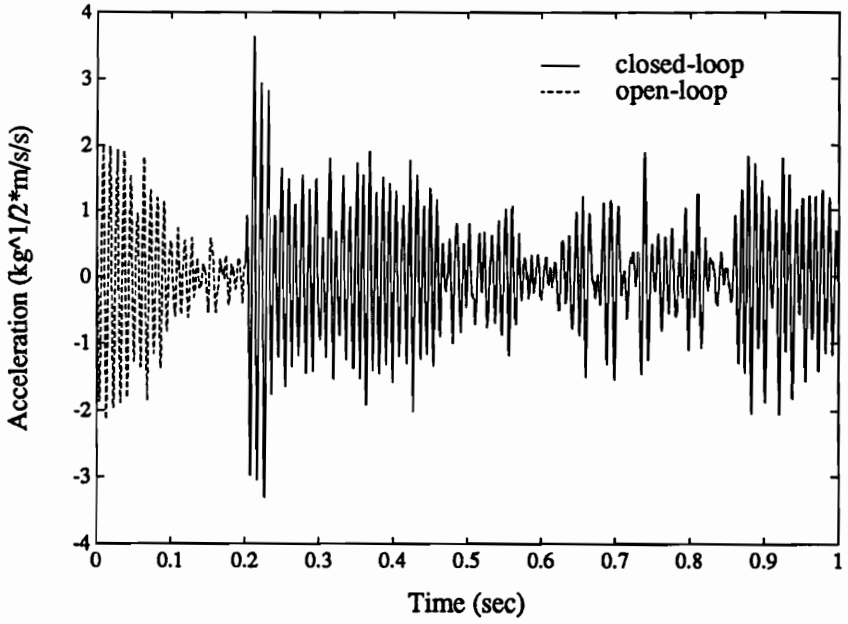

a) simulated data

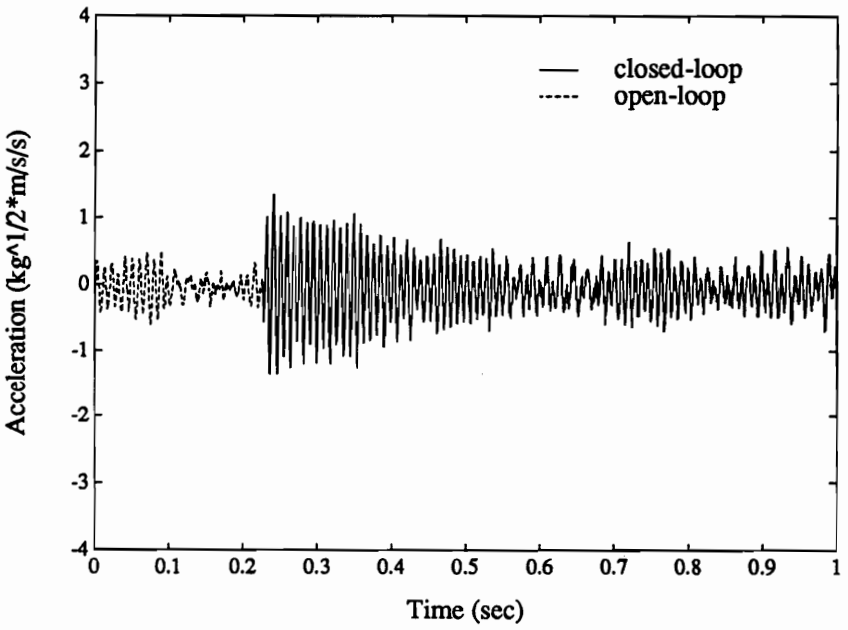

b) experimental data

Figure 5.12: H_∞ Narrowband Disturbance Rejection: Mode 2

Table 5.4: Design Parameters for the H_∞ Controller.

	Harmonic Disturbance	Narrowband Disturbance
Control Weight, ρ	1.1	0.1
Disturbance Filter Damping ζ_f	0.1	0.1
Disturbance Covariance Ξ	500	500
Measurement Covariance Λ	0.5	0.5

The first examination was to drive the system with the narrowband disturbance and then compute the autospectrum of the modal accelerations. This was compared with the open loop data to examine the effect of the controller under actual operating conditions. The second experiment was to drive the system with wide-band (white) noise and calculate the transfer function from the disturbance to the modal accelerations. Both the narrowband and wideband Gaussian disturbance signals used in the tests were digitally generated. They were smoothed using a low-pass filter with a 512Hz cutoff frequency. An additional purpose for this low-pass filter was to limit the spectral content of the disturbance so that unmodelled modes would not be excited. The modal acceleration was also filtered for the transfer function test so that the phase characteristics of the low-pass filters would not affect the results.

In order to obtain adequate information (in a statistical sense) to compute the

autospectra and transfer functions, 75 averages was required for each test. This involved running the experiment for more than 20 minutes for each test. The ability to run the system closed-loop for such an extended period rules out any instability that could occur if only shorter periods were tested.

Experimental Modal Accelerations Autospectra

We first show the autospectra results to show how each controller performs under actual operating conditions, i.e. being driven by narrowband disturbance. As we discussed earlier, the relative phasing of the control and modes one and two causes the mode one response to be attenuated and the mode two response to be amplified. Figure 5.13 shows the autospectrum of the narrowband input disturbance. Figure 5.14 gives a comparison of the first modal and second modal acceleration autospectra. The autospectra for the open-loop as well as all three closed-loop controllers is shown on each plot.

The double hump in the open-loop data is easily explained. The first peak at approximately 50Hz is the plate first mode response. The second peak at approximately 55Hz is due to the forced response from the narrowband noise. As expected, all three controllers provide some degree of disturbance rejection at the disturbance frequency. There is also considerable rejection at the first mode frequency. What is interesting to note is the relative lack of rejection obtained by Rubenstein. His closed-loop, first mode autospectra merely look as though the open-loop autospectra has been decreased approximately 15dB across the whole spectrum; there is still a strong first-mode peak in the closed-loop data.

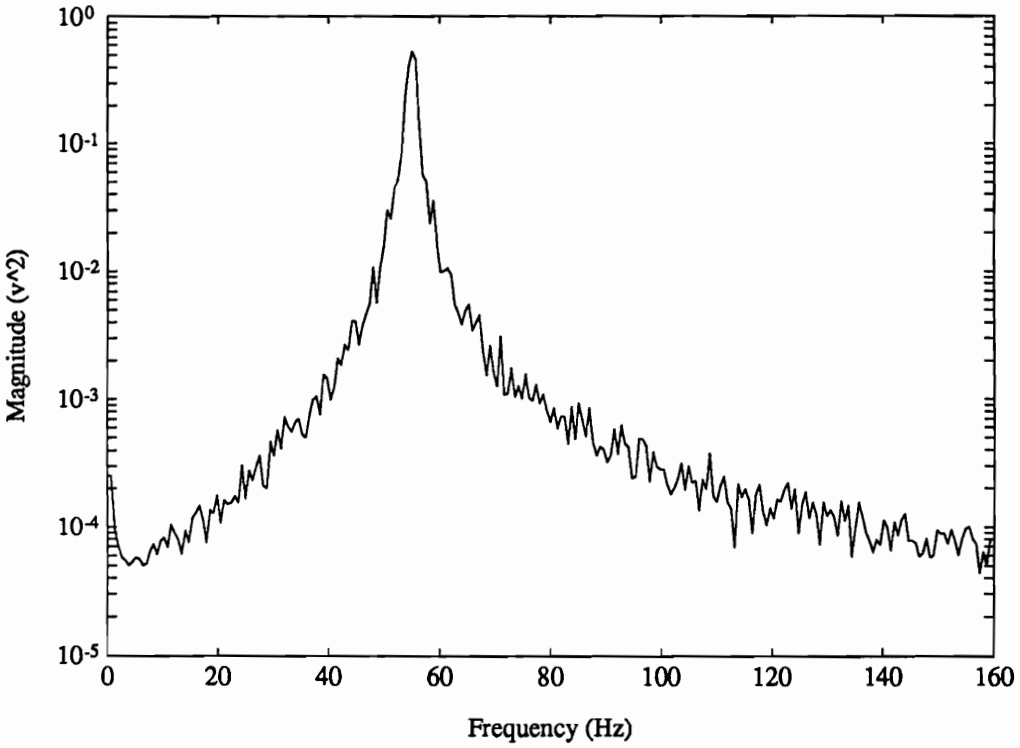

Figure 5.13: Autospectrum of Narrowband Disturbance

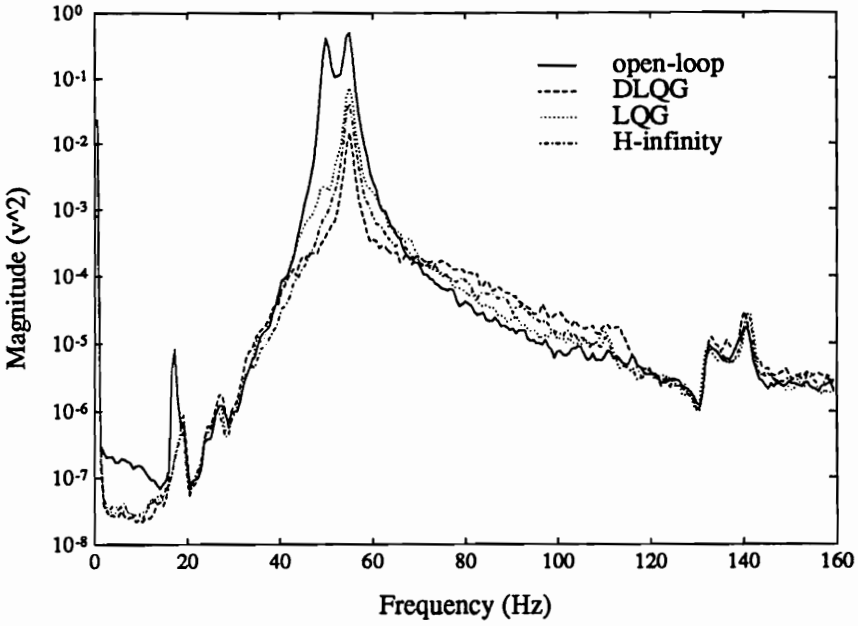

a) mode 1 autospectra

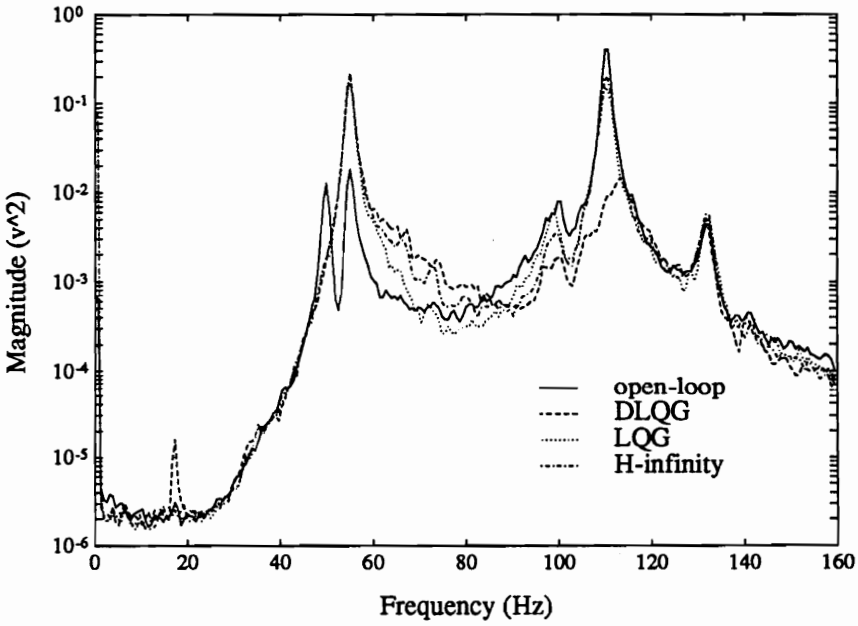

b) mode 2 autospectra

Figure 5.14: Comparison of Narrowband Controllers Modal Autospectra

A comparison of the effectiveness of each controller is shown in tables 5.5, 5.6, and 5.7. Table 5.5 gives the disturbance rejection obtained at the center frequency of the narrowband disturbance (55Hz) for the first modal acceleration. Table 5.6 shows the second modal acceleration autospectra disturbance rejection. As we mentioned previously, the phasing of mode one and mode two cause an increase in the first modal response and a decrease of the second modal response when trying to reject a disturbance near the first mode. Table 5.7 gives the first modal acceleration rejection at the first modal frequency instead of the disturbance frequency.

Table 5.5: First Modal Acceleration Disturbance Rejection at the Disturbance Center Frequency from the Experimental Autospectra (in dB)

DLQG	LQG	H_∞
-13.47	-8.45	-10.94

Table 5.6: Second Modal Acceleration Disturbance Rejection from the Experimental Autospectra (in dB)

	Mode 1 Frequency (49Hz)	Mode 2 Frequency (109Hz)
DLQG	10.88	-14.46
LQG	9.68	-4.24
H_∞	10.51	-3.14

These autospectra data show the same trends we saw in the earlier harmonic data. The DLQG controller provides the most disturbance rejection, while the next best is

Table 5.7: First Modal Acceleration Disturbance Rejection from the Experimental Autospectra at the First Modal Frequency (in dB)

DLQG	LQG	H_∞
-29.25	-23.28	-26.11

the H_∞ controller, and then the LQG controller. On curious aspect, however, is the large reduction of the second modal acceleration of the DLQG controller compared to the other two (> 10dB). It is not apparent why this happens. One important aspect to note for the H_∞ controller is the additional reduction even over the DLQG controller at frequencies below the first modal frequency.

Experimental Transfer Functions

Whereas in the previous section we drove the plate with a narrowband disturbance to determine the modal accelerations autospectra, now we use a wideband Gaussian disturbance source to generate the experimental transfer functions. Both the autospectrum of the wideband disturbance and the transfer functions are shown in figure 5.15.

These experimental data show results similar to the previous experimental autospectra. We see that the DLQG controller provides more disturbance rejection than either the LQG or the H_∞ controllers at both the disturbance frequency and the first modal frequency. Also, the H_∞ controller shows damping over a wider frequency range than both the DLQG and LQG controllers. Numerical data for the rejection obtained is shown in tables 5.8 and 5.9 for the disturbance frequency and first

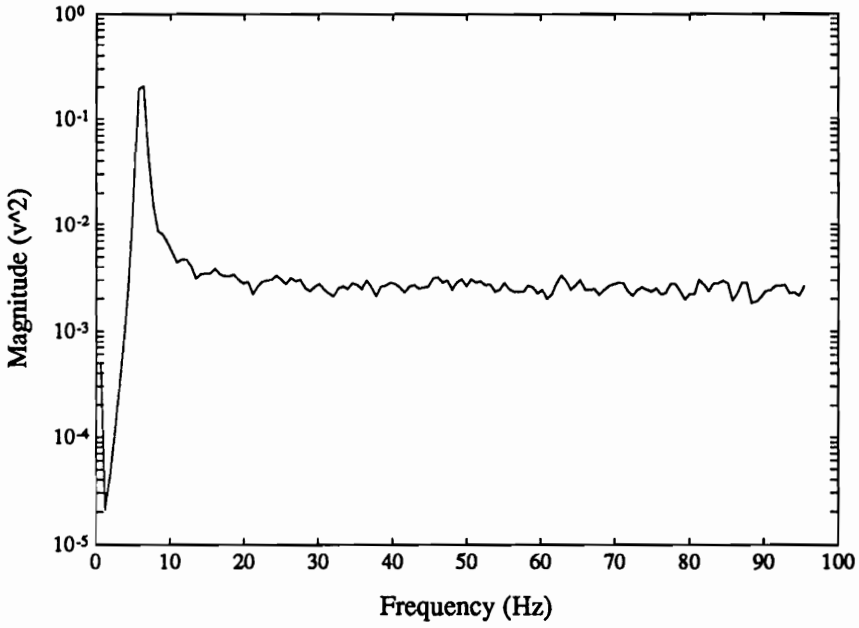

a) disturbance autospectra

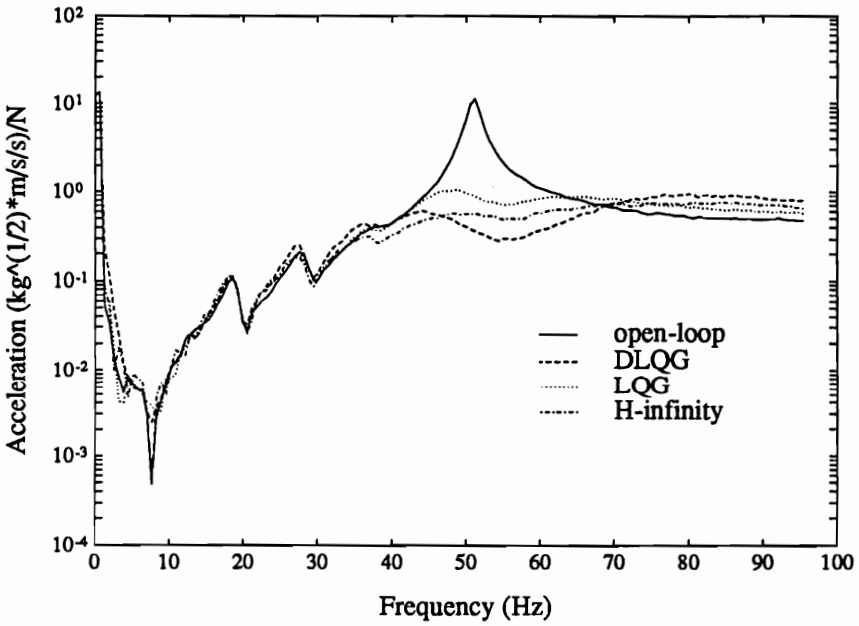

b) mode 1 transfer functions

Figure 5.15: Comparison of Experimental Transfer Functions: Mode 1

modal frequencies respectively. Notice there is reasonable agreement between these data an the numbers computed from the experimental autospectra.

Table 5.8: First Modal Acceleration Disturbance Rejection from the Experimental Transfer Functions at the Disturbance Center Frequency (in dB)

DLQG	LQG	H_∞
-15.82	-8.33	-11.33

Table 5.9: First Modal Acceleration Disturbance Rejection from the Experimental Transfer Functions at the First Mode Frequency (in dB)

DLQG	LQG	H_∞
-29.83	-22.05	-26.01

A couple of artifacts in the experimental data bear mentioning. The notch at 6Hz is a shaker resonance. Both the disturbance and control shaker response functions are given in Rubenstein and show a peak at 6Hz. The two resonances and anti-resonances seen between 20 and 30Hz are a mystery. They may have something to do with the plate mounting, but it is not clear. One thing that is clear, however, is that these types of unmodelled effects can play havoc with model-based controllers like those used here. Fortunately, they do not seem to affect our results.

5.2.5 Impulse Response Comparison

Even though the controllers we designed are for disturbance rejection, we would also like to maximize the damping available so that any unforeseen disturbances are

quickly mitigated. In order to check the additional damping provided by the various controllers, an impulse response test was performed for the open-loop system and the various closed-loop controllers.

The impulse test was performed by turning on the controller (for the closed-loop cases) with no external disturbance and then hitting the center of the plate with a soft-tipped hammer to excite mainly mode one. The hammer was soft-tipped so that less high frequency energy was pumped into the plate so that a curve fit could be performed on the closed-loop data to obtain damping ratios. Tests were repeated until approximately the same maximum magnitude impulse was obtained for each controller tested. Given the low quality of the impact tester, several trials were required before adequate data were obtained.

The open- and closed-loop impulse response plots for the various narrowband controllers are shown in figures 5.16 through 5.17. The damping ratios obtained using the log decrement method are shown in table 5.10. One caveat, however, is that the closed-loop data has so much high frequency information that it is necessary to to low-pass filter it before any data could be extracted for the curve fit. In order to verify that the filtering process did not alter the data, an FFT was performed on the filtered data to check the spectral content was primarily first mode.

Table 5.10: Experimental Mode 1 Damping Ratios

Open-Loop	DLQG	LQG	H_∞
0.009	0.08 – 0.1	0.08 – 0.1	0.08 – 0.1

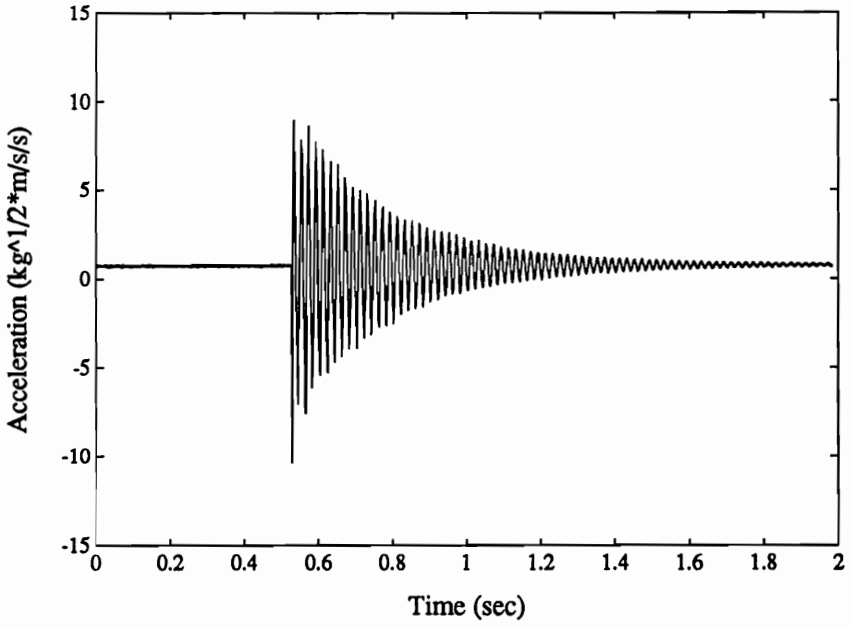

a) open-loop

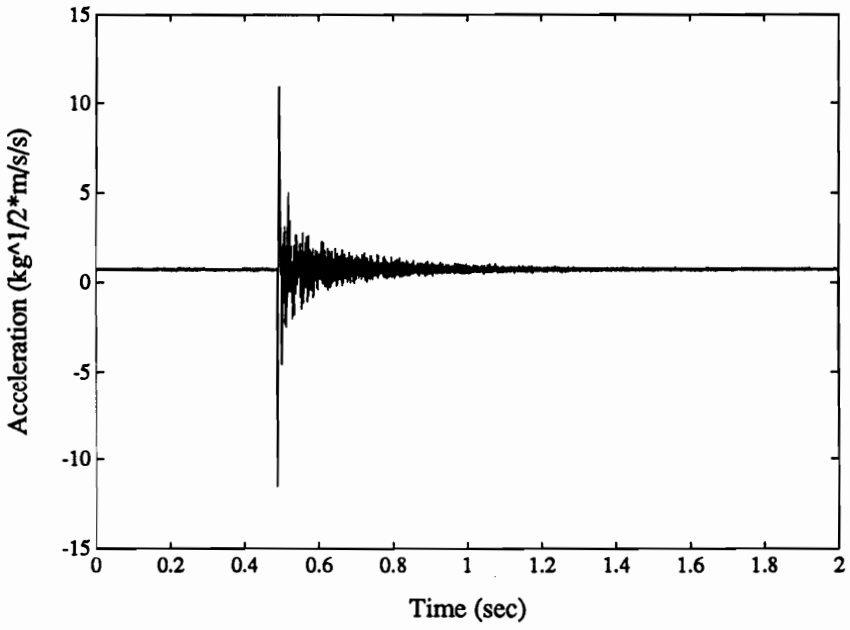

b) DLQG controller

Figure 5.16: Mode 1 Impulse Response: Open-Loop and DLQG

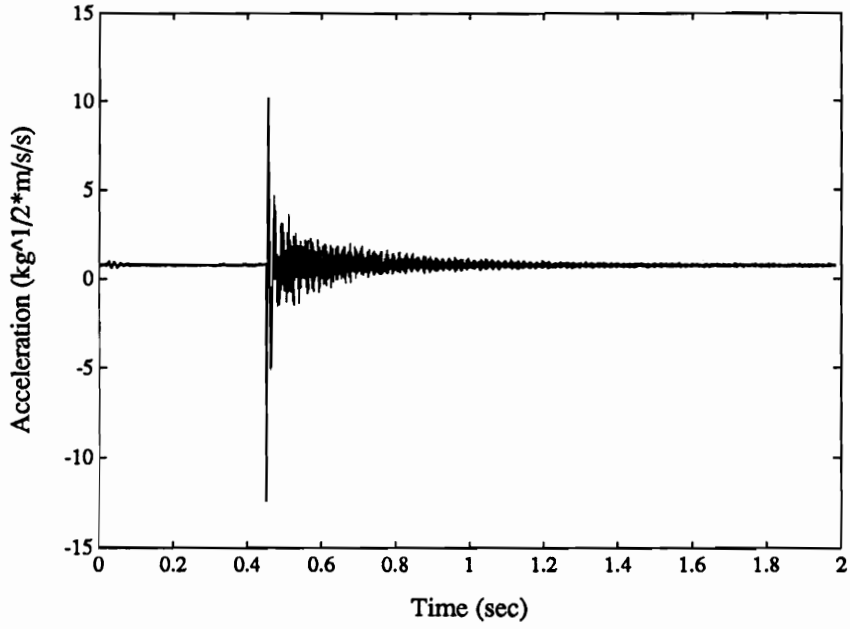

a) LQG controller

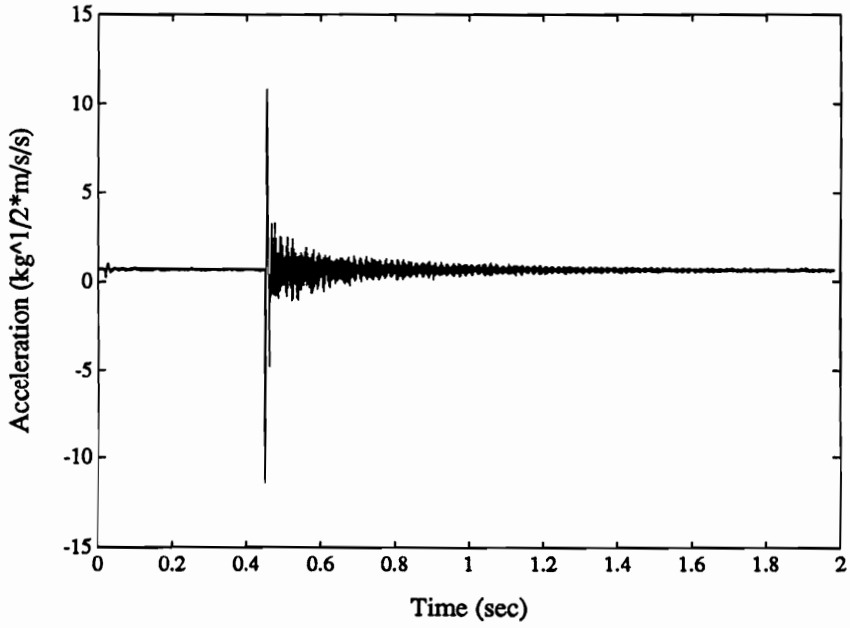

b) H_∞ controller

Figure 5.17: Mode 1 Impulse Response: LQG and H_∞

Additionally, the closed-loop damping ratios shown in table 5.10 are approximate. This is due to the poor original data and the filtering process. For example, the H_∞ transient data make it appear as though the H_∞ controller has the most damping, but the curve fit does not show that quantitatively. The filtering was done only as an expedient so there is some degree of uncertainty in the log decrement data fits. Basically, all three controllers provide an order of magnitude increase in damping. This is also more damping obtained by Rubenstein for his DLQG controller. He was only able to obtain 0.022, (2.2 percent critical) damping with his controller.

Chapter 6

Conclusions and Recommendations for Future Research

This last chapter gives us an opportunity to mull over all of the theory and data presented earlier and hopefully make some sense out of what we saw, or what we thought we saw. Also since this chapter includes recommendations, we pose some possible related, yet previously unmentioned areas of difficulty and interest motivated by the effort required to perform the plate experiments.

In the analytical section of this work, we see how the H_∞ controller is not a state-estimator like the LQG controller. Purely in this context, the utility of such knowledge is not clear. If we include the observations from the simply-supported plate experiments, we see that the H_∞ controller concentrates its control effort where the augmented open-loop system has the maximum "gain" (in a singular value sense). The averaging nature of the LQG controller tends to spread the control effort across a wider frequency range than an H_∞ controller with the same weights and for the disturbance rejection problems of interest this may not be the best choice. Another

thing that was not explicitly mentioned is the ability to design H_∞ controllers using the same approach as in the LQG case.

One obvious extension to the single-disturbance, single-control actuator experiment shown here is to add more disturbances and more control actuators. If we model each disturbance spectrum separately (with the knowledge that the model order increases for each disturbance) instead of treating the problem as a wideband or passband disturbance rejection problem, the H_∞ optimal controller can go after each resonant peak separately (assuming a sufficient number of actuators). Admittedly, LQG would also go after the peaks, but not as aggressively as the H_∞ approach.

In terms of our goal of rejecting persistent disturbances, all three compensator designs, DLQG, LQG, and H_∞ were successful in rejecting the harmonic and narrowband disturbances on the simply supported plate. Using the "minimum acceleration" design procedure developed here as the basis for generating weighting matrices provided approximately the same degree of steady-state disturbance rejection as the ad hoc weighting matrix method used by Rubenstein [53] while at the same time providing five times more damping. The closed-loop DLQG damping ratio for the plate first mode increased from 2.2 to 10 percent critical using the minimum acceleration approach.

One possible connection to the "minimum acceleration" design procedure discussed above that bears further investigation is the weighting of the uncontrollable, augmented disturbance states. Jones [51] arrived at a set of quadratic weights for

LQG that involved these uncontrollable augmented states by posing the direct disturbance cancellation problem and then solving the inverse optimal LQ regulator problem. Unfortunately, Jones did not provide any narrowband or transient results and therefore there are no damping ratios for comparison. The controller-on transient response for his harmonic results did show the same "fast" (0.1 sec) response as the harmonic results presented earlier in this dissertation, however. It may be that there is nothing special about minimum acceleration per se, it might be the penalizing of the uncontrollable disturbance states the gives the performance noted above.

An interesting comparison would be to solve the inverse H_∞ optimal control problem for a direct disturbance cancellation control to see the form of the controlled output equation obtained. Unfortunately, for the general inverse H_∞ optimal control problem, no procedure for finding the controlled output equations exists. Fujii et al. [56] provide necessary and sufficient conditions for the existence of the inverse H_∞ problem, but provide no method for actually obtaining a controlled output equation.

The H_∞ experimental results are important for several reasons. First, there have not been many experiments using H_∞ optimal control (or even LQG for that matter!). Additionally, this is an important comparison between the LQG and H_∞ approaches for persistent disturbance rejection. Both methods provide disturbance rejection which validates the appropriateness of H_∞ for these types of problems; however, the H_∞ controller provides more attenuation over a wider frequency range than the DLQG and LQG controllers. Unfortunately, the continuous-to-discrete controller design approach does not seem to be the appropriate method to use for discrete

systems. We loose about 5-7dB of rejection when the LQG method is compared to the DLQG. This is a strong motivation to use discrete-time H_∞ controller design. It would also be advantageous if there were a corresponding predictor-corrector form for a discrete-time H_∞ controller so control values could be based on a step-ahead prediction like the DLQG.

The next logical step from the "nominal" H_∞ controller design is a robust controller design. The supposed advantage of using an H_∞ controller is the ability to deal with structured plant perturbations using μ-synthesis. A study of the performance/robustness tradeoffs for some set of plant model errors is an important evolutionary step in the use of H_∞ controllers. Another possibility is some type of online system identification to help in the never-ending quest for an analytical model that actually matches reality. One concern with using μ-synthesis is that a stabilizing controller may be found, but the system model may sufficiently removed from reality that there is no closed-loop performance. Some system identification procedure that lets us optimize the model online might be the best way to obtain stability and performance.

An important, related and previously unmentioned area of concern for all of the preceding state-space methods involves the numerical solution of the Hamiltonian eigenvalues. This is often a numerically ill-conditioned problem and even after balancing, the condition numbers encountered can lead to inaccurate results. Research needs to be performed to find better way to solve this problem especially as the numerical problems are exacerbated by increasing model order.

Another unmentioned area concerns the data acquisition system used in the controller. Typically, 12-bit resolution analog-to-digital (ADC) converters are used since the analog electronics are often not much more accurate than that. We found that the quantization noise often gets amplified as data "flows" through the control loop and signals that are supposed to be zero are amplified to unacceptable DC levels. This is especially evident at high gain settings. A solution to this problem is to use 16-bit converters to decrease the effect of this quantization noise.

And in conclusion, we should acknowledge that the field of control system design requires many interdisciplinary skills that are often not emphasized in formal training, but are important nevertheless. The work presented herein required working knowledge of dynamics, modal analysis, instrumentation, real-time programming, linear systems theory, and, yes, even control system theory. Without a broad grasp of the fundamentals in these diverse areas, the ability to take many of the advanced control systems theories and apply them is not likely succeed.

Bibliography

[1] Dorato, P., ed., *Robust Control,* IEEE Press, New York, 1987.

[2] Kalman, R.E., "A New Approach to Linear Filtering and Prediction Problems," *ASME Journal of Basic Engineering,* vol. 82, pp. 34-45, 1960.

[3] Brogan, W.L., *Modern Control Theory,* Prentice-Hall, Inc., Englewood Cliffs, N.J. 1985.

[4] Anderson, B.D.O., and J.B. Moore, *Linear Optimal Control,* Prentice-Hall, Englewood-Cliffs, N.J., 1971.

[5] Dontchev, A.L., *Perturbations, Approximations, and Sensitivity Analysis of Optimal Control Systems,* Lecture Notes in Control and Information Sciences, vol. 52, Springer-Verlag, Berlin, 1983.

[6] Porter, B., and R. Crossley, *Modal Control: Theory and Applicatons,* Taylor and Francis, Ltd., London, 1972.

[7] Dailey, R.L., *Lecture Notes for the Workshop on H_∞ and μ Methods for Robust Control,* American Control Conference 1990, San Diego, CA, May 1990.

[8] Kalman, R.E., "When is a Linear Control System Optimal?," *Trans. ASME, Ser. D (J. Basic Engr.)*, vol. 86, pp. 51-60, Mar. 1964.

[9] Safanov, M.G., and M. Athans, "Gain and Phase Margins for Multiloop LQG Regulators," *IEEE Trans. Automat. Contr.*, vol AC-22, pp. 173-179, Apr. 1977.

[10] Doyle, J.C., "Guaranteed Margins for LQG Regulators," *IEEE Trans. Automat. Contr.,* vol. AC-23, pp. 756-757, Aug. 1978.

[11] Doyle, J.C., and G. Stein, "Robustness with Observers", *IEEE Trans. Automat. Contr.,* vol. AC-24, pp. 607-611, Aug. 1979.

[12] Doyle, J.C., and G. Stein, "Multivariable Feedback Design: Concepts for a Classical Modern Synthesis," *IEEE Trans. Automat. Contr.*, vol. AC-26, no. 1, pp. 4-16, Feb. 1981.

[13] Youla, D.C., Jabr, H.A., and J.J. Bongiorno, Jr., "Modern Weiner-Hopf Design of Optimal Controllers Part II: The Multivariable Case," *IEEE Trans. Automat. Contr.*, vol. AC-21, no. 3, pp. 319-338, June 1976.

[14] Desoer, C.A., Liu, R.-W, Murray, J., and R. Saeks, "Feedback System Design: the Fractional Representation Approach to Analysis and Synthesis," *IEEE Trans. Automat. Contr.*, vol. AC-25, no. 3, pp. 399-412, June 1980.

[15] MacFarlane, A.G.J., and I. Postlethwaite, "The Generalized Nyquist Stability Criterion and Multivariable Root Loci," *Int. J. Contr.*, vol. 25, pp. 81-127, Jan. 1977.

[16] Safanov, M.G., Laub, A.J., and G.L. Hartmann, "Feedback Properties of Multivariable Systems: The Role and Use of the Return Difference Matrix," *IEEE Trans. Automat. Contr.*, vol. AC-26, no. 1, pp. 47-65, Feb. 1981.

[17] Ridgley, D.B., and S.S. Banda, *Introduction to Robust Multvariable Control,* Control Dynamics Branch, Flight Dynamics Laboratory, AD-A165 891, Feb. 1986.

[18] Maciejowski, J.M., *Multivariable Feedback Design*, Addison-Wesley, New York, 1989.

[19] Zames, G., "Feedback and Optimal Sensitivity: Model Reference Transformations, Multiplicative Seminorms, and Approximate Inverses," *IEEE Trans. Automat. Contr.*, vol. AC-26, no. 2, pp. 301-320, Apr. 1981.

[20] Doyle, J.C., "Lecture Notes in Advances in Multivariable Control," *ONR/Honeywell Workshop,*, Minneapolis, MN, 1984.

[21] Francis, B.A., and J.C. Doyle, "Linear Control Theory with an H_∞ Optimality Criterion," *SIAM J. Control and Optimization,* vol. 25, no. 4, pp. 815-844, 1987.

[22] Francis, B.A., *A Course in H_∞ Control Theory,* Lecture Notes in Control and Information Sciences, vol. 88, Springer-Verlag, Berlin, 1987.

[23] Doyle, J.C., "Analysis of Feedback Systems with Structured Uncertainties," *IEE Proc.*, vol. 129, Part D, no. 6, pp. 242-250, Nov. 1982.

[24] Safanov, M.G., "Stability Margins of Diagonally Perturbed Multivariable Feedback Systems," *IEE Proc.*, vol. 129, Part D, no. 6, pp. 251-256, Nov. 1982.

[25] Ball, J.A., Helton, J.W., and M. Verma, "A Factorization Principle for Stabilization of Linear Control Systems," preprint.

[26] Glover, K., and J.C. Doyle, "State-Space Formulae for All Stabilizing Controllers that Satisfy an H_∞ Norm Bound and Relations to Risk Sensitivity," *Systems and Control Letters,* 11, pp. 167-172, 1988.

[27] Doyle, J.C., Glover, K., Khargonekar, P.P., and B.A. Francis, "State-Space Solutions to Standard H_2 and H_∞ Control Problems," *IEEE Trans. on Auotmat. Control,* vol. 34, no. 8, Aug. 1989, pp. 831-847.

[28] Safonov, M.G., Limebeer, D.J.N., and R.Y. Chiang, "Simplifying the H^∞ Theory via Loop-Shifting, Matrix-Pencil and Descriptor Concepts," *Int. J. Control,* vol. 50, no. 6, 1989, pp. 2467-2488.

[29] Glover, K. and J.C. Doyle, "A State Space Approach to H_∞ Optimal Control," *Three Decades of Mathematical System Theory,* Lecture Notes in Control and Information Sciences, Vol. 135, Springer-Verlag, Berlin, pp. 179-218, 1989.

[30] Hvostov, H.S., and M. Luksic, "On the Structure of H_∞ Controllers," *Proceedings of the 1990 American Control Conference,* San Diego, CA, May 1990, pp. 2484-2489.

[31] Chang, B.C., Li, X.P., Banda, S.S., and H.H. Yeh, "Design of an H^∞ Optimal Controller by Using DGKF's State-Space Formulas," *Proceedings of the 29th Conference on Decision and Control,*, Honolulu, Hawaii, pp. 2632-2633, Dec. 1990.

[32] Scherer, C., "H_∞-Control by State-Feedback and Fast Algorithms for the Computation of Optimal H_∞-Norms," *IEEE Trans. on Automat. Contr.,* vol. 35, no. 10, pp. 1090-1099, 1990.

[33] Green, M., and D.J.N. Limebeer, "H_∞ Optimal Full Information Control for Discrete Time Systems," *Proceedings of the 29th Conference on Decision and Control,*, Honolulu, Hawaii, December, 1990, pp. 1769-1774.

[34] Keller, J.P., and B.D.O. Anderson, "H_∞ Optimal Controller Discretization," *Proceedings of the 29th Conference on Decision and Control,*, Honolulu, Hawaii, December, 1990, pp. 1781-1785.

[35] Bernstein, D.S., and W.M. Haddad, "LQG Control with an H_∞ Performance Bound: A Ricatti Equation Approach," *Proceedings of the 1988 American Control Conference,* Atlanta, GA, June, 1988, pp. 796-802.

[36] Zhou, K., Doyle, J., Glover, K., and B. Bodenheimer, "Mixed H_2 and H_∞ Control," *Proceedings of the 1990 American Control Conference,* San Diego, May 1990, pp. 2502-2507.

[37] Yeh, H.-H., Banda, S.S., and Chang, B.-C., "Necessary and Sufficient Conditions for Mixed H_2 and H_∞ Optimal Control," *Proceedings of the 29th Conference on Decision and Control,*, Honolulu, Hawaii, December, 1990, pp. 1013-1017.

[38] Yeh, H.-H., Banda, S.S., Heise, S.A., and A.C. Bartlett, "Robust Control Design with Real-Parameter Uncertainty and Unmodelled Dynamics," *J. Guidance,* vol. 13, no. 6., Nov.-Dec. 1990.

[39] Fan, M.K.H., Tits, A.L., and J.C. Doyle, "Robustness in the Presence of Mixed Parametric Uncertainty and Unmodelled Dynamics," *IEEE Trans. Auto. Control,*, vol. 36, no. 1, Jan. 1991, pp. 25-38.

[40] Zhou, K., and P.P. Khargonekar, "An Algebraic Riccati Equation Approach to H_∞ Optimization," *Systems and Control Letters,* 11, 1988, pp. 85-91.

[41] Sampei, M., Mita, T., and M. Nakamichi, "An Algebraic Approach to H_∞ Output Feedback Control Problems," *Systems and Control Letters,* 14, 1990, pp. 13-24.

[42] Peterson, I.R., Anderson, B.D.O., and E.A. Jonckheere, "A First Principles Solution to the Non-Singular H_∞ Control Problem," Submitted to the International Journal of Robust and Nonlinear Control.

[43] Makila, P.M., "H^∞-Optimization and Optimal Rejection of Persistent Disturbances," *Automatica,* vol. 26, no. 3, pp. 617-618, 1990.

[44] Kawatani, R., Fujii, T., and H. Kimura, "On the role of Disturbance Estimation in H^∞ Control Systems," *Proceedings of the 29th Conference on Decision and Control,*, Honolulu, Hawaii, December, 1990, pp. 200-201.

[45] Fujita, M., Matsumura, F., and K. Uchida, "Experiments on the H^∞ Disturbance Control of a Magnetic Suspension System," *Proceedings of the 29th Conference on Decision and Control,*, Honolulu, Hawaii, December, 1990, pp. 2773-2778.

[46] Balas, G.J., and J.C. Doyle, "Robustness and Performace Tradeoffs in Control Design for Flexible Structures," *Proceedings of the 29th Conference on Decision and Control,*, Honolulu, Hawaii, December, pp. 2999-3010, 1990.

[47] Balas, G.J., Doyle, J.C., Glover, K, Packard, A., and R. Smith, *μ-Analysis and Synthesis Toolbox: MATLAB Functions for the Analysis and Design of Robust Control Systems,* MUSYN, Inc., Minneapolix, MN, 1991.

[48] Uchida, K. and M. Fujita, "On the Central Controller: Characterization via Differential Games and LEQG Control Problems," *Systems and Control Letters,* 13, 1989, pp. 9-13.

[49] Sievers, L.A., and A.H. von Flowtow, "Comparison of Two LQG-Based Methods for Disturbance Rejection," *Proceedings of the 28th. Conference on Decision and Control,* Tampa, Florida, Dec. 1989, pp. 483-485.

[50] Sievers, L.A., and A.H. von Flowtow, "Comparison and Extenstions of Control Methods for Narrowband Disturbance Rejection," *1990 ASME Winter Annual Meeting,* Dallas, Nov. 1990.

[51] Jones, S.H., "Parameter Robust Reduced-Order Control of Flexible Structures," *Ph.D. Dissertation,* Virginia Tech, August 1991.

[52] Stengel, R.F., *Stochastic Optimal Control: Theory and Application,* Wiley, New York, 1986.

[53] Rubenstein, S.P., "An Experiment in State-Space Vibation Control of Steady Disturbances on a Simple-Supported Plate," *M.S. Thesis,* Virginia Tech, August, 1991.

[54] Ellis, G.K., "Design and Programming of a Medium Performance Data Acqusition System Based on Transputers," *Internal Report, Center for Intelligent Mataerial Systems and Structures,* Mechanical Engineering Department, Virginia Tech, Blacksburg, VA, 1991.

[55] Chui, C.K., and G. Chen, "Kalman Filtering with Real-Time Applications," *Springer Verlag,* New York, 1987.

[56] Fujii, T., and P.P. Khargonekar, "Inverse Problems in H_∞ Control Theory and Linear-Quadratic Differential Games," *Proceedings of the 27th Conference on Decision and Control,*, Austin, TX, pp. 26-31, Dec. 1988.

Vita

Graham K. Ellis was born in Montgomery, Alabama on May 28, 1961. After living in Alabama, Kansas, and Maryland, his family moved to Sterling, Virginia in 1968. After graduating from Park View High School in 1979, he attended Virginia Tech and received a BSME and MSME in 1983 and 1984 respectively. After graduation, he worked for the Institute for Computational Mechanics in Propulsion at NASA Lewis Research Center in Cleveland, Ohio for four years. He returned to Virginia Tech persue a Ph.D. in the fall of 1988. As of this writing, the he is still searching for gainful employment.